The effect of membrane characteristics on the performance of membrane distillation system for the treatment of hypersaline brine

by

Abdul Azeez Ismail

A thesis submitted in fulfilment of the requirements for the degree

Master of Engineering: Chemical

in the faculty of

Engineering and the Built Environment

at the

Cape Peninsula University of Technology

Supervised by

Prof Mujahid Aziz

September 2022

DECLARATION

I, Abdul Azeez Ismail, declare that the contents of this thesis represent my own unaided work, and that the thesis/dissertation has not previously been submitted for academic examination towards any qualification. Furthermore, it represents my own opinions and not necessarily those of the Cape Peninsula University of Technology.

September 2022

Signed **Date**

ABSTRACT

South Africa is a water-scarce country that continues to experience significant strain around the availability of water resources that are environmentally and economically sustainable. Importantly, this scarcity in the water supply is expected to increase in the future owing to the ramifications of climate change leading to unpredictable rainfall, which the increased evaporation rates will further exacerbate due to elevated average temperatures.

Membrane Distillation (MD) is a membrane-based, thermally driven separation process. Only vapour molecules pass through a microporous hydrophobic membrane that acts as a physical barrier separating a hot aqueous feed solution from a cold permeate. The driving force for membrane distillation is the transmembrane vapour pressure differential.

Of the various membrane characteristics investigated, membrane pore size was identified as the critical variable in terms of membrane selection. As a result, the research focussed mainly on two polyvinylidene fluoride (PVDF) membranes with pore sizes of 0.22 µm and 0.45 µm.

This study examined the use of two membranes with varying pore sizes to treat brine emanating from industrial wastewater. The key aim of this study was to determine the effects of pore size for the treatment of mining and or industrial wastewaters using MD (focussing on flux rate and scaling limitations). The effect of feed temperature and feed concentration on MD system performance using varying pore sizes was also investigated.

Two types of brines were investigated: Type 1 Brine, a monovalent ion dominant, non-scaling/fouling brine and Type 2 Brine, which was a divalent and trivalent ion dominant brine with scaling and or fouling potential. Both brines provided the necessary coverage regarding the variability in brine wastewater characteristics from industrial and mining sectors. Synthetically prepared feed solutions were used to establish baseline performance characteristics for the membranes. The study also included testing industrial brine emanating from an RO process, emphasising the most suitable membrane properties for this specific type of brine.

The water purity from all investigations yielded acceptable results and very high rejection (>99.94%) with the product water exhibiting low conductivity (<15 µS/cm), which only increased once scaling on the membrane surface and pore wetting caused a decrease in flux rate.

For the results obtained using the Type 1 brine, it was found that for both membrane pore sizes investigated, 0.22 µm and 0.45 µm, an increase in temperature from 40˚C to 80˚C increased the flux rate by up to 6.27 times. Increasing the feed TDS concentration from 35 g/L to 65 g/L did not have any notable effect on the flux rate even when the 0.22 µm and 0.45 µm pore size membranes were subjected to feed concentrations close but below solubility level. The 0.22 µm and 0.45 µm pore size membranes performed similarly, indicating that the vapour pressure driving force was not limited by pore size. However, as the Type 1 brine approached solubility level, the smaller, 0.22 µm pore size membrane performed better in terms of flux and salt rejection. This result may be explained by the crystallising solute in the solution having a small enough particle size to enter the pores of the 0.45 µm pore size membrane but being too large to enter the 0.22 µm pore size membrane's pores.

For the results obtained using the prepared Type 2 brine, it was found that for both membrane pore sizes investigated, 0.22 µm and 0.45 µm, an increase in temperature from 40˚C to 80˚C increased the flux rate by up to 4.22 times. An increase in initial feed TDS concentration 11870 mg/L to 27025 mg/L for the 0.22 µm, and 0.45 µm pore size membranes caused a decrease in the flux of up to 40.3% and 35%, respectively. The smaller 0.22 µm pore size membrane generally performed better in terms of flux for these experiments.

The investigation into the effect of scaling/fouling on the performance of MD 0.22 µm and 0.45 µm pore size membranes for the treatment of Type 2 brine with initial feed TDS concentration of 27025 mg/L showed a significant difference between the varying pore sizes. The larger, 0.45 µm pore size membrane yielded a flux two times higher than the 0.22 µm pore size membrane. The maximum suspended solids in the solution before a significant decline in MD performance for the 0.22 µm and 0.45 µm pore size membranes were found to be approximately 3050 mg/L and 3550 mg/L, respectively. Thus the 0.45 µm pore size membrane was more resistant to scaling when compared to the 0.22 µm pore size membrane.

The use of actual brine investigated showed the 0.22 µm pore size membrane to perform better in terms of flux and permeate quality, when compared to the 0.45 µm pore size membrane, which was due to the maximum TSS not being reached. Hence, 0.22 µm pore size membrane generally performs better until scaling/fouling occurs.

More research into membrane characteristics, particularly porosity and membrane thickness, needs to be investigated to develop cheaper, better-performing membranes that would result in greater interest from industrial sectors to use MD.

In conclusion, this study aimed to add to the body of knowledge and explore MD as a more sustainable industrial wastewater treatment process that reduces wastewater production. There is a significant technological gap in providing a cost-effective brine treatment solution towards achieving zero liquid discharge.

ACKNOWLEDGEMENTS

I begin by praising and thanking Allah the Almighty for giving me the strength to succeed with this project, protecting me and blessing me with my family and friends.

The work described in this thesis was carried out within the Chemical Engineering Department at the Cape Peninsula University of Technology (CPUT).

I wish to thank:

- My supervisor, Prof Mujahid Aziz, for his understanding, integrity, humility, patience, professional guidance, technical proficiency, and continuous support throughout my time as his student. I am incredibly thankful for the wisdom and fatherly advice.

- My co-supervisor, Mr. Jeeten Nathoo, for advising me throughout the project with his wealth of technical expertise.

- The Water Research Commission (WRC) for funding my research.

- The technical and administrative staff in the Chemical Engineering department, Mrs Hannelene Small, Mr Alwyn Bester and Mrs Elizma Alberts, for always going out of their way to help me in every way possible

- The Environmental Engineering Research Group (*EnvERG*) for their support

- All my friends and family for their moral support and constant encouragement

- My parents, for their continued moral and financial support

- My mother and sister for being the pillars of strength and moral support in my life.

DEDICATION

To the amazing women in my life, my mother and sister, my family, and friends, for their unconditional love, support, encouragement, and inspiration. This achievement would not be possible without any of you.

I am forever grateful for your presence in my life.

THANK YOU!

RESEARCH OUTPUTS

Oral Presentation:

Ismail A.A., Aziz M. & Nathoo J. 2021. The outcome of membrane characteristics on membrane distillation performance for the remediation of hypersaline water. Cape Peninsula University of Technology (CPUT) Post Graduate Virtual Conference 2021 [CPUT, Bellville, South Africa, 30 November 2021].

Publications:

Nathoo, J., **Ismail, A.A.,** Aziz, M. & Randall, D., 2022. Essential Considerations for the Implementation of Membrane Distillation Crystallisation in the Treatment of Hypersaline Brines. *WRC Report No. 2763/1/22*

Ismail A.A., Aziz M. & Nathoo J. 2022. PVDF membrane treatment of hypersaline brine with a membrane distillation system. *MDPI Membrane.* Submitted XX September 2022 [Paper ID.: XX-XX-XX]

TABLE OF CONTENTS

DECLARATION i
ABSTRACT ii
ACKNOWLEDGEMENTS v
DEDICATION vi
RESEARCH OUTPUTS vii
TABLE OF CONTENTS viii
LIST OF FIGURES xiii
LIST OF TABLES xv
LIST OF PHOTOGRAPHS xix
LIST OF ABBREVIATIONS xx
Chapter 1 Introduction and Background 2
1.1 Background 2
1.2 Research Problem 4
1.3 Research questions 4
1.4 Aim & objectives 4
1.5 Significance of the study 4
1.6 Delineation 5
1.7 Structure of the thesis 6
Chapter 2 Literature Review 8
2.1 Water Shortages 8
2.2 SA Environmental legislation on industrial wastewater discharge 9
2.3 Mining Wastewater and Composition 10
2.4 Membrane Distillation Crystallisation (MDC) 11
2.4.1 Applications of MDC 13
2.4.1.1 Treatment of brines and salty water 13
2.4.1.2 Treatment of wastewater 13
2.5 Types of Membrane Distillation 14
2.5.1 Direct Contact Membrane Distillation (DCMD) 14

2.5.2 Air Gap Membrane Distillation (AGMD) 14
2.5.3 Vacuum Membrane Distillation (VMD) 14
2.5.4 Sweeping Gas Membrane Distillation (SGMD) 15
2.5.5 Other MD configuration systems 15
2.6 Configurations of MD Modules 18
2.7 Membrane Materials 18
2.8 Membrane Distillation Crystallisation Parameters 19
Modelling of membrane distillation 19
Heat and Mass Transfer 19
a) Heat Transfer 20
b) Mass Transfer 21
2.9 Operative and process parameters affecting transport in MD 23
2.9.1 Temperature 23
2.9.2 Feed concentration 23
2.9.3 Flow rate 24
2.9.4 Fouling 24
2.9.5 Permeate flux 24
2.9.6 Salt Rejection 25
2.9.7 Recovery 25
2.10 Membrane characteristics affecting MDC process performance 26
2.10.1 Polymer type and its intrinsic properties 26
2.10.2 Wetting resistance or Liquid Entering Pressure (LEP) 28
2.10.3 Membrane thickness 31
2.10.4 Membrane pore size and pore distribution 34
2.10.5 Membrane porosity 34
2.10.6 Tortuosity 34
2.10.7 Backing structures 35
2.10.8 Mechanical Strength 36
2.10.9 Cost of production of membranes 36

Chapter 3 Research Methodology 39
3.1 Introduction 39
3.2 Selection of model brines for the study 39
3.2.1 Type 1 brine 39
3.2.2 Type 2 brine 39
3.3 Research Design 41
3.3.1 Experiment 1 41
3.3.2 Experiment 2 43
3.3.3 Experiment 3 44
3.3.4 Experiment 4 45
3.3.5 Experiment 5 46
3.4 Selection of membrane characteristics to be investigated for this study 48
3.5 Experimental procedure 50
3.6 Research Apparatus 53
3.5.1 Equipment 53
3.5.2 Materials 54
Chapter 4 Development of flux model 57
4.1 Introduction 57
4.2 Permeate flux model for Type 1 brine 57
4.2.1 Effect of process parameters on permeate flux for the treatment of Type 1 brine 60
Chapter 5 Results and Discussion 65
5.1 Introduction 65
5.2 Investigating the effect of pore size, Type 1 brine feed concentration and operating feed temperature on MD performance (Experiment 1) 65
5.3 Investigating the effect of scaling/fouling on the performance of MD using commercially available MD membranes for the treatment of prepared Type 1 brine (Experiment 2) 68
5.4 Investigating the effect of pore size, Type 2 brine feed concentration and operating feed temperature on MD performance (Experiment 3) 71
5.4.1 Determining the effect of pore size and feed temperature on the permeate flux for prepared Type 2 brine 72

5.4.2 Investigating the effect of pore size and feed concentration on the permeate flux for prepared Type 2 brine 74

5.5 Investigating the effect of scaling/fouling on the performance of MD for the treatment of prepared Type 2 brine using 0.22 µm and 0.45µm pore size membranes (Experiment 4)..... 76

5.6 Investigating the effect of pore size on the performance of MD using actual industrial brine emanating from an RO process (Experiment 5) 82

Chapter 6 Conclusions and Recommendations 86

6.1 Conclusion 86

6.2 Recommendations 88

Chapter 7 - References 90

Appendices 98

Appendix A 99

Investigating the effect of pore size, Type 1 brine feed concentration and operating feed temperature on MD performance 99

Appendix A.1 101

Appendix A.2 107

Appendix A.3 113

Appendix A.4 119

Appendix A.5 125

Appendix A.6 131

Appendix A.7 137

Appendix A.8 143

Appendix A.9 149

Appendix A.10 155

Appendix B 160

Investigating the effect of scaling/fouling on the performance of MD using commercially available MD membranes for the treatment of Type 1 brine 160

Appendix B.1 162

Appendix B.2 165

Appendix C 167

Investigating the effect of pore size, Type 2 brine feed concentration and operating feed temperature on MD performance 167
Appendix C.1 168
Appendix C.2 172
Appendix C.3 177
Appendix C.4 182
Appendix C.5 187
Appendix C.6 192
Appendix C.7 197
Appendix C.8 202
Appendix C.9 207
Appendix C.10 212
Appendix C.11 217
Appendix C.12 221
Appendix D 225
Investigating the effect of scaling/fouling on the performance of MD using 0.45 µm pore size membrane for the treatment of type Type 2 brine 225
Appendix D.1 226
Appendix D.2 230
Appendix E 232
Investigating the effect of pore size on the performance of MD using actual brine emanating from mining and industrial wastewater 232
Appendix E.1 234
Appendix E.2 237
Appendix F 239
Tank level calibration 239
Appendix G 241
Sample Calculations 241

LIST OF FIGURES

Figure 2-1: Schematic of a typical MDC system (Chan et al., 2005).. 12
Figure 2-2: The four basic MD configurations (a)DCMD, (b) AGMD, (c) SGMD and (d) VMD (Du et al., 2019) 16
Figure 2-3: Membrane distillation Modules (a) Tubular module for hollow fibre, (b) Plate and frame module for flat sheet membrane (Camacho et al., 2013) 18
Figure 2-4: Temperature and pressure profile across MD (Adnan et al., 2012) 19
Figure 2-5: Electrical circuit analogies of resistances in Schofield and DG models (Adnan et al., 2012) 23
Figure 3-1: General configuration of the DCMD experimental set-up 52
Figure 4-1: Normal plot of residuals for Type 1 brine flux model.. 59
Figure 4-2: Predicted values vs Actual values 60
Figure 4-3: Perturbation plot of factor interaction for GVHP membrane for the treatment of Type 1 brine 61
Figure 4-4: 3-dimensional representation of the effect of a variation in the feed temperature and feed concentration on the change in flux for Type 1 brine using the 0.22 µm membrane pore size 62
Figure 4-5: 3-dimensional representation of the effect of a variation in the feed temperature and feed concentration on the change in flux for Type 1 brine using the 0.45 µm membrane pore size 62
Figure 5-1: Change in flux rate with a change in feed temperature at different feed concentration levels for the treatment of Type 1 brine using the 0.22 µm membrane pore size 66
Figure 5-2: Change in flux rate with a change in feed temperature at different feed concentration levels for the treatment of Type 1 brine using the 0.45 µm membrane 66
Figure 5-3: Feed and permeate conductivity as a function of Recovery for (6-hour run, 200 g/L initial TDS) prepared Type 1 brine using 0.22 µm pore size and 0.45 µm pore size membranes 68
Figure 5-4: Effects of concentration on flux rate for the treatment of Type 1 brine 69
Figure 5-5: Effects of feed temperature on flux rate for the treatment of prepared Type 2 brine (Initial feed TDS 11870 mg/L) using a 0.22 µm and 0.45 µm pore size membrane 72
Figure 5-6: Effects of feed concentration and suspended solids for the treatment of prepared Type 2 brine using 0.22 µm (GVHP) and 0.45 µm (HVHP) membrane pore size 74
Figure 5-7: Water recovery and Salt rejection as a function of time for the treatment of Type 2 brine with feed TDS of 27025 mg/L using a 0.22 µm and 0.45 µm pore size membranes......... 75
Figure 5-8: Flux rate and TSS as a function of water recovery for prepared Type 2 brine using the 0.22 µm pore size membrane.. 77

Figure 5-9: Flux rate and TSS as a function of water recovery for prepared Type 2 brine using the 0.45 µm pore size membrane... 78
Figure 5-10: Permeate conductivity and TSS as a function of water recovery for prepared Type 2 brine using the 0.22 µm pore size membrane 79
Figure 5-11: Permeate conductivity and TSS as a function of water recovery for prepared Type 2 brine using the 0.45 µm pore size membrane 79
Figure 5-12: Salt rejection and TSS as a function of water recovery for prepared Type 2 brine using the 0.22 µm pore size membrane 80
Figure 5-13: Salt rejection and TSS as a function of water recovery for prepared Type 2 brine using the 0.45 µm pore size membrane 81

LIST OF TABLES

Table 2-1: Coal mine brine composition (Nathoo et al., 2017) 10
Table 2-2: Uses of most common MD configurations (Kebria & Rahimpour, 2020) 17
Table 2-3: Experimentally determined membrane properties (Nathoo et al., 2017) 28
Table 2-4: Typical commercial flat sheet membranes commonly used in MD (Khayet, 2011) ... 29
Table 2-5: Membrane thickness from various membrane polymers used 32
Table 2-6: Young modulus for different membrane types 36
Table 3-1: NaCl concentration levels investigated 39
Table 3-2: Chemical make-up of synthetic coal mine brine 40
Table 3-3: Chemical make-up of the de-supersaturated synthetic coal mine brine that was treated with RO (stage two RO) 40
Table 3-4: Experimental matrix for Experiment 1 using response surface approach 41
Table 3-5: Type 1 brine NaCl concentration levels used in Experiment 1 42
Table 3-6: Experimental Matrix for Experiment 2 43
Table 3-7: Type 1 brine (NaCl) concentration level used in Experiment 2 43
Table 3-8: Experimental matrix used for Experiment 3 44
Table 3-9: Water analysis data for the actual brine emanating from industrial wastewater used for Experiment 5 46
Table 3-10: Scaling indices for actual brine used in Experiment 5 46
Table 3-11: Merck Millipore GVHP and HVHP membrane characteristics 49
Table 4-1: ANOVA response for the Quadratic model using Design Expert 11 for Type 1 brine 58
Table 5-1: Permeate flux rate of Experiment 2 to determine the effect of scaling/fouling for prepared Type 1 brine 69
Table 5-2: Summary of experimental run results of the prepared Type 2 brine 71
Table 5-3: Summary of Experiment 4 results for scaling/fouling experiments using the prepared Type 2 brine 76
Table 5-4: Results for actual brine after 480 minutes 84
Table A- 1: Membrane specification and initial operating conditions of experimental run 101
Table A- 2: Test number 1 of experimental matrix for Experiment 1 (Run 1) 102
Table A- 3: Test number 1 of experimental matrix for Experiment 1 (duplicate) 103
Table A- 4: Test number 1 of experimental matrix for Experiment 1 (triplicate) 104
Table A- 5: Average experimental flux rate for test number 1 of Experiment 1 105
Table A- 6: Membrane specification and initial operating conditions of experimental run 107
Table A- 7: Test number 2 of experimental matrix for Experiment 1 (Run 1) 108
Table A- 8: Test number 2 of experimental matrix for Experiment 1 (duplicate) 109
Table A- 9: Test number 1 of experimental matrix for Experiment 1 (triplicate) 110

Table A- 10: Average experimental flux rate for test number 2 of Experiment 1 111
Table A- 11: Membrane specification and initial operating conditions of experimental run...... 113
Table A- 12: Test number 3 of experimental matrix for Experiment 1 (Run 1) 114
Table A- 13: Test number 3 of experimental matrix for Experiment 1 (duplicate) 115
Table A- 14: Test number 3 of experimental matrix for Experiment 1 (triplicate) 116
Table A- 15: Average experimental flux rate for test number 3 of Experiment 1 117
Table A- 16: Membrane specification and initial operating conditions of experimental run...... 119
Table A- 17: Test number 4 of experimental matrix for Experiment 1 (Run 1) 120
Table A- 18: Test number 4 of experimental matrix for Experiment 1 (duplicate) 121
Table A- 19: Test number 4 of experimental matrix for Experiment 1 (triplicate) 122
Table A- 20: Average experimental flux rate for test number 4 of Experiment 1 123
Table A- 21: Membrane specification and initial operating conditions of experimental run...... 125
Table A- 22: Test number 5 of experimental matrix for Experiment 1 (Run 1) 126
Table A- 23: Test number 5 of experimental matrix for Experiment 1 (duplicate) 127
Table A- 24: Test number 5 of experimental matrix for Experiment 1 (triplicate) 128
Table A- 25: Average experimental flux rate for test number 5 of Experiment 1 129
Table A- 26: Membrane specification and initial operating conditions of experimental run...... 131
Table A- 27: Test number 6 of experimental matrix for Experiment 1 (Run 1) 132
Table A- 28: Test number 6 of experimental matrix for Experiment 1 (duplicate) 133
Table A- 29: Test number 6 of experimental matrix for Experiment 1 (triplicate) 134
Table A- 30: Average experimental flux rate for test number 6 of Experiment 1 135
Table A- 31: Membrane specification and initial operating conditions of experimental run...... 137
Table A- 32: Test number 7 of experimental matrix for Experiment 1 (Run 1) 138
Table A- 33: Test number 7 of experimental matrix for Experiment 1 (duplicate) 139
Table A- 34: Test number 7 of experimental matrix for Experiment 1 (triplicate) 140
Table A- 35: Average experimental flux rate for test number 7 of Experiment 1 141
Table A- 36: Membrane specification and initial operating conditions of experimental run...... 143
Table A- 37:Test number 8 of experimental matrix for Experiment 1 (Run 1) 144
Table A- 38: Test number 8 of experimental matrix for Experiment 1 (duplicate) 145
Table A- 39: Test number 8 of experimental matrix for Experiment 1 (triplicate) 146
Table A- 40: Average experimental flux rate for test number 8 of Experiment 1 147
Table A- 41: Membrane specification and initial operating conditions of experimental run...... 149
Table A- 42: Test number 9 of experimental matrix for Experiment 1 (Run 1) 150
Table A- 43: Test number 9 of experimental matrix for Experiment 1 (duplicate) 151
Table A- 44: Test number 9 of experimental matrix for Experiment 1 (triplicate) 152
Table A- 45: Average experimental flux rate for test number 9 of Experiment 1 153
Table A- 46: Membrane specification and initial operating conditions of experimental run...... 155

Table A- 47: Test number 10 of experimental matrix for Experiment 1 (Run 1) 156
Table A- 48: Test number 10 of experimental matrix for Experiment 1 (duplicate) 157
Table A- 49: Test number 10 of experimental matrix for Experiment 1 (triplicate) 158
Table A- 50: Average experimental flux rate for test number 10 of Experiment 1 159
Table B- 1: Membrane specification and initial operating conditions of experimental run........ 162
Table B- 2: Test number 1 data for Experiment 2 163
Table B- 3: Membrane specification and initial operating conditions of experimental run........ 165
Table B- 4: Test number 2 data for Experiment 2 166
Table C- 1: Membrane specification and initial operating conditions of experimental run 168
Table C- 2: Test Number 1 data for Experiment 3 (Run1) 169
Table C- 3: Test Number 1 data for Experiment 3 (duplicate).. 170
Table C- 4: Membrane specification and initial operating conditions of experimental run 172
Table C- 5: Test Number 2 data for Experiment 3 (Run1) 173
Table C- 6: Test Number 2 data for Experiment 3 (duplicate).. 174
Table C- 7: Average experimental flux rate for test number 2 of Experiment 3 175
Table C- 8: Membrane specification and initial operating conditions of experimental run 177
Table C- 9: Test Number 3 data for Experiment 3 (Run1) 178
Table C- 10: Test Number 1 data for Experiment 3 (duplicate).. 179
Table C- 11: Average experimental flux rate for test number 3 of Experiment 3 180
Table C- 12: Membrane specification and initial operating conditions of experimental run 182
Table C- 13: Test Number 4 data for Experiment 3 (Run1) 183
Table C- 14: Test Number 4 data for Experiment 3 (duplicate).. 184
Table C- 15: Average experimental flux rate for test number 4 of Experiment 3 185
Table C- 16: Membrane specification and initial operating conditions of experimental run 187
Table C- 17: Test Number 5 data for Experiment 3 (Run1) 188
Table C- 18: Test Number 5 data for Experiment 3 (duplicate).. 189
Table C- 19: Average experimental flux rate for test number 5 of Experiment 3 190
Table C- 20: Membrane specification and initial operating conditions of experimental run 192
Table C- 21: Test Number 6 data for Experiment 3 (Run1) 193
Table C- 22: Test Number 6 data for Experiment 3 (duplicate).. 194
Table C- 23: Average experimental flux rate for test number 6 of Experiment 3 195
Table C- 24: Membrane specification and initial operating conditions of experimental run 197
Table C- 25: Test Number 7 data for Experiment 3 (Run1) 198
Table C- 26: Test Number 7 data for Experiment 3 (duplicate).. 199
Table C- 27: Average experimental flux rate for test number 7 of Experiment 3 200
Table C- 28: Membrane specification and initial operating conditions of experimental run 202
Table C- 29: Test Number 8 data for Experiment 3 (Run1) 203

Table C- 30: Test Number 8 data for Experiment 3 (duplicate)... 204
Table C- 31: Average experimental flux rate for test number 8 of Experiment 3 205
Table C- 32: Membrane specification and initial operating conditions of experimental run 207
Table C- 33: Test Number 9 data for Experiment 3 (Run1) 208
Table C- 34: Test Number 9 data for Experiment 3 (duplicate)... 209
Table C- 35: Average experimental flux rate for test number 9 of Experiment 3 210
Table C- 36: Membrane specification and initial operating conditions of experimental run 212
Table C- 37: Test Number 10 data for Experiment 3 (Run1) 213
Table C- 38: Test Number 10 data for Experiment 3 (duplicate)... 214
Table C- 39: Average experimental flux rate for test number 10 of Experiment 3 215
Table C- 40: Membrane specification and initial operating conditions of experimental run 217
Table C- 41: Test Number 11 data for Experiment 3 (Run1) 218
Table C- 42: Test Number 11 data for Experiment 3 (duplicate)... 219
Table C- 43: Membrane specification and initial operating conditions of experimental run 221
Table C- 44: Test Number 12 data for Experiment 3 (Run1) 222
Table C- 45: Test Number 12 data for Experiment 3 (duplicate)... 223
Table C- 46: Average experimental flux rate for test number 12 of Experiment 3 224
Table D- 1: Membrane specification and initial operating conditions of experimental run 226
Table D- 2: Test Number 1 data for Experiment 4 227
Table D- 3: Membrane specification and initial operating conditions of experimental run 230
Table D- 4: Test Number 1 data for Experiment 4 231
Table E- 1: Membrane specification and initial operating conditions of experimental run........ 234
Table E- 2: Membrane specification and initial operating conditions of experimental run........ 237
Table E- 3: Test Number 2 data for Experiment 5.. 238

LIST OF PHOTOGRAPHS

Photograph 3-1: Commissioned DCMD experimental set-up 55

LIST OF ABBREVIATIONS

AGMD	Air Gap Membrane Distillation
AMD	Acid Mine Drainage
CMB	Coal Mine Brine
CP	Concentration Polarisation
DCMD	Direct Contact Membrane Distillation
DI	Deionised
EC	Electrical Conductivity
EE	Energy Efficiency
LEP	Liquid Entry Pressure
MD	Membrane Distillation
MDC	Membrane Distillation Crystallisation
PE	Polyethylene
PES	Polyether Sulfone
PP	polypropylene
PTFE	Polytetrafluoroethylene
PVDF	Polyvinylidene Fluoride
RO	Reverse Osmosis
RSM	Response Surface Methodology
SA	South Africa
SEM	Scanning Electron Microscopy
SGMD	Sweeping Gas Membrane Distillation
TDS	Total Dissolved Solids
TP	Temperature Polarisation
TSS	Total Suspended Solids
VMD	Vacuum Membrane Distillation
XRD	X-ray diffraction
ZLD	Zero Liquid Discharge

Chapter 1

Introduction

Chapter 1 Introduction and Background

1.1 Background

Due to the rapid increase of the human population and water exploitation, greater environmental awareness on the use and reuse of water is required. There has been a surge in water scarcity among various sectors, such as industry, agriculture, and domestic. Over the last three decades, there have been significant advances in membrane technology, resulting in lower production costs (Balasubramanian, 2013). Membrane technology is progressively becoming the first-line option for various industrial, physical, and chemical processes. Therefore, it is of crucial importance in the water treatment sector of the economies of many nations due to the numerous benefits of membrane separation over thermal technologies (Ashoor et al., 2016).

Saline organic wastewater is one of the most vital targets for wastewater treatment due to its rising trend in many industries such as petroleum, chemical engineering, tanning, pharmaceutical and food (Jiang et al., 2017). The massive generation of rejected water (saline effluent from desalination plants or industry) is usually viewed as a severe environmental risk. In the engineering design of any desalination facility, rejected water disposal is classified as a significant trial and usually appears to be an afterthought (Balasubramanian, 2013) due to extensive application of reverse osmosis (RO) technology. Water recovery in seawater RO operations differs typically from 30-50%, with the remainder rejected (Ji et al., 2010).

Since RO requires large amounts of electrical energy and with the diminishing supply of non-renewable (fossil fuels) resources, the interest in the use of membrane distillation (MD) (the integration of thermal distillation with membrane separation) has grown significantly in recent years. MD can utilise renewable energy such as solar energy (Alsebaeai & Ahmad, 2020).

Membrane Distillation (MD) was patented in 1963 by Bodel (Alsebaeai & Ahmad, 2020). It is a membrane-based, thermally driven separation process whereby only vapour molecules pass through a microporous hydrophobic membrane. It acts as a physical barrier that separates a hot aqueous feed solution from a cold permeate (Alkhudhiri et al., 2012; Camacho et al., 2013). The driving force for membrane distillation is the vapour pressure difference across the membrane, significantly different from other membrane processes driven by the absolute pressure difference (Li et al., 2015). MD has excellent potential to replace conventional desalination processes since it requires lower operating temperatures (~40-60^{o}C) (Ali et al., 2019) and smaller vapour spaces (Taylor et al., 2009).

Crystallisation is a vital separation and purification technology used in numerous industrial processes. Crystal formation is due to the competitive nucleation and growth in supersaturated solutions. Crystallisation utilizing membrane distillation is characterised by laminar conditions that minimise the shear stress, encouraging suitable structured crystalline forms (Ruiz Salmón & Luis, 2018).

Membrane distillation crystallisation (MDC) integrates membrane distillation with crystallisation to recover salts and pure volatile solvents from effluents (Jiang et al., 2017). This integration was first introduced by Drioli and co-workers and could enable nearly complete water recovery and eliminate the secondary disposal problem (Li et al., 2015). MDC is explained when a solution is treated in an MD system. It becomes saturated and then supersaturated with crystals collected in an external crystallizer. In this hybrid separation process, pure solvent and high-quality crystal products are attained simultaneously. In aqueous solution systems, the MDC membrane serves as a mass transfer apparatus to concentrate the aqueous solution by removing the solvent in the vapour phase and as an active surface to generate heterogeneous nucleation (Jiang et al., 2017).

The hydrophobic character of a membrane is of utmost importance to MD. The reason that membranes have been manufactured using polymers such as polypropylene (PP), polytetrafluoroethylene (PTFE) and polyvinylidene fluoride (PVDF) (Curcio & Drioli, 2005). According to studies, PVDF membranes have been widely researched for the use in MD for the treatment of solutions such as isopropanol (Banat et al., 1998), sucrose (Izquierdo-Gil et al., 1999), NaCl (Kimura et al., 1987), HNO_3 (Matheswaran et al., 2007) and hypersaline brine (Nathoo et al., 2017). An investigation for the application of PVDF membranes in desalination for DCMD processes was conducted and showed that little wetting occurred during long term desalination tests (Fan & Peng, 2012).

The effects of membrane characteristics for PVDF membranes such as pore size, membrane thickness, porosity, hydrophobicity, tortuosity and liquid entry pressure (LEP) have been studied for various solutions (Eykens, 2016). Many of these membrane characteristics are yet to be investigated for hypersaline brine solutions using PVDF membranes.

Membrane Distillation Crystallisation is also an attractive wastewater treatment technique because it requires significantly lower operating temperatures (40-60°C) when compared to evaporative crystallisation, thus enabling the efficient use of waste heat streams or renewable energy sources. Furthermore, MDC requires lower hydrostatic operating pressures when compared to reverse osmosis (RO) and can therefore be constructed from less expensive materials.

1.2 Research Problem

Reverse osmosis processes treating mining and industrial wastewater generate unwanted, highly concentrated brine effluent that significantly concerns the environment. Membrane distillation has been identified as a potential solution to treat these effluents successfully. However, the novelty of this application for the treatment of hypersaline brine using PVDF membranes has limited information on the effect of membrane characteristics on the performance of this effluent remediation.

1.3 Research questions

How does the membrane pore size of a PVDF membrane affect an MD system performance?

1.4 Aim & objectives

The research project investigates the applicability of MDC for industrial wastewater treatment with a specific focus on establishing the influence that physical membrane characteristics (specifically pore size) have on the permeate flux rate and fouling/scaling.

The research objectives were as follows:

i. Investigate the effect of different brine types (monovalent and divalent/ trivalent dominant ions) on the salt rejection and permeate flux rate.
ii. Investigate the effect of varying feed temperature and concentration on the salt rejection and permeate flux rate.

1.5 Significance of the study

This project focuses on coalmine wastewater remediation in South Africa, identifying the most suitable membrane properties. The proposed research will benefit the broader knowledge of membrane technology and membrane distillation. This knowledge will assist industrial suppliers and practitioners with invaluable, readily usable information aiming towards a more energy-efficient and sustainable solution, closing a significant technological gap in a cost-effective brine treatment solution towards achieving zero liquid discharge.

1.6 Delineation

This study used PVDF membranes at varying feed concentrations and temperatures to focus on the membrane distillation process's membrane pore size. Simulated hypersaline brackish and coal mining effluent treated by RO and actual industrial brine was used in a pilot-plant setup to evaluate membrane performance and resistance to fouling. All others are delineated.

1.7 Structure of the thesis

This thesis contains six chapters, with a brief introduction as follows:

Chapter 1 includes the introduction and background to this study. The aims and objectives of the research are explained, and the significance of the study is outlined. The research problem and research questions are highlighted.

Chapter 2 gives an in-detail literature study related to the research.

Chapter 3 gives details of the procedures, equipment and apparatus used for data acquisition

Chapter 4 gives results for the development of a flux model using Design Expert 11

Chapter 5 gives the results and discussion regarding each process used and the factors affecting them.

Chapter 6 concludes the research based on the results obtained during experimentation and provides recommendations

CHAPTER 2

Literature Review

Chapter 2 Literature Review

2.1 Water Shortages

Water is fast becoming an endangered resource around the globe caused by increased water demand due to an increase in population, industrialisation, improper treatment and disposal of wastewater, and climate change. An annual increase of 1.5% in water demand is projected for South Africa (SA) (Ochieng et al., 2010).

It is well-known that SA is experiencing a water crisis, implementing water restrictions in the country for the past decade. Over 70% of the water used in rural and urban areas is surface water drawn from rivers, streams, lakes, ponds and springs. SA has also been shown to have a daily water usage per capita greater than the global average. Drought is a natural hazard of South Africa's semi-arid climate and could intensify, resulting in a drought area coverage of up to 90% by 2100. Considering the dependence on natural sources for water and the excessively high consumption with limited supply as well as little to no desalination infrastructure, SA could become a drought-stricken land far before the predictions suggest (Otieno & Ochieng, 2004; Water Research Commission, 2015).

Mining forms a large share of the industry, which has seen a rapid increase since the 1950s. Coal mining forms the largest and most in-demand sector, and the demand continues to increase (Kesieme, 2015). Acid mine drainage (AMD) is a massive problem since water draining from coal and base metal mines often contains sulphuric acid, contaminating freshwater streams and agricultural lands. Also, it is a significant health risk to those consuming the contaminated agricultural products due to its higher heavy metals concentration and very acidic pH levels (Ochieng et al., 2010).

Mining operations on a large and small scale are inherently disruptive to the environment creating immense amounts of waste with long-lasting impacts. Incorrect working practises, and rehabilitation measures account for most environmental degradation during mining activity. Land degradation, soil contamination, air pollution, surface and groundwater pollution are just a few things affected by mining activity (Jhariya et al., 2016).

2.2 SA Environmental legislation on industrial wastewater discharge

The South African government has put in place many laws regarding the preservation of the country's water resources, such as the following:

Section 24 (a) and (b)(1) in the Bill of Rights contained in the Constitution of the Republic of South Africa states that: "Everyone has the right to an environment that is not harmful to their health or well-being, and to have the environment protected, for the benefit of present and future generations, through reasonable legislative and other measures that prevent pollution and ecological degradation" (Republic of South Africa, 1996).

Section 41 (1)(b) of the Constitution of the RSA declares that it is the responsibility of the SA government to secure the well-being of residents of the country (Republic of South Africa, 1996).

The National Water Act (NWA) of 1998 was founded to oversee the responsible usage, development, conservation, and management of South African water resources (WWF-SA, 2016).

2.3 Mining Wastewater and Composition

Mining wastewater typically possesses increased inorganic and organic suspended matter with varying salinity. The general treatment method for mine wastewater is slightly more complex than other types of wastewaters due to the varying feed water composition and the presence of metals.

A large amount of mining wastewater is produced daily during the mining process. Mining industry water usage in Australia accounts for approximately 10% of all the non-agricultural demand and is used for the following (Kesieme, 2015):

- Transporting ore and waste in slurries,
- Mineral separation through a chemical process,
- Centrifugal separation,
- Suppression of dust, and
- Washing and cleaning of equipment.

In a study conducted by Nathoo et al. (2017), the source of a coal mine brine (CMB) specimen was generated from RO coal mine pit water, and a synthetic coal mine brine was created. The composition of the coal mine brine can be seen in Table 2-1.

Table 2-1: Coal mine brine composition (Nathoo et al., 2017)

Species	mg/L
Silicic acid	18.2
Sodium ion$^{(+1)}$	2456
Potassium ion$^{(+1)}$	96.33
Calcium ion$^{(+2)}$	528.42
Magnesium ion$^{(+2)}$	451.74
Iron ion$^{(+2)}$	0.04
Manganese ion$^{(+2)}$	0.09
Copper(II) ion$^{(+2)}$	1.00×10^{-3}
Zinc ion$^{(+2)}$	5.00×10^{-3}
Ammonium ion$^{(+1)}$	4
Barium ion$^{(+2)}$	0.05
Strontium ion$^{(+2)}$	14.95
Chloride ion$^{(-1)}$	481.12
Carbonate ion$^{(-2)}$	39.16
Bicarbonate ion$^{(-1)}$	695.12

Sulfate ion$^{(-2)}$	7413.63
Phosphate ion$^{(-3)}$	0.619
Nitrate ion$^{(-1)}$	4.78
Fluoride ion$^{(-1)}$	1.62

2.4 Membrane Distillation Crystallisation (MDC)

MDC combines an MD unit with a crystalliser. In the MD unit, a microporous hydrophobic membrane is situated between two streams, i.e., a hot feed saline solution and a cold pure water stream (distillate). Due to a vapour pressure difference, water vapour passes through the pores from the feed to the distillate side. The vapour pressure difference is achieved by keeping the feed at a sufficiently higher temperature than the distillate. The saline solution becomes supersaturated because of water evaporation. It flows to a crystalliser where supersaturation is alleviated by crystal formation. MDC allows the use of low enthalpy energy sources. The process is basic, compact and doesn't require costly materials since moderate temperatures and pressure close to atmospheric is sufficient (July 2017).

The advantages of the MDC technique compared to conventional crystallisation techniques, i.e., circulating magma crystalliser, is apparent. In the latter instance, solvent evaporation and solute crystallisation occur in the same region. This causes temperature gradients between the surface and the bulk of the body, which usually compromises the suspension uniformity of the crystalline products. These two phenomena occur in separate reactors in MDC. The solvent evaporation occurs within the MD module and the crystallisation in a separate crystalliser. Additionally, membrane distillation crystallisers operating under forced solution flow conditions are characterised by an axial flux in the laminar regime of the crystallising solution through the membrane fibres. This induces well-organised orientation of the particles, resulting in crystals with improved quality and size distribution, which is significant when crystals need to go through additional treatment or reactions (Curcio & Drioli, 2005).

The warm brine (retentate) flows counter-current to the cold distillate (pure water) in MDC processes (such as in direct contact membrane distillation (DCMD) configuration). A microporous hydrophobic membrane separates the two streams. When the water is removed from the retentate, it increases the concentration supersaturation of various species in the mother liquor—followed by the nucleation and crystal growth within the crystalliser. Ideally, the crystallisation process is controlled where the bulk of crystal formation is isolated to the crystallised to minimise crystal deposition on the membrane since it is highly unfavourable because of deterioration in system performance due to membrane fouling (scaling) and blocking of the membrane pores (Pantoja et al., 2013).

The maximum achievable recovery is limited in an RO process by membrane fouling and scaling at concentrations beyond the maximum antiscalant tolerance levels. Since precipitation within the RO element is to be avoided, MD could be applicable in zero (or near zero) liquid discharge applications seeing as relatively high fluxes can be obtained at salt concentrations higher than are suited for an RO application (Camacho et al., 2013).

This requires proper management of precipitating salts to avoid membrane fouling, which is significantly less detrimental to the membrane, given that the scaling does not occur at elevated pressures as can be observed in an RO process. One way of managing these salts is with MDC. This method has been explored for NaCl and Na_2SO_4 solutions, where it was found that at specific feed concentrations, the flux declines due to crystal formation on the membrane surface. This reduces the membrane's salt rejection characteristics because salts can penetrate the pores. Using MD together with MD crystallisation allows for improved separation of salts from solution, and this concept has the potential to expand into other industries, such as drug development (Camacho et al., 2013).

Figure 2-1 illustrates a typical MDC configuration used to recover the crystalline salts.

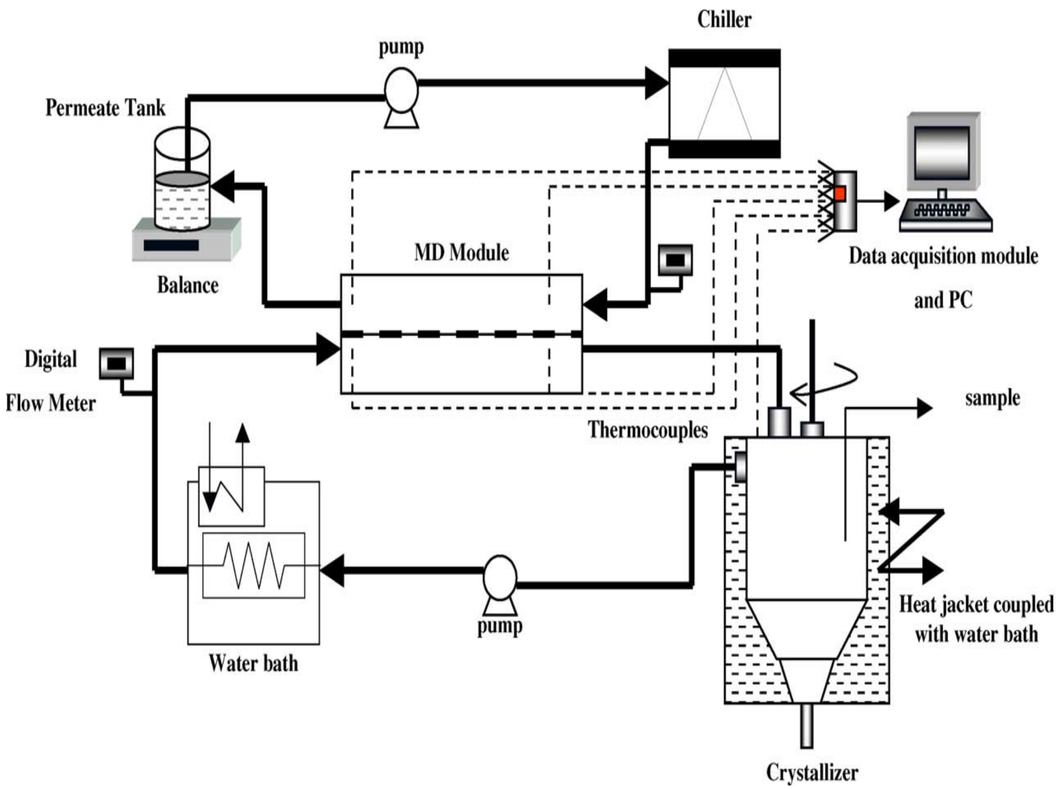

Figure 2-1: Schematic of a typical MDC system (Chan et al., 2005)

Applications of MDC

The large variety of applications offered by the membranes and the future outlook on this technology is that it is promising and a competitive alternative to conventional crystallises for chemical production. The major applications are being developed for the desalination of seawater and brine, wastewater treatment for the recovery of high-purity silver or sodium sulphate, CO_2 capture, nanotechnology, etc. (Ruiz Salmón & Luis, 2018).

2.4.1.1 Treatment of brines and salty water

Since the ideal is water production and brine recovery, brine crystallisation has been advanced recently, and many alternatives have been suggested. A zero salty water discharge using continuous MDC, which combines DCMD with crystallisation, was proposed (Chen et al., 2014). High fluxes over 25 L/m^{2}hr have been obtained (Ruiz Salmón & Luis, 2018). Water and NaCl production were decreased when the permeate flow rate decreased and the permeate temperature increased under the considered study conditions. An increase in feed temperature and flow rate were maximised because of the complex interaction between the MD unit and the crystalliser. High feed flow rates decreased the residence time in the crystalliser and hindered salt crystallisation which reduced the NaCl production. This causes the concentration in the effluent stream to increase, which is recycled, decreasing the water production flux (Ruiz Salmón & Luis, 2018).

2.4.1.2 Treatment of wastewater

MDC emerges as a promising technology to replace, implement or complement currently applied methods which are in many cases technically obsolete or inappropriate for newer application fields. Therefore, an environment is becoming more necessary since industries are forced to adhere to increasingly restricted requirements. New water plants use membrane technology, such as reverse osmosis (RO), instead of conventional technology (Lee et al., 2011). Desalination processes mainly focus on water treatment and not on the disposal of brines and hence becomes a problem since the most straightforward practice is to discharge the waste into the environment (Creusen et al., 2013).

2.5 Types of Membrane Distillation

Four main categories of MD differ on how the permeate is processed (Camacho et al., 2013); however, many new configurations have been investigated recently. Figure 2-2 below illustrates the four basic MD configurations:

2.5.1 Direct Contact Membrane Distillation (DCMD)

The hot and cold fluids contact both sides of the membrane, producing reasonably high flux. Vapour is transferred from the feed side to the permeate side through the membrane's pores based on a vapour pressure difference as a result of the temperature gradient. The vapour condenses in the membrane module. DCMD is best suited for concentrated aqueous solutions and desalination applications (Alkhudhiri et al., 2012). This configuration is the most straightforward configuration regarding design and has a high gained output ratio. However, it has relatively high conductive heat losses and thermal polarization due to the constant contact between the feed side. The membrane on the permeate side and the volatile substances are expected to wet the membrane distillate side because of a slight contact angle with the membrane or a low surface tension (González et al., 2017).

2.5.2 Air Gap Membrane Distillation (AGMD)

The feed fluid is in contact with the membrane, whilst stagnant air exists between the membrane and the condensation surface on the product side. The vapour passes through the air gap and condenses inside the membrane. The flux generated from AGMD is usually low and has the highest energy efficiency due to a decrease in heat transfer from inlet to outlet. It is well suited for most membrane distillation applications but mostly when energy accessibility is low (Alkhudhiri et al., 2012; Osman et al., 2011).

2.5.3 Vacuum Membrane Distillation (VMD)

A pump is used to form a vacuum in the permeate membrane side. The product side of the membrane has air under reduced pressure or vapour, which creates a vacuum that eliminates gas trapped in the pores. It also improves the mass flux. The permeate gas is condensed to form the product. A benefit is that the heat lost by conduction is negligible. VMD is suitable for removing volatiles from an aqueous solution (Alkhudhiri et al., 2012).

2.5.4 Sweeping Gas Membrane Distillation (SGMD)

A cold inert or sweep gas is used to strip the vapour produced on the product side of the membrane. This gas flows to a condenser, where the fluid is collected. The flowing gas reduces the boundary layer resistance, which improves the mass flux. SGMD is well suited for removing volatiles from an aqueous solution (Wang & Chung, 2015).

2.5.5 Other MD configuration systems

Basic configurations of MD have been modified to improve transmembrane fluxes (TMFs) and energy efficiency. Some of these novel configurations included: liquid gap MD (LGMD), material gap MD (MGMD), multi-effect MD (MEMD), vacuum enhanced DCMD (VEDCMD) permeate gap MD (PGMD), vacuum multi-effect MD (V-MEMD), osmotic MD (OMD) and multi-stage MD (MSMD) (Alsebaeai & Ahmad, 2020).

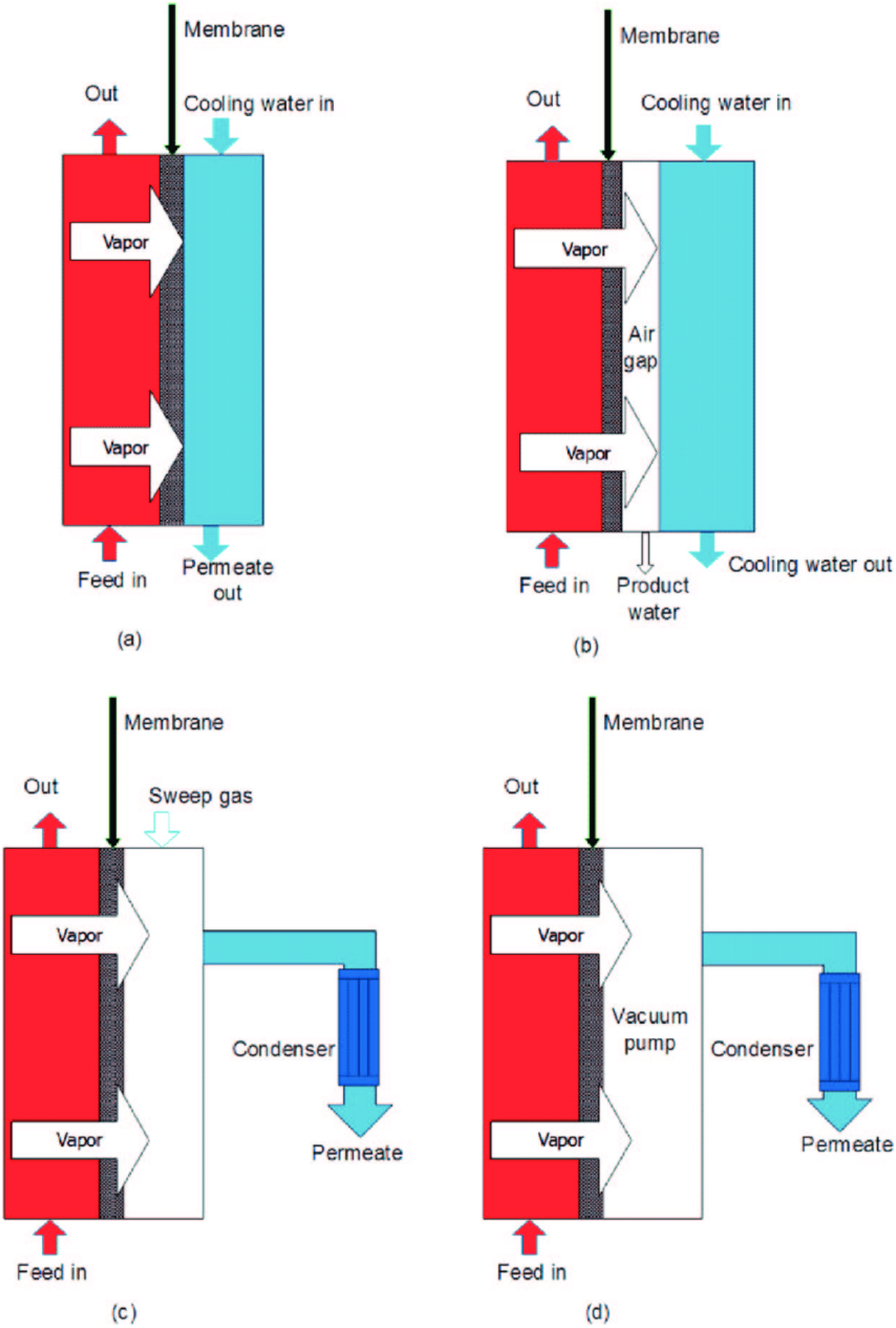

Figure 2-2: The four basic MD configurations (a)DCMD, (b) AGMD, (c) SGMD and (d) VMD (Du et al., 2019)

Table 2-2: Uses of most common MD configurations (Kebria & Rahimpour, 2020)

MD configuration	Application area	Advantages	Disadvantages
Direct contact membrane distillation (DCMD)	• Seawater desalination • Crystallisation • Treatment of dye effluents • Arsenic removal from aqueous solution	• High permeate flux • Considered at commercial scale	• High conductive heat loss
Vacuum membrane distillation (VMD)	• Seawater desalination • Treatment of alcoholic solution • Recovery of aroma compounds • Treatment of textile wastewaters	• High permeate flux • Considered at commercial scale	• High risk of membrane pore wetting • Process complexity
Air gap membrane distillation (AGMD)	• Seawater desalination • The concentration of fruit juices • Separation of azeotropic mixtures • VOC removal	• Low conductive heat loss • Process simplicity • Low risk of temperature polarisation	• Lower flux than DCMD and VMD
Sweeping gas membrane distillation (SGMD)	• Brackish water desalination • Separation of azeotropic mixtures • VOC removal	• Reduction of the barrier to the mass transport through forced flow	• High risk of temperature polarization • Process complexity

2.6 Configurations of MD Modules

The tubular plate and frame modules are the two major MD module configurations. Both of these modules have been implemented in the pilot plant trials. A hollow fibre membrane is fitted in hollow fibre tubular modules. This configuration causes an extremely high packing density (3000m^2/m^3). Due to its large active area and small footprint, hollow fibre modules have great potential in commercial and industrial applications. Plate and frame modules are suitable for flat sheet membranes and can be used for DCMD, AGMD, VMD and SGMD. The packing density is generally about 100-400 m^2/m^3, notably lower than hollow fibre modules. This configuration allows multiple layers of flat sheet MD membranes to increase the effective area and is very easy to construct. This module is widely used in laboratory experiments for testing the influence of membrane properties and process parameters on the flux or energy efficiency of membrane distillation (Camacho et al., 2013)

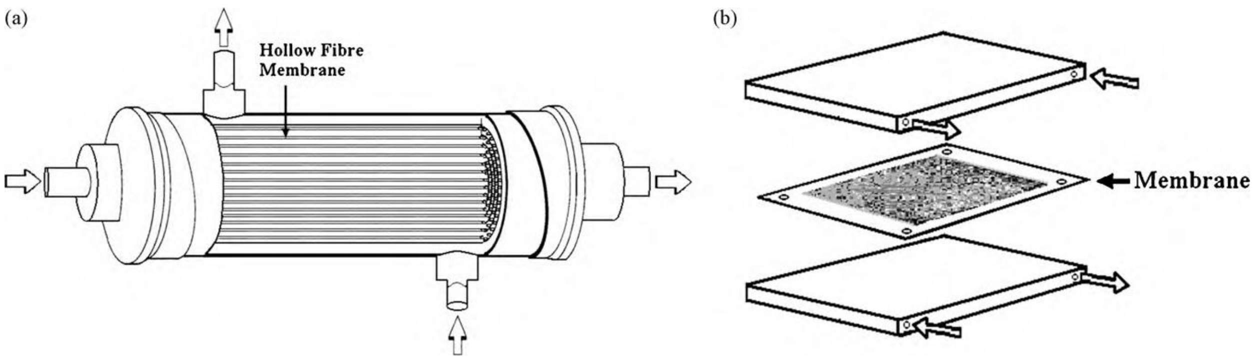

Figure 2-3: Membrane distillation Modules (a) Tubular module for hollow fibre, (b) Plate and frame module for flat sheet membrane (Camacho et al., 2013)

2.7 Membrane Materials

Polytetrafluoroethylene (PTFE), polypropylene (PP) and polyvinylidene fluoride (PVDF) are the most commonly used materials to produce MD membranes. These membranes have a porosity in the range of 0.60 to 0.90. The pore size is in the range of 0.2 to 1.0 µm, and the thickness is 0.04 to 0.25 mm. PTFE has the highest hydrophobicity of the three materials with the most extensive contact angle to the water, decent chemical and thermal stability, and oxidation resistance. However, since it has the highest conductivity, it will cause greater heat transfer through PTFE membranes. PP exhibits good thermal and chemical resistance. PVDF has good hydrophobicity, mechanical strength and thermal resistance (Camacho et al., 2013).

2.8 Membrane Distillation Crystallisation Parameters

The two main underlying phenomena that govern the efficiency of an MDC process are the heat and mass transfer of the system; these are discussed below, along with other parameters that affect an MDC process.

Modelling of membrane distillation

Heat and Mass Transfer

A vapour liquid interface occurs because of the hydrophobic nature of the membranes at every pore. In DCMD, hot brine transported over one side of the hydrophobic membrane creates a surface for vaporization. At the same time, cold permeate is passed on the other side of the membrane, causing condensation of the water vapour. The driving force for water vapour transfer is the difference in water vapour partial pressure due to temperature differences on both sides (Li & Sirkar, 2016). Mass and heat transfer for MD can be divided into five regions as seen in Figure 2-4: the bulk feed, boundary layer, across the membrane, permeate boundary layer and permeate bulk regions. The mass flux, *J* (kg/m^{2}hr), is defined as the ratio of diffusing mass flux to the membrane area (Adnan et al., 2012).

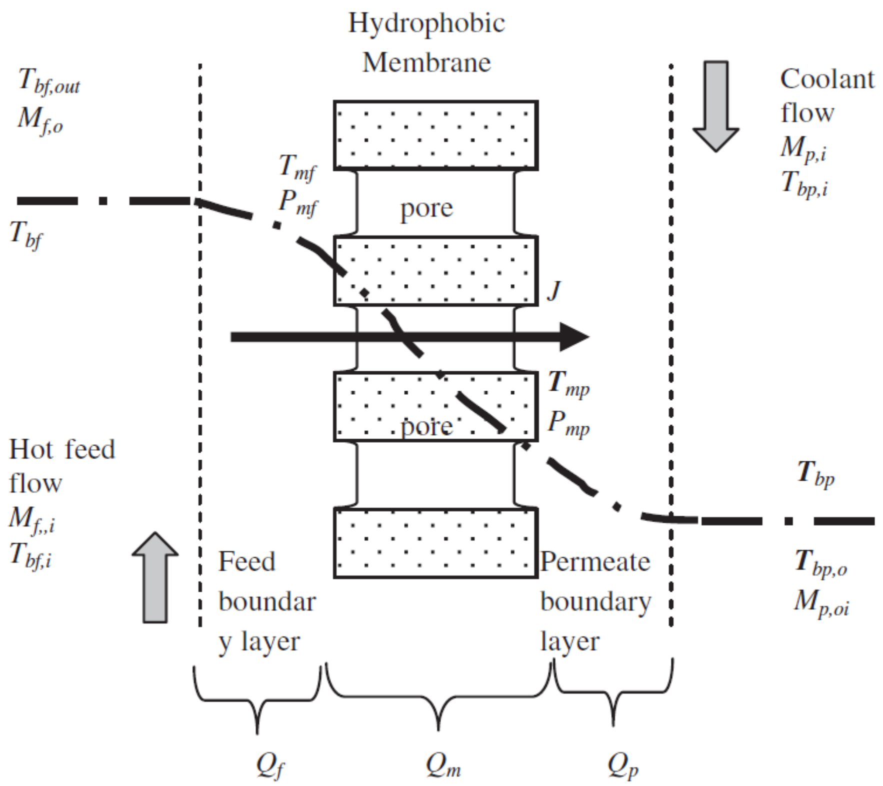

Figure 2-4: Temperature and pressure profile across MD (Adnan et al., 2012)

a) Heat Transfer

Membrane distillation is a non-isothermal process, and two mechanisms coincide to allow heat transfer through the membrane: latent heat and conduction heat transfer (Alkhudhiri et al., 2012). Heat loss due to conduction (Q_c) is caused by a temperature difference on either side of the membrane. The heat required for the evaporation of the vapour molecules associated with flux (Q_N) serves as efficient heat transport. The Energy efficiency (EE) can be calculated by the ratio of the efficient heat due to flux to the total heat flux through the membrane (Eykens et al., 2016).

$$\mathbf{Q_C = \frac{k_m}{\delta}(T_{f,m} - T_{p,m})}$$ **Equation 2-1**

$$\mathbf{Q_N = \Delta H_W N}$$ **Equation 2-2**

$$\mathbf{EE = \frac{Q_N}{Q_N + Q_C}}$$ **Equation 2-3**

Where ΔH_W is the enthalpy of vaporisation of water, $T_{f,m}$ (^oC) and $T_{p,m}$ (^oC) are the interfacial temperatures at the membrane on the brine and permeate side, and k_m is the thermal conductivity of the membrane (Eykens et al., 2016).

The heat transfer in direct contact membrane distillation (DCMD) occurs in three regions (Alkhudhiri et al., 2012; Yun et al., 2006):

Heat transfer by convection in the feed boundary layer:

$$\mathbf{Q_f = h_f(T_f - T_{f,m})}$$ **Equation 2-4**

Total heat transfer through the membrane utilizing conduction and convection due to vapour movement across the membrane and assuming the effect of mass transfer on heat transfer to be ignored (Phattaranawik et al., 2003).

$$\mathbf{Q_m = \frac{k_m}{\delta}(T_{f,m} - T_{p,m}) + J\Delta H_v = h_m(T_{f,m} - T_{p,m})}$$ **Equation 2-5**

Where h_m is the heat transfer coefficient of the membrane. Heat transfer by convection on the permeate boundary layer can be written as:

$$\mathbf{Q_p = h_p(T_{p,m} - T_p)}$$ **Equation 2-6**

Hence, at a steady state, the overall heat transfer flux through the membrane is shown:

$$\mathbf{Q} = \mathbf{Q_f} = \mathbf{Q_m} = \mathbf{Q_p}$$ **Equation 2-7**

$$\mathbf{h_f}\left(\mathbf{T_f} - \mathbf{T_{f,m}}\right) = \frac{\mathbf{k_m}}{\boldsymbol{\delta}}\left(\mathbf{T_{f,m}} - \mathbf{T_{p,m}}\right) + \mathbf{J\Delta H_v} = \mathbf{h_p}(\mathbf{T_{p,m}} - \mathbf{T_p})$$ **Equation 2-8**

$$\mathbf{Q} = \mathbf{U}(\mathbf{T_f} - \mathbf{T_p})$$ **Equation 2-9**

Where U is the overall heat transfer coefficient, notably, the heat conduction can be ignored for non-sported thin membranes as well as for high operating temperatures. Heat transfer by convection is also ignored in MD except for AGMD (Alkhudhiri et al., 2012).

b) Mass Transfer

Mass transfer depends on membrane pore size, porosity, thickness, and other factors. Both feed and permeate solutions directly contact the membrane under atmospheric conditions in DCMD.

There are very important diffusion mechanisms used to describe the total mass transfer in MD. The general form can be seen below:

$$\mathbf{J} = \frac{\mathbf{M}}{\mathbf{RT}}\mathbf{R_i}\boldsymbol{\nabla}\mathbf{p}$$ **Equation 2-10**

Where M is the molecular mass of the volatile component, R is the gas constant, T is the average temperature, R_i is the resistance to mass transport i, and ∇p is the saturated pressure gradient. The pressure gradient is only evaluated across the thickness of the membrane and can be simplified by making ∇p the pressure difference across the membrane (Adnan et al., 2012).

Schofield’s Model and the Dusty Gas Model are the two most appropriate electrical circuit analogies used to model MD's resistance to mass transport. Both models consider the Knudsen, molecular and viscous diffusions; however, they differ in resistance to transport. Viscous and Knudsen diffusions are parallel for both models, but in the DGM, the molecular diffusion’s resistance is in series with the Knudsen diffusion (Adnan et al., 2012).

Mass transport across the membrane occurs in three regions in DCMD. It depends on the pore size and the mean free path of the transferring species: Knudsen region, ordinary-diffusion region and transition region (Qtaishat et al., 2007). The mass transfer mechanisms of DCMD greatly depend on the Knudsen number (K_n) (Li & Sirkar, 2016):

$$\mathbf{K_n} = \frac{\boldsymbol{\lambda_w - a}}{\mathbf{d_p}}$$ **Equation 2-11**

Suppose the mean free path of transporting water molecules exceeds the membrane pore size (Kn>1 or r<0.5λ, where r is pore radius). In that case, the molecule-pore wall collisions are dominant over the molecule-molecule collisions, which will result in Knudsen type of flow prevailing as the mechanism that describes the water vapour migration through the pores of the membrane. The net DCMD permeability can be expressed for this as seen below (Khayet, 2011; Qtaishat et al., 2007):

$$\mathbf{B_m^K} = \frac{2}{3}\frac{\boldsymbol{\varepsilon r}}{\boldsymbol{\tau\delta}}\left(\frac{\mathbf{8M}}{\boldsymbol{\pi}\mathbf{RT}}\right)^{\frac{1}{2}}$$ **Equation 2-12**

Where ε, τ, r and δ are the porosity, pore tortuosity, pore radius and thickness of the hydrophobic membrane, respectively. *R* is the gas constant, and *T* is the absolute temperature.

Air is permanently entrapped within the membrane's pores with pressure values close to atmospheric pressure in a DCMD process. Hence, if $K_n < 0.01$ ($r > 50\lambda$), molecular diffusion describes the mass transport in continuum region caused by stagnant air trapped within each of the membrane pores due to the low solubility of air in water. The following relationship can be used for the net DCMD membrane permeability (Qtaishat et al., 2007):

$$\mathbf{B_m^D} = \frac{\boldsymbol{\varepsilon}}{\boldsymbol{\tau\delta}}\frac{\mathbf{PD}}{\mathbf{P_a}}\frac{\mathbf{M}}{\mathbf{RT}}$$ **Equation 2-13**

Where P_a is the air pressure, *P* is the total pressure inside the pore (assumed to be constant and equal to partial air and water liquid), and *D* is the water diffusion coefficient. The value of the PD (Pa.m^2/s) for water-air can be calculated with the following equation (Qtaishat et al., 2007):

$$\mathbf{PD} = \mathbf{1.895} \times \mathbf{10^{-5}T^{2.072}}$$ **Equation 2-14**

In the transition region, $0.01 < K_n < 1$ ($0.5\lambda < r < 50\lambda$), the molecules of liquid water collide with one another, and diffusion takes place among the air molecules. The mass transport takes place under both the Knudsen and ordinary-diffusion mechanisms, and the following equation determines water liquid permeability (Qtaishat et al., 2007):

$$\mathbf{B_m^C} = \left[\frac{3}{2}\frac{\boldsymbol{\tau\delta}}{\boldsymbol{\varepsilon r}}\left(\frac{\boldsymbol{\pi}\mathbf{RT}}{\mathbf{8M}}\right)^{1/2} + \frac{\boldsymbol{\tau\delta}}{\boldsymbol{\varepsilon}}\frac{\mathbf{P_a}}{\mathbf{PD}}\frac{\mathbf{RT}}{\mathbf{M}}\right]^{-1}$$ **Equation 2-15**

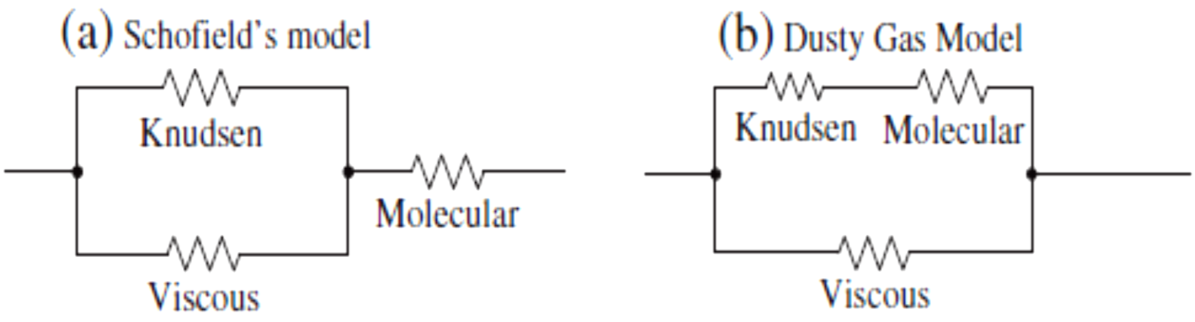

Figure 2-5: Electrical circuit analogies of resistances in Schofield and DG models (Adnan et al., 2012)

2.9 Operative and process parameters affecting transport in MD

2.9.1 Temperature

An increase in feed temperature will result in a greater vapour pressure differential, which, in turn, increases the mass flux through the membrane.

On the other hand, there will be increased heat loss in the system considering conductive heat loss, and the temperature difference is directly proportional. These factors also increase the TP effect (Camacho, et al., 2013).

Conversely, an increase in the permeate temperature will decrease mass flux due to the vapour pressure differential. A decrease in the permeate temperature should have a smaller increase in the flux than an increase in the feed temperature because of the exponential increase in the vapour pressure with temperature.

2.9.2 Feed concentration

Variability in the concentration of solutes in a solvent affects the vapour pressure, which is the salt concentration in water for this study. Raoult's law can be used to approximate the vapour pressure of dilute solutions with Equation 2-16 (Van Ness & Abott, 1999):

$$\mathbf{P^{Sat}} = \mathbf{X_{solv}} \times \mathbf{P^{0}_{solv}} \qquad \textbf{Equation 2-16}$$

Where P^{Sat} is the vapour pressure of the solution, X_{solv} is the mole fraction of the solvent and P^0_{solv} is the vapour pressure of the pure solvent at a particular temperature.

From Equation 2-16, it can be seen that an increase in feed concentration results in a decrease in vapour pressure of the solution and, by extension, a decrease in permeate flux since vapour pressure is the driving force. Furthermore, an increase in feed concentration leads to increased solution viscosity. This would yield a smaller Reynolds number, indicating less turbulent flow and decreasing mass flux.

2.9.3 Flow rate

An increase in feed flow rate decreases the thermal boundary layer, thereby reducing the effect of temperature polarization and improving the mass flux. However, an increase in flow rate also leads to increased hydrostatic pressure, leading to membrane pore wetting if the liquid entry pressure (LEP) is exceeded (Onsekizoglu, 2012). Similarly, an increase in permeate side flow rate reduces the TP effect.

2.9.4 Fouling

Fouling will reduce the effective membrane area and decrease mass flux. Furthermore, due to the reduced flow, there will also be an increase in the temperature polarisation effect. Fouling may also introduce wettability of the pores, thereby allowing solutes to pass through the membrane (Gryta, 2001).

2.9.5 Permeate flux

Permeate flux is defined as the volume of water extracted per unit surface area of the MD membrane. The flux can be calculated according to the following formula (Nathoo et al., 2017):

$$\boldsymbol{Flux = J_v = \frac{Q}{A} = \frac{Volume\ of\ water\ extracted\ (ml) \times \frac{1\ (l)}{1000\ (ml)}}{Membrane\ (m^2) \times Time\ period\ (hr)}} \qquad \textbf{Equation 2-17}$$

Where Q, A and J_v are the volumetric flow rate of permeate (L/hr), the effective area of the membrane (m^2) and the permeate flux respectively.

2.9.6 Salt Rejection

Salt rejection or contaminant removal is defined as the removal of a contaminant from the feed stream by the membrane and is calculated using $\boldsymbol{R}\ (\%) = \mathbf{1} - (\frac{\boldsymbol{EC_{permeate}}}{\boldsymbol{EC_{feed}}})\boldsymbol{\times}\mathbf{100}$

Equation 2-18:

$$\boldsymbol{R}\ (\%) = \mathbf{1} - (\frac{\boldsymbol{EC_{permeate}}}{\boldsymbol{EC_{feed}}})\times\boldsymbol{100} \qquad \textbf{\textit{Equation 2-18}}.$$

Rejection is often presented as a percentage. Membrane distillation aims to remove dissolved salts which is why measuring the system's salt rejection is a good indicator of performance (Aziz & Kasongo, 2019).

$$\boldsymbol{R}\ (\%) = \mathbf{1} - (\frac{\boldsymbol{EC_{permeate}}}{\boldsymbol{EC_{feed}}}) \times \mathbf{100} \qquad \textbf{Equation 2-18}$$

Where $EC_{permeate}$ (µS/cm), EC_{feed} (mS/cm) and R% are the permeate conductivity, feed conductivity and salt rejection, respectively.

2.9.7 Recovery

Recovery is defined as the fraction of the feed water which becomes permeate water. Generally, a high recovery is good but if the recovery rate becomes too high it can cause soluble salts to precipitate and may lead to the occurrence of scaling and fouling (Kucera, 2011).

2.10 Membrane characteristics affecting MDC process performance

The following characteristics are viewed as integral to the performance of MD membranes:

i. **Hydrophobicity** – should be hydrophobic or have at least one hydrophobic layer
ii. **Pore size and porosity** – should be microporous
iii. **Membrane thickness and tortuosity** – should have a low resistance to mass transfer
iv. **Thermal characteristics** – should have low thermal conductivity to prevent heat loss across the membrane and should exhibit good thermal stability in extreme temperatures
v. **Chemical stability** – should have a high resistance to chemicals, such as acids and bases

Hydrophobic microporous membranes initially developed for microfiltration applications are typically used in most commercial MD system applications. However, these membranes are not optimized for the MD process (Eykens 2016, Teoh & Chung, 2009). Consequently, further optimisation of these repurposed membranes specifically for application in an MD process could significantly enhance the MD process.

The membrane type and its characteristics influence the membrane's efficiency and operation. A correlation between trans-membrane flux and membrane characteristics is given by the following relationship (Kullab, 2011):

$$\mathbf{N} \propto \frac{\mathbf{r}^{\mathbf{a}}\boldsymbol{\varepsilon}}{\boldsymbol{\tau}\boldsymbol{\delta}_{\mathbf{m}}} \qquad \textbf{Equation 2-19}$$

Where r is the average pore size for Knudsen diffusion ($a = 1$) or the average squared pore size for viscous flux ($a = 2$), ε is the membrane porosity, τ is the membrane tortuosity, and δ_m is the membrane thickness.

General considerations of typical membrane characteristics are as follows: liquid entering pressure (LEP), membrane thickness, membrane porosity and tortuosity, membrane pore size and distribution, which essentially affect membrane performance and transmembrane flux.

Polymer type and its intrinsic properties

Many membranes applied on a pilot or commercial scale are made of one of the following materials: Polytetrafluoroethylene (PTFE), Polyvinylidene fluoride (PVDF), or polypropylene (PP). The polymers have an excellent wetting resistance due to the low surface tension on the surfaces. Recently, Polyethylene (PE) and modified Polyethersulfone (PES) membranes are becoming common commercial membranes and are currently being explored for their application in MD (Eykens, 2016).

To date, three common types of DCMD membrane configurations are in use, namely hollow fibre, tubular or flat sheet. The membrane is typically made from PP, PVDF, PVDF-PTFE composite material, as a flat sheet or plate, whereas the membrane is usually made from PP, PTFE, and PVDF (Camacho, et al., 2013). The flat sheet configuration has a much smaller contact area than the tubular configuration. Still, it is much easier to construct, clean and perform experiments.

Commercial PE, PVDF and PP membranes showed higher salt retention on the membrane interface (Eykens, 2015). On the scale-up, pilot experiments revealed that salt retention was lower by 1 - 2%. The lower retention of salt was best explained by the fact that there were minor defects in the membrane, which were difficult to prevent in thin electrospun membranes.

One of the fundamental properties is the thermal conductivity of the membrane. The thermal conductivity of the membrane must be low as possible to reduce the heat loss due to the conduction in the membrane wall as presented in $\mathbf{Q_C} = \frac{\mathbf{k_m}}{\boldsymbol{\delta}}(\mathbf{T_{f,m}} - \mathbf{T_{p,m}})$ **Equation 2-1**.

Where Q_c is the heat loss through conduction, d is the membrane thickness, $T_{f,m}$ and $T_{p,m}$ are the feed and permeate temperatures, respectively and k_m is the thermal conductivity of the membrane, which is a property of the structure, porosity, and the intrinsic thermal conductivity of the polymer. Furthermore, a higher mechanical and chemical stability membrane to withstand the Furthermore,

Table

Table

Polymer	**Density (kg/m^3)**	**Surface (x10$^-$**	**Thermal**	**Thermal**	**Melting**	**Contact (˚)**
PTFE	2.16	19.1	0.25	0.29	342	135
PVDF	1.78	30.3	0.17	0.21	165	130
PP	0.91	30	0.11	0.20	160	141

PE	0.92	33.2	0.1	0.3	96	120
PES	1.37	1.37	0.145	0.16	340	140

Material

From

Wetting resistance or Liquid Entering Pressure (LEP)

The wetting resistance or Liquid Entering Pressure (LEP) is the minimum transmembrane pressure required for the feed solution to wet the largest membrane pore size and is a significant membrane characteristic. LEP depends on the maximum pore size and membrane hydrophobicity. It is directly related to feed concentration and the presence of organic solutes, which usually reduce the LEP. The LEP is dependent on both the membrane characteristics and on feed composition and can be estimated by $\mathbf{LEP}= -\mathbf{2b}-\mathbf{B}\boldsymbol{\gamma}_{\mathbf{L}}\mathbf{cos\theta}⬚\mathbf{r}_{\mathbf{max}}⬚ = \boldsymbol{P_f} - \boldsymbol{P_p}$ **Equation 2-20** (Dow, et al., 2008) :

$$\mathbf{LEP} = \frac{-\mathbf{2b}-\mathbf{B}\boldsymbol{\gamma}_{\mathbf{L}}\mathbf{cos\theta}}{\mathbf{r}_{\mathbf{max}}} = \boldsymbol{P_f} - \boldsymbol{P_p}$$ **Equation 2-20**

Where P_f and P_p are the hydraulic pressure on the feed and permeate side, γ_L is the liquid surface tension, θ is the liquid-solid contact angle (liquid surface tension), r_{max} is the maximum pore radius, and B is a geometric pore coefficient determined by pore structure (equal to 1 for cylindrical pores). The impact of salt concentration (NaCl) on the water surface tension was studied and found to be:

$$\boldsymbol{\gamma}_{\mathbf{new}} = \boldsymbol{\gamma}_{\mathbf{i}} + \mathbf{1.467c_f}$$ **Equation 2-21**

Where γ_i is the surface tension of pure water at 25°C (72 mN/m). As a result, membranes with a high contact angle (high hydrophobicity), small pore size, low surface energy, and high surface tension for the feed solution possess a high LEP value (Alklaibi & Lior, 2005).

The effect of pore size on LEP is more evident when a solution of low surface tension is processed. To avoid wetting membrane pores, the pore size must be as small as possible, which contradicts the requirement of higher MD permeability suggesting that the maximum pore size to prevent wetting should be between 0.1 – 0.6 μm (Alkhudhiri, et al., 2012).

Typical LEPs are reported for values of about 5.5 bar. Table 2-3 reports typical values for surface energies for some polymeric materials.

Table 2-4: Typical commercial flat sheet membranes commonly used in MD (Khayet, 2011)

Trade name	**Manufacturer**	**Material**	**Mean pore size (um)**	**LEP_W (kPa)**
TF200	Gelman	PTFE/PP	0.20	282
TF450	Gelman	PTFE/PP	0.45	138
TF1000	Gelman	PTFE/PP	1.00	48
GVHP	Millipore	PVDF	0.22	204
HVHP	Millipore	PVDF	0.45	280
FGLP	Millipore	PTFE/PE	0.20	124
Gore	Millipore	PTFE	0.20	368
Gore	Millipore	PTFE	0.45	288
Gore	Millipore	PRFE/PP	0.20	463

Table 2-4 shows typical commercial flat sheet membranes commonly used in MD along with the characteristics such as material, mean pore size and LEP.

2.10.3 Membrane thickness

(i) Membrane thickness effect on thermal efficiency

Most of the commercially available membranes used in MD have thicknesses ranging from 20 – 200 µm (Wu, 2014). In some cases, the membranes have thicknesses up to 300 µm, although these membranes and their use are not standard. The membrane's thickness gives essential information on both the membrane's mechanical strength and the expected fluxes (Xu & Huang, 1988).

While studies regarding DCMD considered the optimal membrane properties for seawater desalination, few studies have focused on the optimal membrane properties in the high concentration regime; mainly aiming at optimizing the membrane thickness (Field et al., 2013; Ali et al., 2012; Rao, Hiibel, & Childress, 2014; Essahli, 2013).

There is an inversely proportional relationship between the membrane thickness and the permeate flux (Adnan et al., 2012). The permeate flux is reduced as the membrane becomes thicker because the mass transfer resistance increases, while heat loss is reduced as the membrane thickness increases. A theoretical study was conducted relating the effect of membrane thickness to the flux or model equations (Lagana et al., 2000).

The conclusion drawn from this study was that the optimum membrane thickness lies between 30 – 60 µm. Literature addressing membrane thickness is presented in Table 2-5.

Table 2-5: Membrane thickness from various membrane polymers used

Author	Membrane Type	Remarks	NaCl concentration (wt.%)	Feed Conditions
(Gostoli & Sarti, 1987)	PTFE (60 μm) PTFE + air gap (1 cm)	The flux of thin membranes is more affected by salinity	0.3	T_m= 50 ^{0}C ΔT =5-30 ^{0}C V = 0.35 m/s
(Lagana et al., 2000)	PP (120 μm)	Optimal thickness (30 – 60 um)	-	-
(Martinez, 2003)	GVHP (100 μm)	Optimal thickness depending on concentration (10 – 60 um)	0-20	T_f = 40 ^{0}C T_p = 20 ^{0}C V =0.35 m/s
(Wu et al., 2014)	Electrospun PVDF	Optimal δ depending on heat transfer in the channels feed temperature and membrane permeability (10-20 um)	0 – 9	T_f = 45 – 65 ^{0}C T = 20 ^{0}C
(Wu et al., 2014)	Electrospun PVDF (27 – 58 μm)	Optimal δ depending on heat transfer in the channels, feed temperature and membrane permeability (10 – 20 μm)	0 – 9	Tf = 45 – 65 ^{0}C T_p = 20 ^{0}C v = not specified
(Martinez & Maroto, 2008)	GVHP (100 μm), TF200(60 μm)	Asymptotic value for larger δ, sharp decline of energy efficiency at low δ especially at higher concentrations	0 – 20	T_f = 40 ^{0}C T_p = 20 ^{0}C v = 0.35 m/s
(Essahli, 2013)	Electrospun PVDF (144 – 1529 μm)	Asymptotic value for larger δ, decline of energy efficiency at low δ, especially at higher concentrations	0 – 6	T_f = 40 – 80 ^{0}C T_p = 20 ^{0}C v = not specified

A sharp drop in the energy efficiency at low membrane thickness, which was consistent with findings in other bodies of literature was found (Martinez & Maroto, 2008). The membrane thickness is a significant parameter in determining the resistance to mass transfer. Thus, to achieve a high permeability on the membrane, the membrane should be as thin as possible. On the other hand, the better thermal efficiency can be achieved when the membrane is as thick as possible; this is because, in membrane distillation, heat loss by conduction takes place through the membrane matrix as can be seen by $\mathbf{Q_C} = \frac{\mathbf{k_m}}{\boldsymbol{\delta}}(\mathbf{T_{f,m}} - \mathbf{T_{p,m}})$ **Equation 2-1** (Lawson, 1997; Schofield, 1987).

It is generally accepted that the permeability is enhanced by reducing the membrane thickness by increasing the porosity and pore size.

(i) Membrane thickness effect on salinity

Previous studies have also been carried out on the membrane thickness and the salinity of the brine solutions. Some studies have confirmed that thin membranes are more suitable (Lagana et al., 2000; Elssahli, 2013). Also, other studies have indicated that at thicker membrane structures, the membranes perform better at higher salinities.

Salinity plays an integral part in the determination of optimal membrane thickness. Flux is more affected by concentration for thin membranes. The presence of salt reduces the water vapour partial pressure in the feed. With decreasing membrane thickness, the effect of salinity becomes more pronounced. At a specific thickness, reducing the driving force due to temperature polarization and salts counterbalances the increased permeability, resulting in an optimum membrane thickness for flux (Gostoli et al., 1987).

At high salinities, thin membranes can only be used if sufficient driving force is provided. Moreover, thinner membranes are more sensitive to salinity than thicker membranes (Eykens et al., 2016). The transmembrane flux for MD using supported PVDF and PTFE membrane showed that thicker membranes had higher flux in high salt concentration due to decreased temperature polarisation across the membrane. Thus, the thin membranes' flux and energy efficiency are severely reduced with increasing salinity, especially at low-temperature differences and flow velocities (Martinez & Maroto, 2008).

2.10.4 Membrane pore size and pore distribution

Several investigations have focused on a few membranes with most likely variation in membrane pore size (Phattaranawick et al., 2003; Woods et al., 2011). Membranes with pore sizes between 100 nm to 1 µm are usually used in MD systems, upon which the permeate flux increases with increasing membrane pore size. The mass transfer mechanism can be determined based on the membrane pore size and the mean free path through the membrane pores taken by transferred molecules (water vapour). Large pore size is required for high permeate flux, while the pore size should be small to avoid liquid penetration (El-Bourawi, et al., 2006).

Several authors have reported that it would be worthwhile to use mean pore size to determine the vapour transfer coefficient instead of the pore size distribution (Phattaranawick et al., 2003; Martinez, 2003; Imdakm & Matsuura, 2005; Khayet, 2011). A reasonable vapour transfer coefficient when the mean pore size and pore size distribution was used (Martinez, 2003).

2.10.5 Membrane porosity

Membrane porosity refers to the void volume fraction of the membrane (defined as the volume of the pores divided by the total volume of the membrane).

The porosity (ε) can be determined by the Smolder–Franken equation (Khayet & Matsuura, 2001).

$$\boldsymbol{\varepsilon = 1 - \frac{\rho_m}{\rho_{pol}}}$$ **Equation 2-22**

Where ρ_m and ρ_{pol} are the densities of membrane and polymer material, respectively.

Membrane porosity contributes significantly to the flux, temperature polarisation and thermal efficiency (Zhang et al. 2010). The high porosity was favourable for high flux, low-temperature polarisation coefficient (θ) and high thermal efficiency. Membrane porosity in the MD system varies from 30 to 85% (El-Bourawi et al., 2006).

2.10.6 Tortuosity

Tortuosity (τ) is the deviation of the pore structure from the cylindrical shape. As a result, the higher the tortuosity value, the lower the permeate flux (Surapit et al., 2006)

$$\tau = \frac{(2-\varepsilon)^2}{\varepsilon}$$ **Equation 2-23**

A lower tortuosity and higher porosity increase membrane permeability and result in a higher flux for all membrane thicknesses. The energy efficiency is improved for lower tortuosity, higher porosity and lower membrane thermal conductivity. In these cases, the flux is improved. At the same time, heat loss due to conduction is not affected (in the case of tortuosity) or even reduced (porosity and thermal conductivity).

2.10.7 Backing structures

Commercial membranes used in MD have low thicknesses, typically not more than 200 µm. Thus, thinner membranes less than 60 µm are damaged due to low mechanical stability and mechanical defects. A way to remedy this is by using supporting material consisting of nylon or scrim supports (Adnan et al., 2012). In other instances, hydrophobic polymers such as PE or PP are also used for this purpose. However, as the pore size of these nonwoven supports is above 1 µm, the support material is considered to be wetted during the MD operation. Whilst the supporting material adds mechanical strength to the membrane, it also imposes an additional resistance in the process. The role of backing layers has not yet been investigated quantitatively at a larger scale. However, it was noted that backing layers affect membrane structure, especially on the thermodynamic phenomenology (Winter et al., 2013). The addition of support material reduced the flux across the membrane. It was understood that a complex network of thermal resistances is formed by the presence of a backing material, the material itself forming an additional resistance to the heat transfer. The cross-sectional area for diffusion might also be imparted by the backing layers' presence and absence. This results in the additional mass transfer resistance (Mastuura, 2005)

Non-supported membranes had better performance than supported membranes due to the absence of flux blockage at the permeate side and further temperature polarisation by the membrane support material. However, their findings could not be very conclusive of the effect, as their study was limited only to PTFE membranes (Adnan et al.,2012).

To date, few systematic studies have been performed on the optimal properties of the hydrophobic layer in supported composite membranes (Martinez et al., 2008). The influence of the hydrophobic material thermal conductivity can be neglected (Qtaishat et al., 2007).

The properties of the support layer also affect the membrane distillation performance and can be adjusted to increase the membrane performance by (Qtaishat et al., 2007; Su, 2010):

- Reduction of the support thickness to reduce the temperature polarization and increase the flux
- Increased thermal conductivity results in more heat transfer through the wetted support, less temperature polarization, and a higher driving force and flux through the hydrophobic membrane layer.

2.10.8 Mechanical Strength

Membranes exhibit a degree of deformation before fracture. These are evaluated in terms of the stress and strain before fracture. Table 2-6 illustrates the different stress and strain with the corresponding. Young's modulus values for different membrane types (Eykens et al., 2016):

Table 2-6: Young modulus for different membrane types

Membrane	Strain at break (%)	Stress at break (MPa)	Young's modulus (MPa)
PE	21	19.3	81
PES	20	16.5	549
PP	70	1.2	19
PTFE	192	13.2	8
PVDF	19	5.7	156

Routine tests showed that unsupported PP and PTFE membranes needed little stress to deform, thus displaying more strain at breakage and bending. On the other hand, PVDF has a lower break strain, thus requiring much more stress to break the membrane by (Eykens et al., 2016).

2.10.9 Cost of production of membranes

The most commonly used membranes in MD include the stretched PTFE and PE membranes, and the phase invented PVDF and PP membranes. The cost of the membrane depends on several factors, most prominently the method of production. Literature survey has pointed out that the stretching process mainly produces PTFE membranes, making the membrane material much more expensive (Eykens, 2016). In addition, the authors argued that the production of thicker membranes is equally costly. On the other hand, commercially useable PP, PVDF and surface modified PES membranes are produced by isotropic phase inversion. However, literature still lacks clear and conclusive statements on the cost of the membranes.

CHAPTER 3

Research Methodology

Chapter 3 Research Methodology

3.1 Introduction

In this chapter, the details are given regarding equipment and materials and experimental procedures followed during all experimental runs conducted. Descriptions of the instruments used are also included.

All experiments were conducted at the Cape Peninsula University of Technology, Bellville, Chemical Engineering and Chemistry Building.

3.2 Selection of model brines for the study

Two characteristically distinct brines with varying dominant ion valences and scaling propensities (Type 1 and Type 2) were investigated. A description of the characteristics of Type 1 and Type 2 brines is provided below:

3.2.1 Type 1 brine

Type 1 brine was a monovalent ion dominant sodium chloride hypersaline solution with little to no scaling or fouling propensity within the range of water recoveries anticipated using membrane distillation. The NaCl concentration levels investigated can be seen in Table 3-1.

Table 3-1: NaCl concentration levels investigated

Chemicals	Molecular weight (g/mol)	Concentration (mg/L)		
Sodium Chloride (NaCl)	58,44	35 000	50 000	65 000

3.2.2 Type 2 brine

Type 2 brine contained a combination of monovalent and divalent ionic species. As a result of the presence of calcium, magnesium, sulphate and bicarbonate ions, Type 2 brine had a propensity towards scaling/fouling within the range of water recoveries anticipated using membrane distillation.

Both synthetic and actual brine solutions that fell within the classification of Type 2 brine were investigated in this study. The synthetic brine was used to simulate actual brine samples generated from brackish water reverse osmosis (RO) processes associated with industrial and or coal mining applications.

The composition of the synthetic Type 2 brine investigated in this study is shown in Table 3-2 :

Table 3-2: Chemical make-up of synthetic coal mine brine

Chemicals	Molecular weight (g/mol)	Concentration (mg/L)	Feed TDS (mg/L)
Sodium Bicarbonate ($NaHCO_3$)	84,01	687,89	11870
Sodium Sulphate (Na_2SO_4)	142,04	7530,39	
Sulphuric Acid (H_2SO_4)	98,08	834,10	
Magnesium Chloride ($MgCl_2$)	95,21	1585,92	
Calcium Chloride ($CaCl_2$)	110,98	1248,01	

The synthetic Type 2 brine was de-supersaturated using simulation software, and the outputted solution was put through an RO simulation process. The composition of the more concentrated synthetic Type 2 brine investigated in this study is shown in Table 3-3.

Table 3-3: Chemical make-up of the de-supersaturated synthetic coal mine brine that was treated with RO (stage two RO)

Chemicals	Molecular weight (g/mol)	Concentration (mg/L)	Feed TDS (mg/L)
Sodium Bicarbonate ($NaHCO_3$)	84,01	1611,14	27025
Sodium Sulphate (Na_2SO_4)	142,04	17838,98	
Sulphuric Acid (H_2SO_4)	98,07	834,1	
Magnesium Chloride ($MgCl_2$)	95,21	3772,32	
Calcium Chloride ($CaCl_2$)	110,98	2968,56	

3.3 Research Design

During this research, a quantitative research approach was used. A research design was developed to understand better and relate to the aims and objectives outlined in Chapter 2. Experiments 1-5 were used to easily describe the different investigations of the research.

3.3.1 Experiment 1

Experiment 1 aimed to determine the ideal membrane pore size and operating conditions for Type 1 Brine using membrane distillation and was developed using Design Expert 11 software to determine a permeate flux model. This study also aimed to identify the effect of increasing concentration on the performance of the membrane distillation system using the commercially available membrane distillation membranes, $GVHP_{0.22\ \mu m}$ and $HVHP_{0.45\ \mu m}$.

The experimental matrix for Experiment 1 can be seen in Table 3-4 for test numbers 1-10. These experiments allowed a predictive permeate flux model for Type 1 brine to be determined.

Table 3-4: Experimental matrix for Experiment 1 using response surface approach

Test Number	Feed temperature (ºC)	NaCl concentration (g/L)	Membrane	Pore Size (µm)
1	80	65	HVHP	0.45
2	60	35	GVHP	0.22
3	40	65	HVHP	0.45
4	40	50	GVHP	0.22
5	60	50	HVHP	0.45
6	80	35	GVHP	0.22
7	40	35	HVHP	0.45
8	60	65	GVHP	0.22
9	80	35	HVHP	0.45
10	80	50	GVHP	0.22

The process conditions for Experiment 1 were as follows:
Brine used: Prepared Type 1 brine
Brine composition: NaCl-H_2O solution: 35 g/L, 50 g/L, 65 g/L
Temperature: T_{feed} = 40˚C, 60˚C, 80˚C and T_{perm} = 10˚C

Flowrates: F_{feed} = 130 L/hr
Run time: 3 hours

The range of ionic concentrations of the various aqueous species in the Type 1 brine investigated in this study are provided in Table 3-5 below:

Table 3-5: Type 1 brine NaCl concentration levels used in Experiment 1

Chemicals	**Molecular weight (g/mol)**	**Concentration (mg/L)**		
Sodium Chloride (NaCl)	58,44	35 000	50 000	65 000

The preliminary benchmark performance testing on the prepared membranes was to be carried out using a high salinity, >35000 mg/L NaCl-H_2O, solution Type 1 brine to ascertain the effect of varying the selected key membrane characteristic, i.e., pore size had on the membrane distillation performance response variable (membrane flux, water recovery and water purity).

3.3.2 Experiment 2

The aim of Experiment 2 was to determine the effects of scaling/fouling on the performance (focussed on membrane flux, water recovery and water purity) of the MD system using the commercially available MD membranes, $GVHP_{0.22\ \mu m}$ and $HVHP_{0.45\ \mu m}$, for the treatment of Type 1 brine which should theoretically have little to no scaling potential. These experiments were allowed to run for 6 hours at a feed temperature of 60˚C, and volume readings were taken at 30-minute intervals. The experimental matrix for Experiment 2 can be seen in Table 3-6 below:

Table 3-6: Experimental Matrix for Experiment 2

Test Number	Feed temperature (ºC)	NaCl concentration (g/L)	Membrane	Pore Size (µm)
1	60	200	GVHP	0.22
2	60	200	HVHP	0.45

Since the solubility of NaCl in water is approximately 360 g/L, an initial feed TDS concentration below the solubility level was selected to be tested in order to determine whether a very high concentration would result in fouling. It was for this reason that an initial feed TDS of 200g/L was selected as seen in Table 3-7.

Table 3-7: Type 1 brine (NaCl) concentration level used in Experiment 2

Chemicals	Molecular weight (g/mol)	Concentration (mg/L)
Sodium Chloride (NaCl)	58,44	200 000

The process conditions for Experiment 2 were as follows:

Brine used: Prepared Type 1 brine

Brine composition: NaCl-H_2O solution: 200 g/L

Temperature: T_{feed} = 60˚C and T_{perm} = 10˚C

Flowrates: F_{feed} = 130 L/hr

Run time: 6 hours

3.3.3 Experiment 3

Experiment 3 aimed to determine the ideal membrane pore size and operating conditions for Type 2 Brine using MD under specific operating conditions of feed temperature and feed water concentration for prepared brine. This study also aimed to identify the effect of increasing concentration on the performance of the membrane distillation system using the commercially available membrane distillation membranes, $GVHP_{0.22\ \mu m}$ and $HVHP_{0.45\ \mu m}$.

The process conditions for Experiment 3 were as follows:
Brine used: Prepared Type 2 brine
Brine composition: The prepared Type 2 brine studied is shown in Table 3-2 and Table 3-3.
Feed TDS concentrations of prepared Type 2 brines: 11870 mg/L and 27025 mg/L
Temperature: T_{feed} = 40°C, 60°C, 80°C and T_{perm} = 10°C
Flowrates: F_{feed} = 130 L/hr
Run time: 3 hours

The experimental matrix used for Experiment 3 is shown in Table 3-8:

Table 3-8: Experimental matrix used for Experiment 3

Test Number	Pore Size (µm)	Feed Temperature (°C)	Product Temperature (°C)	ΔT (°C)	Feed and product flow rate (L/hr)	Synthetic brine concentration (mg/L)
1	0,22	40	10	30	130	11870
2	0,45	40	10	30	130	11870
3	0,22	60	10	50	130	11870
4	0,45	60	10	50	130	11870
5	0,22	80	10	70	130	11870
6	0,45	80	10	70	130	11870
7	0,22	40	10	30	130	27025
8	0,45	40	10	30	130	27025
9	0,22	60	10	50	130	27025
10	0,45	60	10	50	130	27025
11	0,22	80	10	70	130	27025
12	0,45	80	10	70	130	27025

3.3.4 Experiment 4

The aim of Experiment 4 was to determine the effects of scaling/fouling on the performance (focussed on membrane flux, water recovery and water purity) of the membrane distillation system using the commercially available MD membranes, $GVHP_{0.22\ \mu m}$ and $HVHP_{0.45\ \mu m}$, for the treatment of prepared Type 2 brine. These experiments were allowed to run for as long as a volume reading could be taken.

TSS (total suspended solids) concentration was measured during these experiments to determine the level at which the suspended solids concentration in the solution would have a majorly detrimental effect on overall system performance. Theoretical TSS was also calculated using OLI Stream Analyzer (2012) software.

The process conditions for Experiment 4 were as follows:
Brine used: Prepared Type 2 brine
Brine composition: The prepared Type 2 brine investigated in this study is shown in .
Feed TDS concentrations of prepared Type 2 brines: 27025 mg/L
Temperature: T_{feed} = 60˚C and T_{perm} = 10°C
Flowrates: F_{feed} = 130 L/hr

3.3.5 Experiment 5

Experiment 5 aimed to determine the ideal membrane pore size and operating conditions for Type 2 brine using MD under specific operating conditions of feed temperature and feed water concentration for brine emanating from mining and industrial wastewater. This study also aimed to identify the effect of increasing concentration on the performance of the membrane distillation system using the commercially available membrane distillation membranes, $GVHP_{0.22\ \mu m}$ and $HVHP_{0.45\ \mu m}$.

As can be seen from the water analysis provided in Table 3-9, the water is classified as Type 2 brine because it contains monovalent and divalent species. The scaling indices for the actual brine can be seen in Table 3-10 which indicates that the actual brine has high scaling tendencies.

Table 3-9: Water analysis data for the actual brine emanating from industrial wastewater used for Experiment 5

Component	Concentration (mg/L)
Ca^{2+}	98,01
Mg^{2+}	107,93
Na^{+}	1131,28
K^{+}	25
Fe^{3+}	0,79
Mn^{2+}	0,79
SO_4^{2-}	424,58
Cl^{-}	1793,54
HCO_3^{-}	263,09
CO_3^{2-}	1,75
CO^{2}	0,84

Table 3-10: Scaling indices for actual brine used in Experiment 5

Scalant Type	(%)
$CaCO_3$	121,64
$Fe(OH)_3$	920,58
$Mn(OH)_2$	306,86

The process conditions for Experiment 5 were as follows:

Brine used: Actual industrial brine

Temperature: T_{feed} = 60˚C and T_{perm} = 10ºC

Flowrates: F_{feed} = 130 L/hr

Run time: 3 hours

3.4 Selection of membrane characteristics to be investigated for this study

By and large, the selection criteria for the membrane characteristics investigated for this study was based on the literature review in Chapter 2. The information collected helped identify the most crucial membrane characteristics to be investigated and the possible ranges to consider.

PVDF membranes were selected for this study because they have been widely used in previous studies and have shown good hydrophobic tendencies. More knowledge regarding the applicability of PVDF membranes for the treatment of hypersaline industrial brine is needed as well as determining the ideal membrane characteristics for this effluent.

A summary of the key findings can be seen below:

Hydrophobic membranes initially developed for microfiltration applications are typically used in most commercial MD system applications. Most of the membranes used recently have good hydrophobicity. Many polymer materials used, such as PVDF, PP, PTFE, PE, and PES, have excellent wetting resistance due to the surface's low surface tension (Eykens, 2016). All of these polymers yield high contact angle within the range of 120-140˚ which is very significant on the hydrophobicity (Lafuma & Quéré, 2003).

An inverse relationship was identified between membrane thickness and permeate flux. The membrane thickness gives important information on both the mechanical strength, heat conductivity and the fluxes to be expected. Whilst decreasing the thickness yields high permeability, increased thickness leads to better heat efficacy. It is generally accepted that the permeability is enhanced by reduction in the membrane thickness, by increasing the porosity and pore size. Many of the commercially available membranes used in MD have a thickness ranging 20-200 µm (Wu et al., 2014). A safe range for membrane thickness of 100-150 µm was selected so as to achieve high fluxes whilst still considering mechanical strength and structural integrity of the membranes used.

Membrane pore sizes between 100 nm to 1 µm are usually used in MD systems, upon which the permeate flux increases with increasing membrane pore size. Typical commercial flat sheet membranes commonly used and studied range between 0.1 µm to 1 µm. The maximum pore size to prevent wetting should be between 0.1 – 0.6 µm. Large pore size is required for high permeate flux, while the pore size should be small to avoid liquid penetration. A safe and reasonable range for pore size should be determined for use in MD systems treating different types of brines Alkhudhiri et al., 2012).

Membrane porosity greatly contributes to the flux, temperature polarisation and thermal efficiency. The high porosity was favourable for high flux, low-temperature polarisation coefficient (θ) and high thermal efficiency (Zhang et al., 2012). Membrane porosity in the MD system varies from 30 to 85%. However, most studies aim towards the upper end of the range whilst still taking caution in not compromising the structural integrity of the membrane due to the large packing volume of the pores of the membrane (El-Bourawi et al., 2006).

The characteristics of the GVHP and HVHP membranes are provided in Table 3-11 below.

Table 3-11: Merck Millipore GVHP and HVHP membrane characteristics

Supplier	Merck Millipore	
Membrane Name	GVHP	HVHP
Max operating temp (ºC)	85	85
Pore size (µm)	0,22	0,45
Porosity (%)	75	75
Thickness (µm)	125	125
Polymer type	PVDF	PVDF

The GVHP and HVHP membranes provided a good balance between selecting membranes that are representative of those readily available on a commercial scale and being used for membrane distillation, whilst simultaneously also meeting the criteria of having a large enough differential in pore size between the two membranes which was central to achieving the objectives of this study.

3.5 Experimental procedure

The general configuration of the DCMD experimental set-up used for all experiments can be seen in Figure 3-1.

The feed and product temperatures were set to the required temperatures at the entrance to the membrane module. These had to be controlled indirectly by adjusting the heat exchanger temperatures.

Before switching on the experimental apparatus, the valves to the membrane module were closed for both the feed and product sides. Four litres of the sample solution were prepared and poured into the feed tank. The conductivity probe was submerged into the solution. The product tank was then filled with sufficient deionised water to submerge the conductivity probe.

The circulating temperature control systems for each side of the membrane module, i.e., feed and permeate side, were switched on and set to the required temperatures. The pump speed was set to the maximum pump flow rate of 25 L/min to achieve the highest heat transfer rate.

The membrane was installed into the module with two rubber gaskets/O-rings to keep the membrane in place and seal the system.

When the tanks had reached the required operating temperatures, the valves to the membrane module were opened, and the pumps switched on. The system was given sufficient time to stabilise before data logging was initiated as the circulating lines and membrane module temperature had to reach the required temperature. During this time, the inlet temperature for both the feed (T_1) and product (T_3) side into the membrane module was monitored to ensure they were at the required temperatures for the specific runs. The heat exchanger temperatures were adjusted accordingly if T_1 and T_3 were not at the required level.

Change in volume was obtained by recording the tank level readings every 10-minutes for the first 180-minute of a run and subsequently 30 minutes or 1-hour intervals for runs extending beyond 180-minutes in duration.

This was done by stopping the pumps briefly, recording the level and switching the pumps on again. For instances where the level readings could not be obtained at a specific sampling time for whatever reason during any of the experimental runs, these were omitted from the average flux calculated for each experimental run and marked with a dash symbol in the raw data.

All experiments had a duration of 3 hours except for the effect of fouling experiments conducted on Type 1 and Type 2 brine. As stated in the Research Design, these experiments were run for a more extended period.

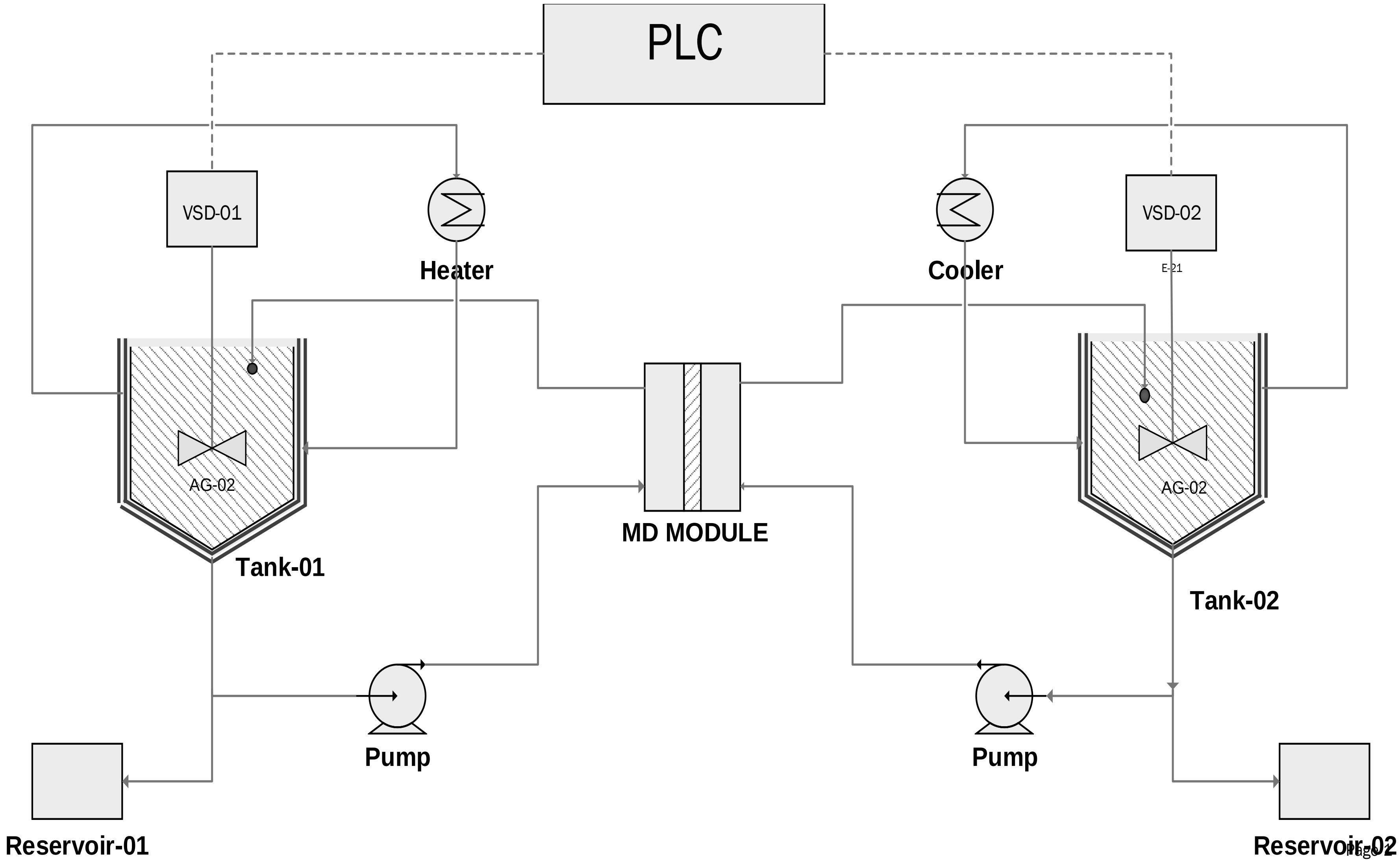

Figure 3-1: General configuration of the DCMD experimental set-up

Research Apparatus

3.5.1 Equipment

The following apparatus and equipment were used for all the experiments:

- **Peristaltic pumps**

Watson-Marlow 620S peristaltic pumps were used on both the feed and product side to pump the solution to and from the jacketed tank and membrane unit.

- **Overhead agitators**

The overhead agitators were used to ensure the solutions in the feed and product side were well mixed and to keep a constant rpm during the process.

- **Multimeter**

The multimeter was used to measure EC, TDS and tank temperature.

- **Heating and cooling thermostats**

A Lauda RP 845 was used to cool and maintain the desired temperature for the product side solution

A Lauda RE 420 Eco Silver was used to heat and maintain the desired temperature for the product side.

A 4 L jacketed crystalliser with level indicator was used on the feed side to crystallise out any salts from solution and record changes in the feed volume. It can be seen in Photograph 3-1 labelled [1].

- **4 L jacketed reactor with level indicator**

A 4L jacketed reactor with level indicator was used on the product side to hold and recirculate cold permeate to cool the membrane at the module. The level indicator was used to record changes in the permeate volume. It can be seen in Photograph 3-1 labelled [2].

- **MD module unit with thermocouples**

The MD module was used to hold the membrane in place and the thermocouples measured the temperatures of the solutions at the entry and exit for the feed and product sides of the module. The level indicator was used to record changes in the permeate volume. It can be seen in Photograph 3-1 labelled [3].

3.5.2 Materials

The following consumables were used during experiments

- $NaCl$
- $NaHCO_3$
- Na_2SO_4
- H_2SO4
- $MgCl_2$
- $Ca(OH)_2$

Photograph 3-1: Commissioned DCMD experimental set-up

Chapter 4

Development of flux model

Chapter 4 Development of flux model

4.1 Introduction

The Design Expert 11 software was used to analyse the measured response of permeate flux of NaCl.$H_2$0 solution at varying feed concentrations (35, 50 and 65 g/l), feed temperatures (40 ˚C, 60 ˚C and 80˚C) and membrane pore sizes (0,22 µm and 0,45 µm). A response surface methodology approach was used, and a quadratic model was seen to show the best fit for the data. The experimental matrix used for Experiment 1 as seen in Table 3-4 was applied for the development of the permeate flux model.

4.2 Permeate flux model for Type 1 brine

The significance test for the regression models and individual model coefficients was determined for all responses using the statistical software package, ANOVA. The analysis of variance for the flux quadratic model can be seen in Table 4-1 and shows the significant model terms affecting the flux decline.

R^2 and adjusted R^2 values were also presented which indicated the degree of fit, defined as the ratio of the explained variation to the total variation. The analysis suggested a good model fit should be for a R^2 of at least 0.9854. The adjusted R^2 value was found to be 0.9900, a difference of less than 0.2, suggesting that this quadratic model was a good fit for the data.

The P-value is lower than 0.05 which means the model term is significant. An F-value of 358.07 implies the model is significant since there is only a 0.01% chance that an F-value this large could occur due to noise. According to the model, feed temperature is significant and has the greatest influence on the response i.e., permeate flux.

Table 4-1: ANOVA response for the Quadratic model using Design Expert 11 for Type 1 brine

Source	Sum of squares	df	Mean Square	F-value	P-value	
Model	11838,20	8,00	1479,78	358,07	<0,0001	Significant
A- Feed temperature (˚C)	9583,73	1,00	9583,73	2319,06	<0,0001	
B- Concentration (g/L)	11,15	1,00	11,15	2,70	0,1154	
C- Membrane pore size (µm)	4,62	1,00	4,62	1,12	0,3024	
AB	0,55	1,00	0,55	0,13	0,7185	
AC	20,22	1,00	20,20	4,89	0,0383	
BC	3,93	1,00	3,93	0,95	0,3407	
A2	223,04	1,00	223,04	53,97	<0,0001	
B2	7,75	1,00	7,75	1,88	0,1853	
Residual	86,78	21,00	4,13			
Lack of fit	13,86	1,00	13,86	0,065		Not significant
Pure Error	72,92	20,00	3,65			
Cor Total	11924,99	29,00				

Source	Adjusted R^2	Predicted R^2
Quadratic	0,99	0,9854

Equation 4-1 below shows the final model in terms of coded factors. A represents the feed temperature (ºC), B represents the feed concentration (g/L), and C represents the pore size (µm).:

$$\mathbf{flux = 22.55 + 22.98A - 0.7837B + 0.4363C - 0.2046AB + 1.05AC + 0.4652BC + 6.26A^2 + 1.17B^2} \quad \textbf{Equation 4-1}$$

Final equations in terms of actual factors can be seen for each pore size investigated. For Equation 4-2 and Equation 4-3, T represents the feed temperature (˚C), and C represents the feed concentration (g/L):

$$\mathbf{flux_{GVHP,0.22} = 27.81439 - 0.748949T - 0.561393C - 0.000682TC + 0.015660T^2 + 0.005191C^2}$$ **Equation 4-2**

$$\mathbf{flux_{HVHP,0.45} = 19.25581 - 0.643455T - 0.499364C - 0.000682TC + 0.015660T^2 + 0.005191C^2}$$ **Equation 4-3**

The equation in terms of actual factors can be used to make predictions about the response for given levels of each factor. Here, the levels are specified in the original units for each factor. The coded equation, Equation 4-1, was useful for identifying the relative impact of the factors by comparing the factor coefficients.

The permeate flux data obtained from running the test runs were evaluated by plotting the normal probability (%) against the externally studentized residuals as seen in Figure 4-1 below. The linear line of fit observing the relationship between normal probability and externally studentized residuals is appropriate. A good fit means that no response transform was required, and the normality of the data did not experience any specious problem.

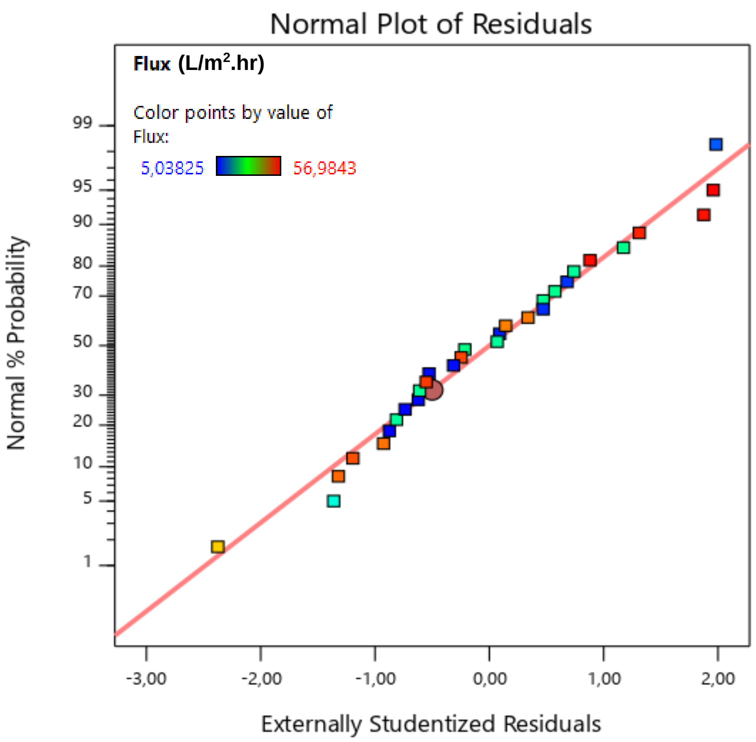

Figure 4-1: Normal plot of residuals for Type 1 brine flux model

The relationship between the actual and the predicted values are shown in Figure 4-2, which indicates that the developed model was acceptable for the prediction of permeate flux since the predicted values were very close to the actual experimental values.

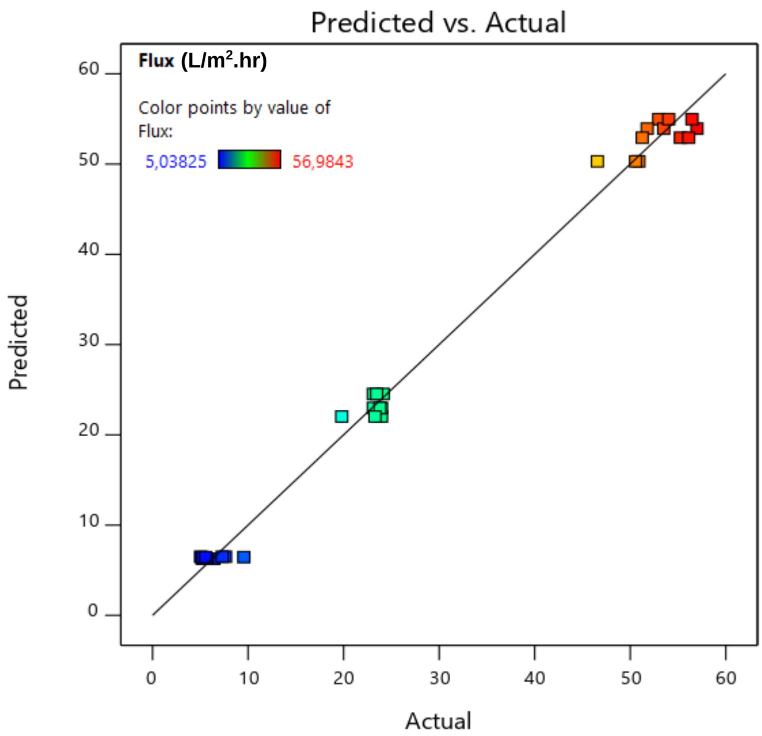

Figure 4-2: Predicted values vs Actual values

4.2.1 Effect of process parameters on permeate flux for the treatment of Type 1 brine

The purpose for predicting the permeate flux was to develop a model, to assist in the selection of a suitable range for process optimisation. The permeate flux observed during DCMD was directly related to the process parameters investigated, providing some interaction effect.

Figure 4-3 shows a perturbation plot displaying the effect of concentration and feed temperature on permeate flux for 0.22 µm pore size membranes.

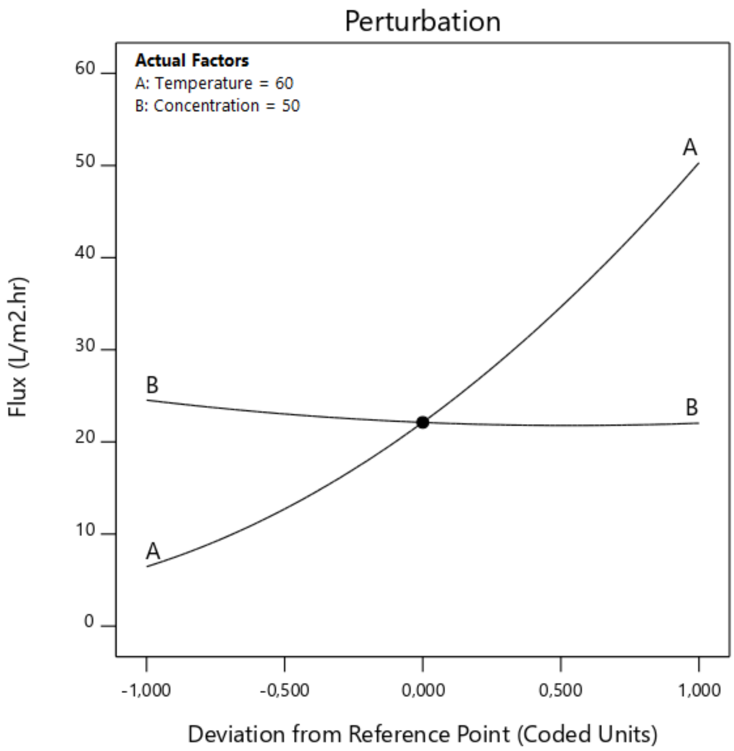

Figure 4-3: Perturbation plot of factor interaction for GVHP membrane for the treatment of Type 1 brine

A perturbation plot allowed for a comparison of the effect of factors at a certain point in the design space, however it does not show the effect of interactions of the factors. The points selected to represent factors A and B in Figure 4-3 is feed temperature at 60ºC and feed concentration at 50 g/L, respectively. Factor C represents the pore size of the membrane used ($GVHP_{0.22\ \mu m}$). The primary factor that affected the permeate flux for Type 1 brine when using MD, appeared to be feed temperature. The effect of concentration was not significant according to the perturbation plot above.

Figure 4-4 and Figure 4-5 below give a 3-dimensional representation, showing the effect of a variation in feed temperature and feed concentration on the change in flux, for the treatment of Type 1 brine for the 0.22 µm and 0.45 µm membrane pore sizes respectively.

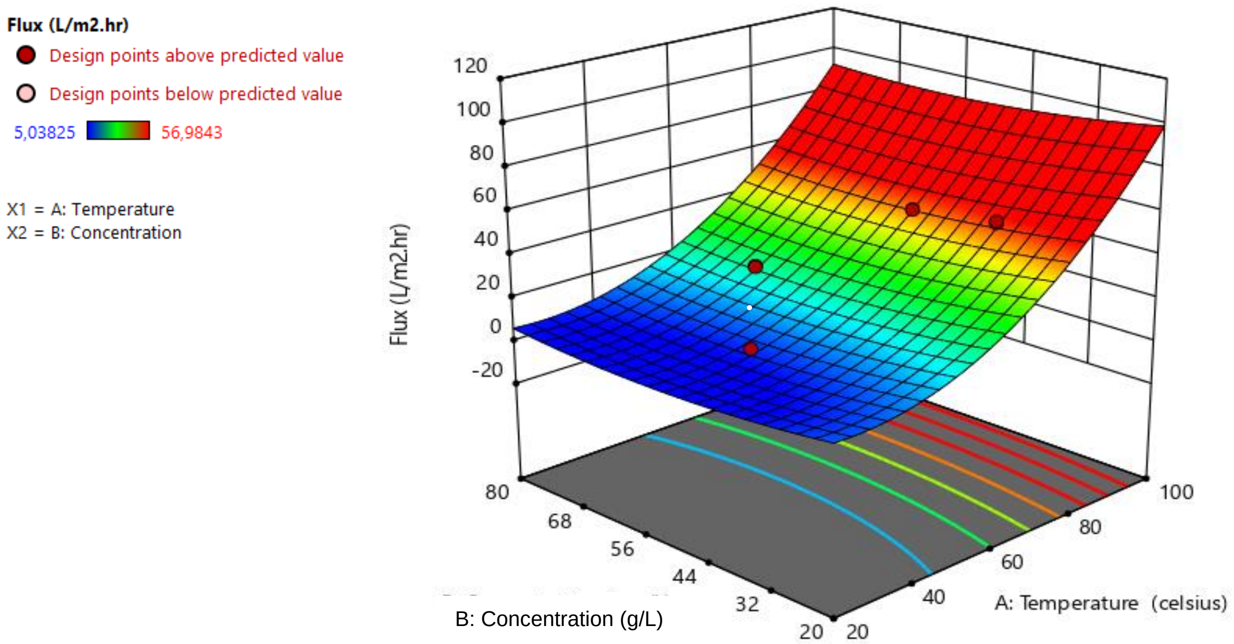

Figure 4-4: 3-dimensional representation of the effect of a variation in the feed temperature and feed concentration on the change in flux for Type 1 brine using the 0.22 µm membrane pore size

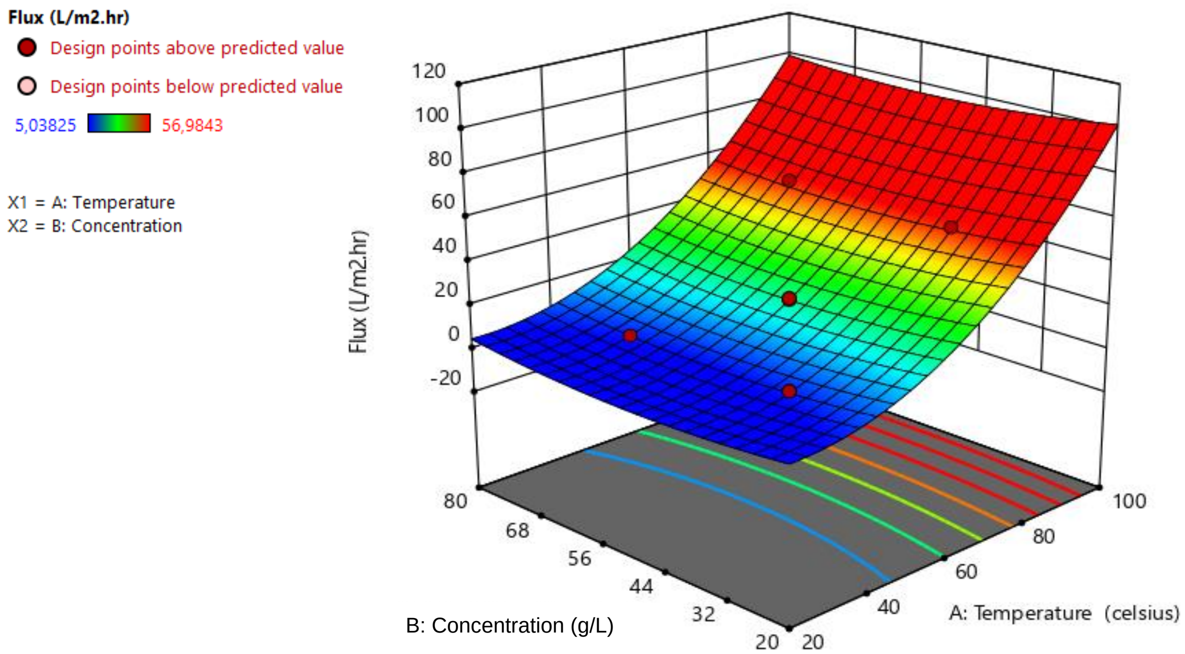

Figure 4-5: 3-dimensional representation of the effect of a variation in the feed temperature and feed concentration on the change in flux for Type 1 brine using the 0.45 µm membrane pore size

The 3-dimensional plots clearly showed that an increase in feed temperature results in an increase in permeate flux whereas increasing feed concentration has little to no effect on the permeate flux. This trend was observed for both the 0.22 µm and 0.45 µm membrane pore sizes for the treatment of Type 1 brine.

Chapter 5

Results and Discussion

Chapter 5 Results and Discussion

5.1 Introduction

The results presented in this chapter were split according to the different types of brine used i.e., Type 1 brine and Type 2 brine, and explained in the order established by the research design in Chapter 3. Many of the results shown in this study was obtained as average values from repeated experiments.

The effect of pore size with a change in feed temperature and feed concentration was investigated for Type 1 and Type 2 brine on MD system performance and membrane scaling.

5.2 Investigating the effect of pore size, Type 1 brine feed concentration and operating feed temperature on MD performance (Experiment 1)

The experimental matrix seen in Table 3-4 was used to determine experimental data. The same data used for the development of the permeate flux model in Chapter 4 was also used to determine the findings of Experiment 1.

Figure 5-1 and Figure 5-2 show the permeate flux versus feed temperature at different concentration levels of each test run conducted for the treatment of Type 1 brine using 0.22 μm and 0.45 μm pore size membranes respectively. Raoult's Law was used to determine the vapour pressure driving force at the different feed concentrations and feed temperatures for the prepared NaCl Type 1 brine (Van Ness & Abott, 1999). The data point, presented at 65 g/L feed concentration and 60˚C feed temperature in Figure 5-1, is significantly lower and deviates from the observed trend hence it can be stated that it was an outlying data point.

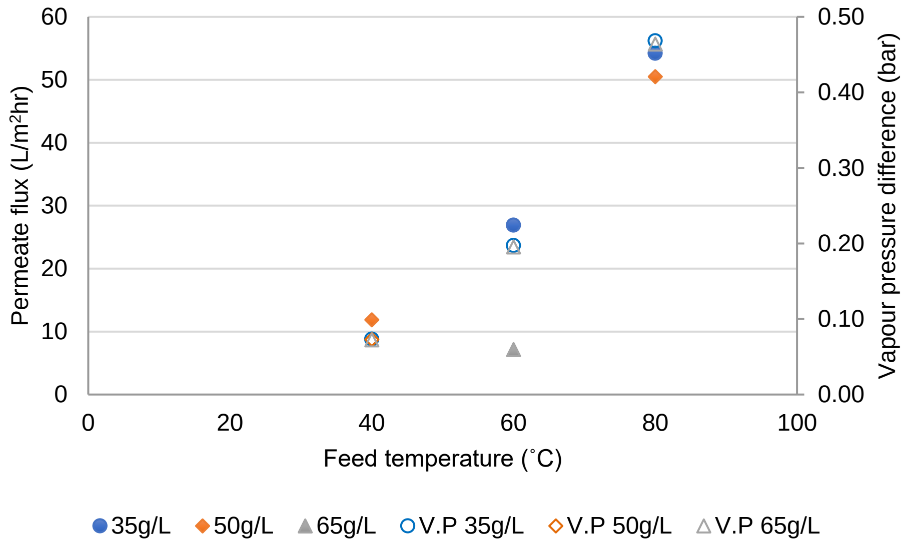

Figure 5-1: Change in flux rate with a change in feed temperature at different feed concentration levels for the treatment of Type 1 brine using the 0.22 µm membrane pore size

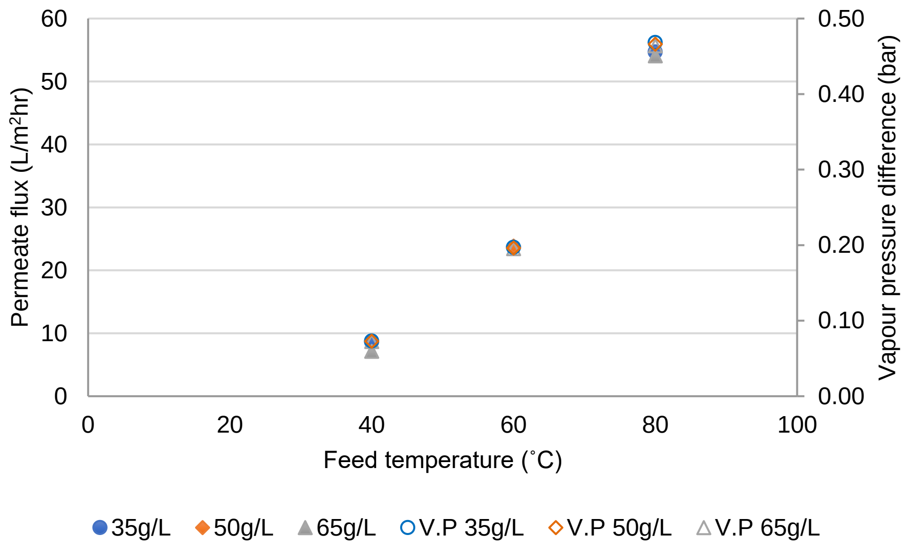

Figure 5-2: Change in flux rate with a change in feed temperature at different feed concentration levels for the treatment of Type 1 brine using the 0.45 µm membrane

Both the 0.22 µm and 0.45 µm pore size membranes displayed similar performance, in terms of flux, at the same operating conditions and also responded the same to an increase in feed temperature. As the feed temperature increased, the two different pore sized membranes both exhibited higher flux rates which indicates that the pore sizes studied for Experiment 1 were sufficient and did not limit the vapour pressure driving force increase as a result of an increase in feed temperature. Also, the fluxes closely match the vapour pressure trends for both membranes as was expected and the vapour pressure at the different concentration levels are almost identical which further supports that concentration at the lower TDS levels should have little to no impact on the flux rate (Fan & Peng, 2012).

5.3 Investigating the effect of scaling/fouling on the performance of MD using commercially available MD membranes for the treatment of prepared Type 1 brine (Experiment 2)

The aim of Experiment 2 was to determine the effects of scaling/fouling on the performance (focussed on membrane flux, water recovery and water purity) of the membrane distillation system using the commercially available membrane distillation membranes, 0.22 µm and 0.45 µm, for the treatment of Type 1 brine, which should theoretically have little to no scaling potential.

The experimental test runs conducted for Experiment 2 can be seen in Table 3-4 and the experimental methodology described in Chapter 3 was followed for tests 1 and 2. The process conditions of all test runs for Experiment 2 were shown in the Research design and the characteristics of the prepared Type 1 brine can be seen in Table 3-7.

Table 5-1 and Figure 5-3 show a 6-hour long experiment using an initial NaCl concentration of 200 g/L, at feed and permeate temperature of 60ºC and 10ºC, respectively, to compare the performance of the two membrane pore sizes at significantly higher TDS levels but still below solubility level of NaCl.

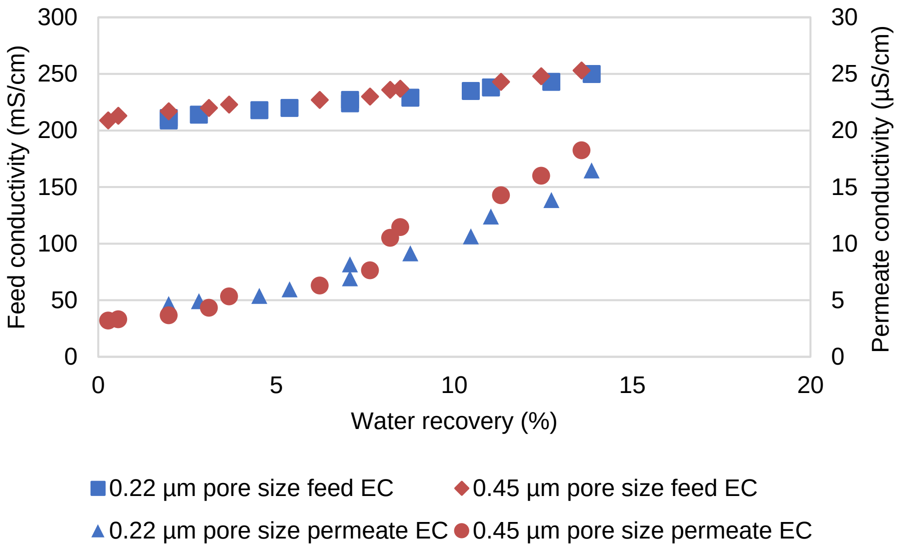

Figure 5-3: Feed and permeate conductivity as a function of Recovery for (6-hour run, 200 g/L initial TDS) prepared Type 1 brine using 0.22 µm pore size and 0.45 µm pore size membranes

Table 5-1: Permeate flux rate of Experiment 2 to determine the effect of scaling/fouling for prepared Type 1 brine

Membrane pore size (µm)	Permeate Flux (L/m^2.hr)
0.22	25.54
0.45	20.85

The 0.22 µm pore size membrane yielded a flux 18.4% higher than the 0.45 µm pore size membrane at these conditions, which is significant. The minor reduction in flux, when comparing the lower concentration runs to the significantly higher 235 g/L run, resulted from the decrease in the water vapour pressure under the high NaCl concentration (Fan & Peng, 2012). Other reasons include the concentration and thermal polarisation in the boundary layer of the feed solution (Lawson and Lloyd, 1996).

Figure 5-4 shows the results of Experiment 2 which was aimed at determining the effects of scaling on the performance (focussed on membrane flux, water recovery and water purity) of the membrane distillation system using the commercially available membrane distillation membranes, 0.22 µm and 0.45 µm, for the treatment of Type 1 brine.

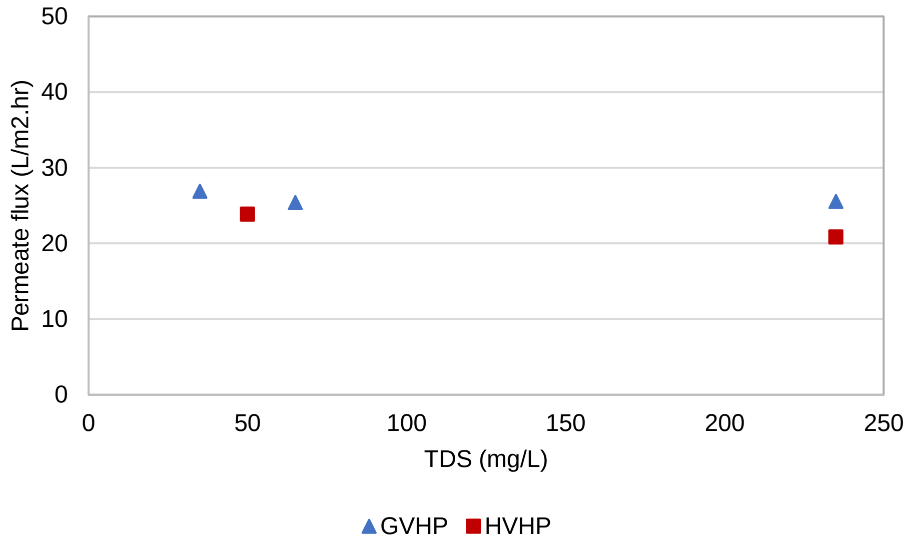

Figure 5-4: Effects of concentration on flux rate for the treatment of Type 1 brine

Figure 5-4 indicates that there is not much variance in flux with a change in concentration, even when the feed TDS concentration is increased from 65 g/L to 235 g/L. This is to be expected and is in agreement with Raoult's Law (Eykens et al., 2016). However, the minor reduction in flux with increasing feed concentration is caused by increasing effect of the salt concentration polarisation, adding more resistance to vapour permeation across the membrane (Khalifa et al., 2017). According to Raoult's Law the vapour pressure is less affected by the amount of solute in the solution and more affected by the solvent molal concentration. As the solvent molal concentrations for the concentrated solutions are all above 99%, the vapour pressure is not expected to change significantly for the Type 1 brine used in Experiment 2.

The 0.22 µm and 0.45 µm membrane pore sizes have shown very little difference in performance as was seen in Experiment 1. Typically, the larger 0.45 µm pore size membrane, yields higher flux for Type 1 brine (Eykens et al., 2016). However, the runs conducted for Experiment 2 where the initial feed TDS was significantly higher and approaching solubility, the smaller 0.22 µm pore size membrane performed significantly better in terms of flux. This may be as a result of the solute precipitating out of the solution having a small enough particle size to enter the pores of the larger, 0.45 µm pore size membrane but too large to enter the 0.22 µm pore size membrane.

The final conductivity of the test run for the 0.22 µm pore size membrane was approximately 10% lower than the 0.45 µm pore size membrane showing that the 0.22 µm pore size membrane yielded better flux and water purity under these conditions.

5.4 Investigating the effect of pore size, Type 2 brine feed concentration and operating feed temperature on MD performance (Experiment 3)

Experiment 3 was aimed at investigating the effect of pore size, synthetic Type 2 brine feed concentration and operating feed temperature on MD performance. The experimental matrix in Table 3-8 and process conditions can be seen in Chapter 3-

A summary of the flux rates and salt rejection of all the 180-minute test runs for the treatment of the prepared Type 2 brine is presented in Table 5-2 below:

Table 5-2: Summary of experimental run results of the prepared Type 2 brine

Feed TDS (mg/L)	Membrane pore size (µm)	Ave. flux (L/m^2.hr)	Salt Rejection (%)
11870	**40ºC feed temperature**		
	0.22	11.39	99.97
	0.45	11.06	99.94
	60ºC feed temperature		
	0.22	19.04	99.96
	0.45	25.11	99.97
	80ºC feed temperature		
	0.22	48.04	99.97
	0.45	40.13	99.97
27025	**40ºC feed temperature**		
	0.22	7.56	99.98
	0.45	12.60	99.99
	60ºC feed temperature		
	0.22	15,18	99,99
	0.45	15.90	99.99
	80ºC feed temperature		
	0.22	28.67	99.98
	0.45	26.17	99.98

5.4.1 Determining the effect of pore size and feed temperature on the permeate flux for prepared Type 2 brine

Figure 5-5 shows the effect of feed temperature for the treatment of prepared Type 2 brine using membranes with 0.22 µm and 0.45 µm pore sizes. The chemical composition of the prepared Type 2 brine used for this run can be seen in Table 3-2. The general trend for both membranes is that an increase in feed temperature resulted in an increase in flux rate. This is explained by the fact that the vapor pressure difference is the main driving force for the mass transfer and that vapour pressure difference and flux rate are directly proportional which can be clearly observed by the larger, 0.45 µm pore size membrane (Khalifa et al., 2017). At 40ºC the driving force is very low and yields an unfeasible flux rate when compared to other membrane separation processes. Alternatively low-grade heat such as solar energy could be applied.

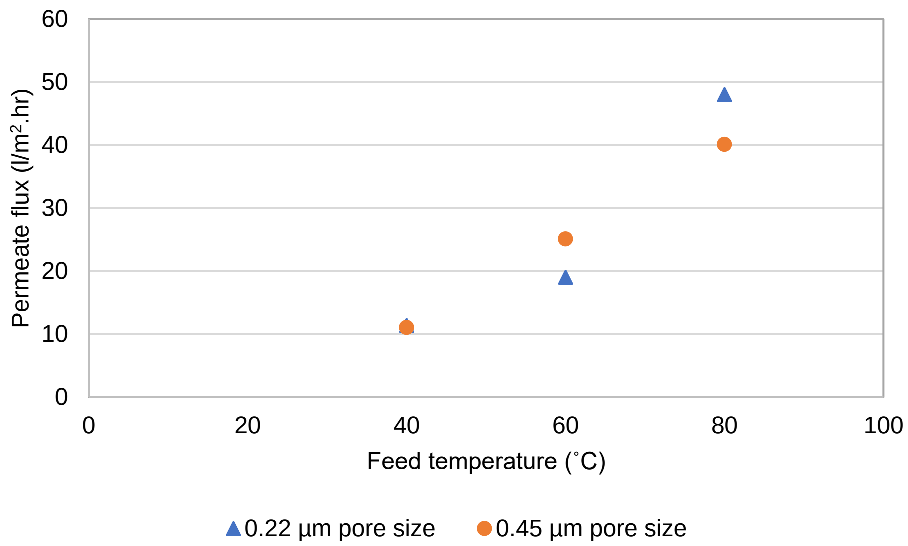

Figure 5-5: Effects of feed temperature on flux rate for the treatment of prepared Type 2 brine (Initial feed TDS 11870 mg/L) using a 0.22 µm and 0.45 µm pore size membrane

The results confirmed that when keeping the material type and other characteristics constant besides pore size, the membrane with the smaller pore size has a higher flux and lower wetting tendency. The larger, 0.45 µm pore size membrane, only yielded higher flux under specific temperature conditions and until wetting occurred. This relationship can be attributed to the change of mass transfer modality from Knudsen diffusion to Knudsen-Poiseuille type according to the Kinetic theory of gases (Bhattacharya et al., 2014). Viscous flow starts and eventually dominates the mass transfer mechanism if the average pore size is bigger than the mean free path of the molecules. This causes an increase in an increase in transport of the liquid and ions in the feed to the product side which results in a higher wetting tendency. LEP and contact angle appear more significant when considering the maximum pore size of the membrane. A smaller maximum pore diameter has a greater impact on the LEP (Damtie et al., 2018).

Table 5-2 shows a flux rate increase of 4.2 times and 3.63 times was observed when increasing the feed temperature from 40ºC to 80ºC for the 0.22 µm and 0.45 µm membrane pore sizes, respectively. This is significant in flux rate for temperatures that can be achieved using waste heat and renewable energy sources such as solar heat (Qtaishat & Banat, 2012).

5.4.2 Investigating the effect of pore size and feed concentration on the permeate flux for prepared Type 2 brine

To determine the effects that a change in feed concentration has on the flux rate, two Type 2 brine solutions of varying concentrations were prepared and investigated with the 0.22 µm and 0.45 µm membrane pore sizes. The chemical makeup of the two varying feed TDS concentration, 11870 mg/L and 27025 mg/L prepared Type 2 brines can be seen in Table 3-2 and Table 3-3, respectively. The process conditions for the test runs conducted to determine the effect of feed concentration can be found in Chapter 3 – Research Design. The feed temperature for these test runs were set to 60˚C and the product temperature was set to 10˚C.

The plot in Figure 5-6 below shows the relationship between permeate flux and TDS as well as theoretical TSS and TDS.

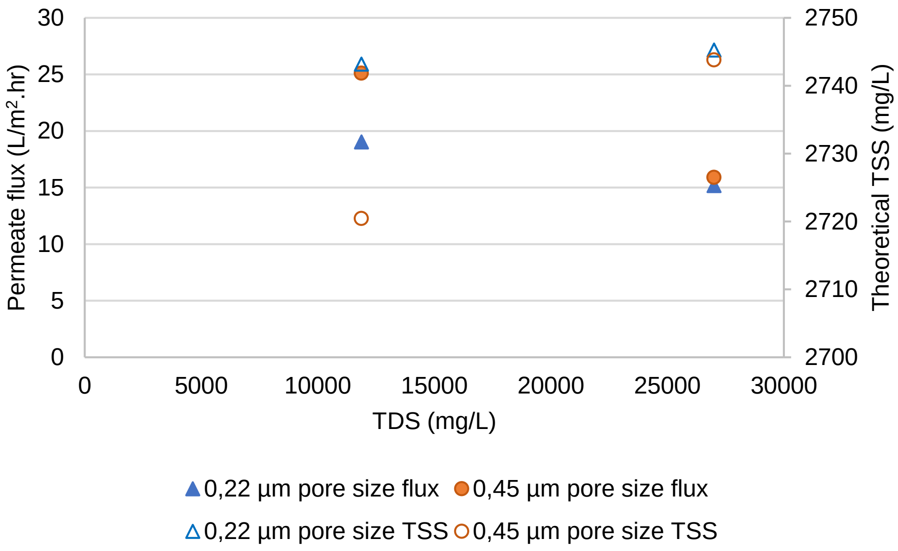

Figure 5-6: Effects of feed concentration and suspended solids for the treatment of prepared Type 2 brine using 0.22 µm (GVHP) and 0.45 µm (HVHP) membrane pore size

According to Raoult's Law, the vapour pressure is negligibly affected by the amount of solute in the solution but rather based on the solvent molal concentration and because the solvent molal concentrations for the concentrated solutions are all above 99%, the vapour pressure is expected to not change significantly. Therefore, the difference in flux of approximately 30% different concentrations can be assumed to be due to scaling/fouling since the initial brine would need to be concentrated 60 times in order for the concentration to have a 10% effect on the vapour pressure.

The theoretical TSS and permeate flux versus TDS plot in Figure 5-6 shows that the increase in feed TSS as the feed concentration increases, has an undesirable effect on the flux. The change in feed TSS indicates that there is fouling occurring as a result of an increase in solids precipitating out thus reducing the flux rate. The smaller 0.22 µm pore size membrane performs worse in terms of flux as the TSS increases compared to the 0.45 µm pore size membrane. This could be explained by the difference in LEP between the pore sizes, since membrane pore size has an inverse relationship with LEP (Alkhudhiri et al., 2012).

Figure 5-7 shows that approximately 50 minutes into the experiment using the prepared 27025 mg/L Type 2 brine, the larger 0.45 µm membrane pore size began to experience wetting as a cause of fouling. The high vapour pressure driving force as a result of an increase in feed temperature to 80ºC yielded higher flux but also accelerated the wetting tendency since the rate of fouling increased.

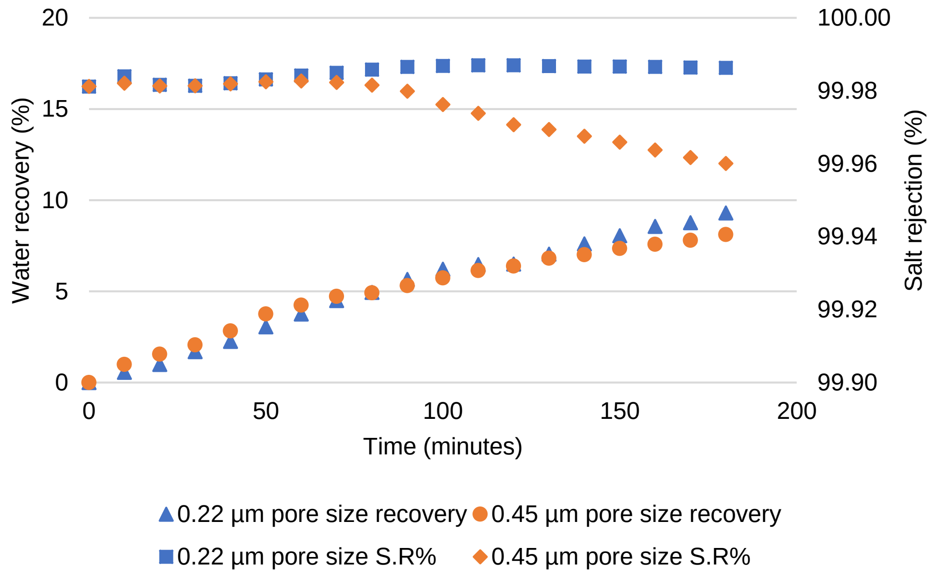

Figure 5-7: Water recovery and Salt rejection as a function of time for the treatment of Type 2 brine with feed TDS of 27025 mg/L using a 0.22 µm and 0.45 µm pore size membranes

5.5 Investigating the effect of scaling/fouling on the performance of MD for the treatment of prepared Type 2 brine using 0.22 µm and 0.45µm pore size membranes (Experiment 4)

Experiment 4 was performed at 60ºC feed temperature and 10ºC permeate temperature to determine the effect of scaling/fouling resulting from a dynamic increase in the feed water concentration and increasing suspended solids on the MD system performance.

The experiment was run using 4 L of the prepared Type 2 brine with an initial feed concentration of 27025 mg/L, until either the feed solution's volume change could no longer be measured because there was very little solution left or because the flux reduced significantly due to scaling/fouling.

Table 5-3 summarises the results obtained from the scaling/fouling effects experiment for the treatment of prepared Type 2 (feed TDS 27025 mg/L) brine using the 0.22 µm and 0.45 µm pore size membranes

Table 5-3: Summary of Experiment 4 results for scaling/fouling experiments using the prepared Type 2 brine

Membrane pore size (µm)	Average Flux ($L/m^2.hr$)	Salt Rejection (%)	Recovery (%)	Cumulative permeate volume (mL)	Running time (hrs)
0.22	10,58	99,93	38,17	1526,85	35,0
0.45	23,10	99,97	55,14	2205,45	24,0

The average flux rate and TSS as a function of water recovered from the feed can be seen in Figure 5-8 and Figure 5-9 for the 0.22 µm and 0.45 µm pore size membranes respectively. The flux rates represented are the average fluxes for the water recovery ranges, 0-10%, 11-20%, 21-30%, 31-40% and 41-50%.

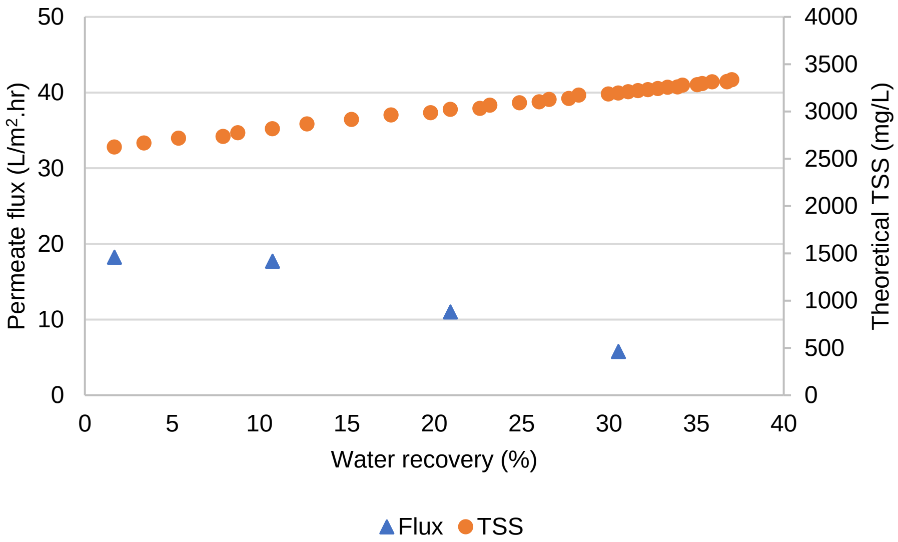

Figure 5-8: Flux rate and TSS as a function of water recovery for prepared Type 2 brine using the 0.22 µm pore size membrane

For the 0.22 µm pore size membrane, the flux appears to be consistent up to 10% water recovery, after which it starts to decline at a faster rate which can be seen in Figure 5-8. The water transfer across the membrane and loss by evaporation causes the feed to become more concentrated causing the saturation of some of the salts to be reached. More salts continue to crystallise out and consequently deposit onto the membrane surface, resulting in membrane scaling. This was supported by the TSS increasing as the water recovery increased (Kamranvand et al., 2021).

The active membrane surface area is reduced due to a build-up of crystals which means less water can be transferred. The flux declined from an average initial of 15 L/m^2.hr to an average of approximately 5 L/m^2.hr. This went on for a further 17 hours at which point the flux rate declined to 2.61 L/m^2.hr with a total water recovery of 38.74%. The run was allowed to continue until volume level readings could no longer be taken, which occurred after 35 hours of running time. The average flux for the 0.22 µm during this run was 10.58 L/m^2.hr which is significantly lower than what was observed for the experiments run over a 3-hour period in Experiment 6 using the same initial Type 2 feed brine concentration.

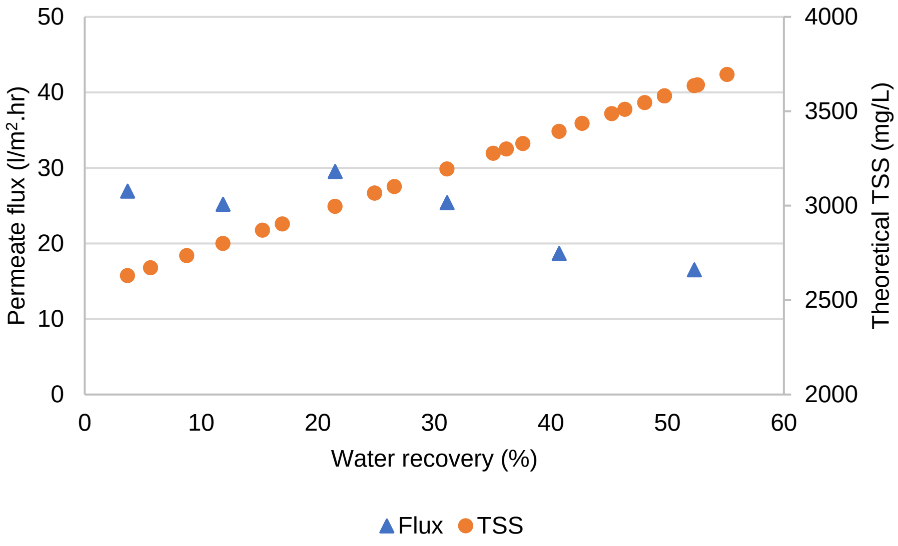

Figure 5-9: Flux rate and TSS as a function of water recovery for prepared Type 2 brine using the 0.45 µm pore size membrane

Figure 5-9 represents significantly better results for the 0.45 µm pore size membrane when comparing it to the 0.22 µm pore size membrane. The average flux achieved over the experimental run was 23.1 L/m^2.hr which shows that the 0.45 µm pore size membrane yielded a flux rate 2.2 times greater than that of the 0.22 µm pore size membrane. The running time to achieve the same point at which the 0.22 µm pore size membrane's experiment was stopped only took 24 hours. The water recovery was also 55.14% which was significantly more water recovered than what was achieved with the 0.22 µm pore size membrane.

Increasing TSS appeared to have minimal effect on the flux rate for this experimental run using the 0.45 µm pore size membrane. The larger pore size membrane yielding better MD performance results is to be expected for industrial wastewater when considering the same membrane material. However, larger pore sized membranes also have higher wetting tendency (Damtie et al., 2018).

Figure 5-10 and Figure 5-11 show the conductivity and TSS as a function of water recovery for prepared Type 2 brine using the 0.22 µm and 0.45 µm pore size membranes respectively. It is clear for both pore sizes that as the water recovery increases, the permeate conductivity and TSS increase as well. The decrease of volume in the feed tank means the water recovery increases, resulting in the feed TDS concentration to increase. This causes more solids to precipitate out and thus the TSS increases.

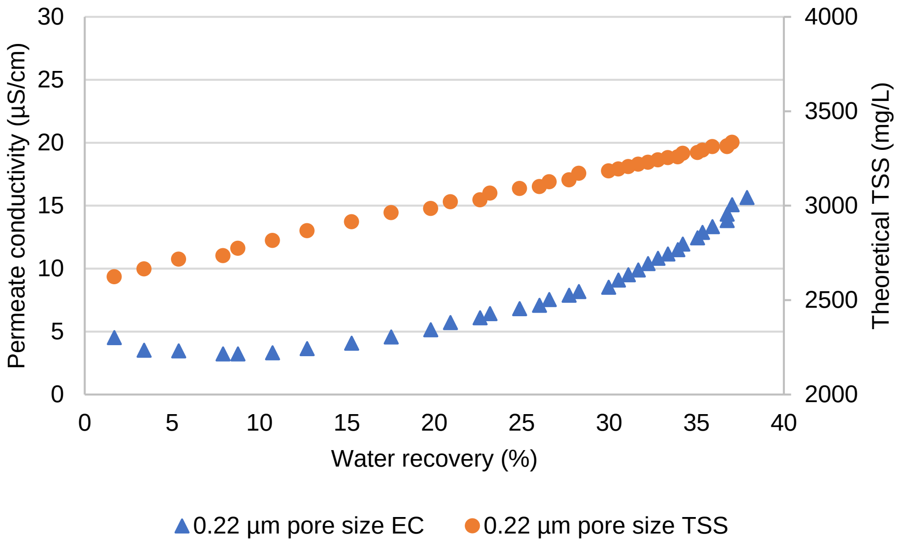

Figure 5-10: Permeate conductivity and TSS as a function of water recovery for prepared Type 2 brine using the 0.22 µm pore size membrane

The initial product conductivity for the 0.22 µm pore size membrane was 4.52 µS/cm and initially dropped as a result of the permeate from the membrane treatment being purer than the initial EC in the product tank. After approximately 9% water recovery, the product EC began to increase, and the final EC measurement for the experiment was 15.65 µS/cm indicating that scaling began to occur and there was salt passage to the product tank through the membrane (Damtie et al., 2018).

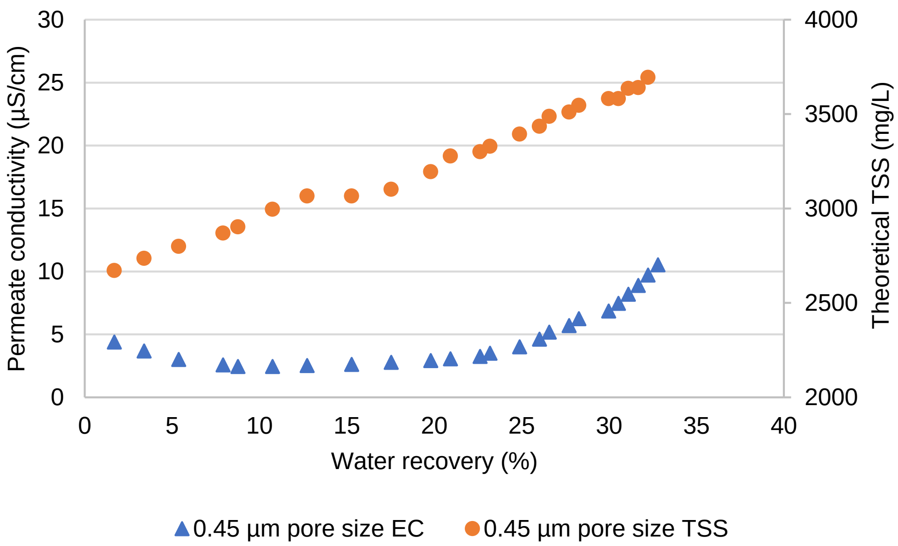

Figure 5-11: Permeate conductivity and TSS as a function of water recovery for prepared Type 2 brine using the 0.45 µm pore size membrane

Figure 5-11 showed the initial product conductivity for the 0.45 µm pore size membrane was 4.39 µS/cm and initially dropped as a result of the permeate from the membrane treatment being purer than the initial EC in the product tank. The EC began increasing at a significantly higher water recovery of approximately 30% and the final EC measurement for the experiment was 10.52 µS/cm. The increase in permeate EC was much less substantial for the 0.45 µm pore size membrane when compared to the water quality of the product water from the 0.22 µm pore size membrane experiment. This result is due to the 0.45 µm pore size membrane producing a significantly higher flux and hence also producing significantly more permeate (causing the permeate EC to remain lower). It still indicates some salt passage, however it is very minimal in comparison (Tijing et al., 2015).

Figure 5-12 and Figure 5-13 exhibit the salt rejection and TSS as a function of water recovery for prepared Type 2 brine using the 0.22 µm and 0.45 µm pore size membranes, respectively. The plots below give a good indication of the effects of TSS on the salt rejection and the point at which severe scaling/fouling begins to occur.

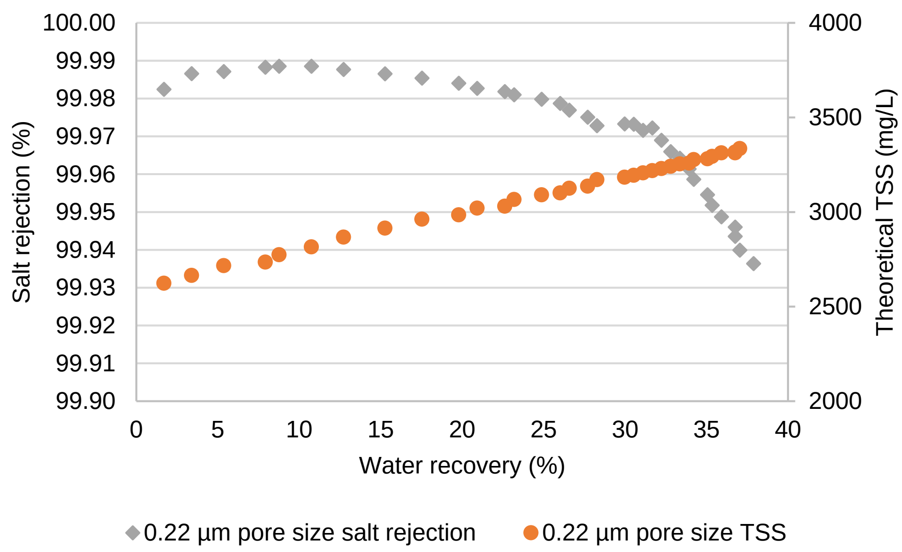

Figure 5-12: Salt rejection and TSS as a function of water recovery for prepared Type 2 brine using the 0.22 µm pore size membrane

In Figure 5-12, the salt rejection achieved using the 0.22 µm pore size membrane appears to have reached a rejection as low as 99.94% having yielded a salt rejection above 99.98% for over 17 hours and recovery of 27.71%. The salt rejection takes a sharp dip at approximately 30% recovery and 3000 mg/L. Hence it could be said that the range at which the maximum TSS which the system should no longer be run using a 0.22 µm pore size membrane is 2900-3100 mg/L. This range factored in the influence that TSS had on the flux rate, the permeate conductivity and the salt rejection (Tijing et al., 2015).

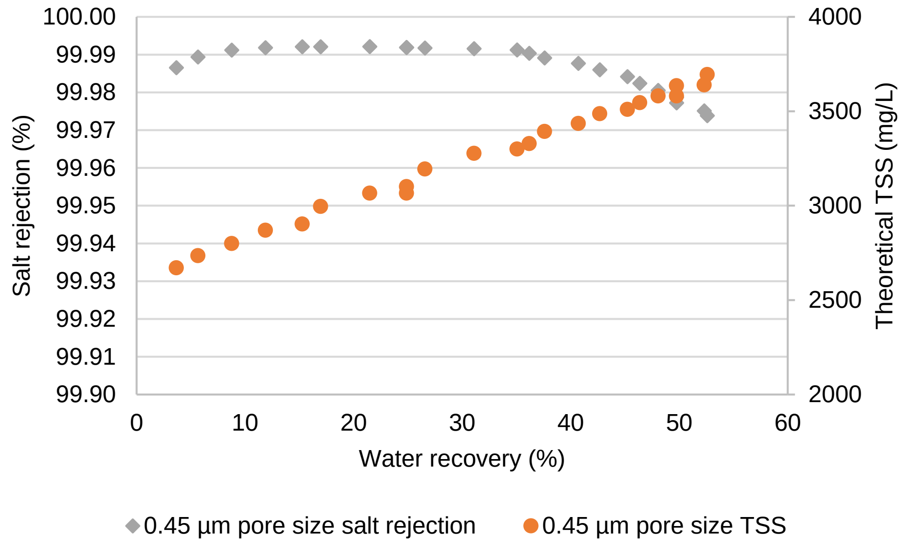

Figure 5-13: Salt rejection and TSS as a function of water recovery for prepared Type 2 brine using the 0.45 µm pore size membrane

Figure 5-13 shows that the salt rejection for the 0.45 µm pore size membrane dropped to only 99.97% after over 50% water was recovered and yielded a very high rejection of 99.9% for the first 45% of the recovered water. The range at which the maximum TSS which the system should no longer be run using a 0.45 µm pore size membrane is 3100-3300 mg/L. This range factored in the influence that TSS had on the flux rate, the permeate conductivity and the salt rejection.

5.6 Investigating the effect of pore size on the performance of MD using actual industrial brine emanating from an RO process (Experiment 5)

Experiment 5 used actual brine emanating from an RO process. The characteristics of the actual brine along with its scaling tendencies can be seen in Table 3-9 and Table 3-10 These experimental runs were conducted at a feed and permeate temperature of 60ºC and 10ºC respectively, using the 0.22 µm and 0.45 µm pore size membrane for an 8-hour period. The process conditions can be seen in Chapter 3-
Two characteristically distinct brines with varying dominant ion valences and scaling propensities (Type 1 and Type 2) were investigated. A description of the characteristics of Type 1 and Type 2 brines is provided below:

3.2.3 Type 1 brine

Type 1 brine was a monovalent ion dominant sodium chloride hypersaline solution with little to no scaling or fouling propensity within the range of water recoveries anticipated using membrane distillation. The NaCl concentration levels investigated can be seen in Table 3-1.

Table 3-1: NaCl concentration levels investigated

Chemicals	Molecular weight (g/mol)	Concentration (mg/L)		
Sodium Chloride (NaCl)	58,44	35 000	50 000	65 000

3.2.4 Type 2 brine

Type 2 brine contained a combination of monovalent and divalent ionic species. As a result of the presence of calcium, magnesium, sulphate and bicarbonate ions, Type 2 brine had a propensity towards scaling/fouling within the range of water recoveries anticipated using membrane distillation.

Both synthetic and actual brine solutions that fell within the classification of Type 2 brine were investigated in this study. The synthetic brine was used to simulate actual brine samples generated from brackish water reverse osmosis (RO) processes associated with industrial and or coal mining applications.

The composition of the synthetic Type 2 brine investigated in this study is shown in Table 3-2 :

Table 3-2: Chemical make-up of synthetic coal mine brine

Chemicals	Molecular weight (g/mol)	Concentration (mg/L)	Feed TDS (mg/L)
Sodium Bicarbonate ($NaHCO_3$)	84,01	687,89	11870
Sodium Sulphate (Na_2SO_4)	142,04	7530,39	
Sulphuric Acid (H_2SO_4)	98,08	834,10	
Magnesium Chloride ($MgCl_2$)	95,21	1585,92	
Calcium Chloride ($CaCl_2$)	110,98	1248,01	

The synthetic Type 2 brine was de-supersaturated using simulation software, and the outputted solution was put through an RO simulation process. The composition of the more concentrated synthetic Type 2 brine investigated in this study is shown in Table 3-3.

Table 3-3: Chemical make-up of the de-supersaturated synthetic coal mine brine that was treated with RO (stage two RO)

Chemicals	Molecular weight (g/mol)	Concentration (mg/L)	Feed TDS (mg/L)
Sodium Bicarbonate ($NaHCO_3$)	84,01	1611,14	27025
Sodium Sulphate (Na_2SO_4)	142,04	17838,98	
Sulphuric Acid (H_2SO_4)	98,07	834,1	
Magnesium Chloride ($MgCl_2$)	95,21	3772,32	
Calcium Chloride ($CaCl_2$)	110,98	2968,56	

Research Design. The results can be seen in Table 5-4.

Table 5-4: Results for actual brine after 480 minutes

Membrane	Membrane pore size (μm)	Average Flux (L/m^2.hr)	Salt Rejection (%)
GVHP	0.22	18,89	99,97
HVHP	0.45	14,33	99,95

The flux obtained after 480 minutes was 18.89 L/m^2.hr and 14.33 L/m^2.hr for the 0.22 μm and 0.45 μm pore size membranes, respectively. The final water recoveries achieved for the 0.22 μm and 0.45 μm pore size membranes were 16.4% and 12.4%, respectively.

The 0.22 μm pore size membrane yielded a slightly higher flux than the prepared Type 2 brine with a feed TDS of 11870 mg/L and significantly higher than prepared Type 2 brine with a feed TDS of 27025 mg/L under the same conditions. This difference could be as an account of all the additional ions and organic matter present in the actual brine compared to the synthetic brine. The 0.45 μm membrane performed similarly to the prepared Type 2 brine with 27025 mg/L feed TDS. No major flux decline was observed when comparing the 180-minute run to the 480-minute run (Mericq et al., 2010).

The reason for the larger 0.45 μm pore size membrane performing worse in Experiment 5 could be due to the particle size of the suspended solids in the actual brine solution being smaller than the pore diameter of the membrane. This may have resulted in particles being small enough to enter the larger 0.45 μm pore size membrane which would have caused wetting.

Chapter 5

Conclusions and Recommendations

Chapter 6 Conclusions and Recommendations

6.1 Conclusion

This study investigated the effects of pore size on MD performance for the treatment of two characteristically distinct brines with varying dominant ion valences and scaling propensities (referred to as Type 1 and Type 2) with varying feed temperature and feed concentration.

The two types of brines investigated were: Type 1 brine, a monovalent ion dominant, non-scaling/fouling brine and Type 2 brine, a divalent and trivalent ion dominant brine with scaling or fouling potential. Both brines provided the necessary coverage regarding the variability in brine wastewater characteristics from the industrial and mining sectors.

Along with using synthetically prepared feed solutions to establish baseline performance characteristics for different membranes, the study also included testing actual industrial brine emanating from an RO process, emphasising the most suitable membrane properties for this specific type of brine.

The water purity from the investigations yielded acceptable results and very high rejection (>99.94%) with the product water exhibiting low conductivity (<15 µS/cm), which only increased once scaling on the membrane surface and pore wetting caused a decrease in flux rate.

For the results obtained using the Type 1 brine, it was found that for both membrane pore sizes investigated, 0.22 µm and 0.45 µm, an increase in temperature from 40˚C to 80˚C increased the flux rate by up to 6.27 times. Increasing the feed TDS concentration from 35 g/L to 65 g/L did not have any notable effect on the flux rate even when the 0.22 µm and 0.45 µm pore size membranes were subjected to feed concentrations close to but below solubility level. The 0.22 µm and 0.45 µm pore size membranes performed similarly, indicating that pore size was not a limiting factor in the vapour pressure driving force.

For the results obtained using the prepared Type 2 brine, it was found that for both membrane pore sizes investigated, 0.22 µm and 0.45 µm, an increase in temperature from 40˚C to 80˚C increased the flux rate by up to 4.22 times. An increase in feed TDS concentration from 11870 to 27025 mg/L for the 0.22 µm and 0.45 µm pore size membranes caused a decrease in the flux of up to 40.3% and 35%, respectively. The smaller 0.22 µm pore size membrane generally performed better for these experiments.

The investigation into the effect of scaling/fouling on the performance of MD using 0.22 µm and 0.45 µm pore size membranes for the treatment of Type 2 brine with feed TDS concentration of 27025 mg/L showed a significant difference between the varying pore sizes. The larger, 0.45 µm pore size membrane yielded a flux 2.2 times higher than the 0.22 µm pore size membrane. The maximum suspended solids in the solution before a significant decline in MD performance for the 0.22 µm and 0.45 µm pore size membranes were found to be approximately 3050 mg/L and 3550 mg/L, respectively. This showed that the 0.45 µm pore size membrane was more resistant to scaling/fouling when compared to the 0.22 µm pore size membrane.

Finally, the use of actual brine investigated showed the 0.22 µm pore size membrane to perform better when compared to the 0.45 µm pore size membrane. This was owing to the maximum TSS not being reached, and hence 0.22 µm pore size membrane generally performs better until scaling/fouling occurs.

6.2 Recommendations

Further studies should investigate the effects of particle size distribution on the MD performance of varying pore size membranes. The effects of porosity should also be investigated for brine emanating from industrial and mining wastewater. This would help better understand the cause of fouling and why the smaller pore size membrane responds so poorly to increasing TSS and scaling/fouling.

Although advancements in membrane modifications have accelerated in the past few years, more research needs to develop cheaper membranes for this purpose since the number of commercially available membranes manufactured specifically for MD use has not increased much.

CHAPTER 7

References

Chapter 7 - References

Adnan, S., Hoang, M., Wang, H. & Xie, Z., 2012. Commercial PTFE membranes for membrane distillation application:Effect of microstructure and support material.. *Desailination,* Volume 284, pp. 297 - 308.

Ali, M., Summers, E., Arafat, H. & J.H.L.V. 2012. Effects of memebrane properties on water production cost in small-scale membrane distillation systems.. *Desalination,* Volume 306, pp. 60-71.

Ali, M., Summers, H. & al., A. e., 2012. Effects of membrane properties on water production cost in small scale membrane distillation systems.. *Desalination,* Volume 306, pp. 60 - 74.

Alkhudhiri, A., Darwish, N. & Hilal, N., 2012. Membrane distillation: A comprehensive review. *Desalination,* 02, Volume 287, pp. 2-18.

Alklaibi, A. & Lior, N., 2005. Membrane-distillation desalination:Status and potential. *Desilination,* 171(2), pp. 111 - 131.

Alsebaeai, M.K. & Ahmad, A.L. 2020. Membrane distillation: Progress in the improvement of dedicated membranes for enhanced hydrophobicity and desalination performance. *Journal of Industrial and Engineering Chemistry*, 86: 13–34. https://doi.org/10.1016/j.jiec.2020.03.006.

Ashoor, B.B., Mansour, S., Giwa, A., Dufour, V. & Hasan, S.W. 2016. Principles and applications of direct contact membrane distillation (DCMD): A comprehensive review. *Desalination*, 398.

Alves, V. & Coelhoso, I., 2006. Orange juice concentration by osmotic evaporation and membrane distillation:A comparative study.. *Journal of Food Engeering,* Issue 74, pp. 125 - 133.

Aziz, M. & Kasongo, G. 2019. Scaling prevention of thin film composite polyamide Reverse Osmosis membranes by Zn ions. Desalination, 464(April): 76–83. https://doi.org/10.1016/j.desal.2019.04.021.

Balasubramanian, P., 2013. A brief review on best available technologies for reject water (brine) management in industries. *International Journal Of Environmental Sciences,* 3(6), pp. 2010-2018.

Banat, F. & Simandi, J., 1998. Desalination by Membrane Distillation:A Parametric Study. *Seperation Science and Technology,* 33(2), pp. 201 - 226.

Bandini, S. & Sarti, G., 1999. Heat and Mass Transport Resistances in Vacuum Membrane Distillation Per Drop. *AIChE Journal,* 45(7), pp. 1422 - 1433.

Bhattacharya, M., Dutta, S.K., Sikder, J. and Mandal, M.K., 2014. Computational and experimental study of chromium (VI) removal in direct contact membrane distillation. *Journal of Membrane Science*, *450*, pp.447-456.

Burgoyne, A. & Vahdati, M., 2000. Direct Contact Membrane Distillation. *Seperation Science and Technology,* 35(8), pp. 1257 - 1284.

Camacho, L. et al., 2013. Advances in Membrane Distillation for Water Desalination and Purification Applications. *Water,* Volume 5, pp. 94-196.

Chan, M.T., Fane, A.G., Matheickal, J.T. & Sheikholeslami, R. 2005. Membrane distillation crystallization of concentrated salts - Flux and crystal formation. *Journal of Membrane Science*, 257(1–2): 144–155.

Chen, G., Lu, Y., Krantz, W.B., Wang, R. & Fane, A.G. 2014. Optimization of operating conditions for a continuous membrane distillation crystallization process with zero salty water discharge. *Journal of Membrane Science*, 450: 1–11. http://dx.doi.org/10.1016/j.memsci.2013.08.034.

Creusen, R., van Medevoort, J., Roelands, M., van Renesse van Duivenbode, A., Hanemaaijer, J.H. & van Leerdam, R. 2013. Integrated membrane distillation-crystallization: Process design and cost estimations for seawater treatment and fluxes of single salt solutions. *Desalination*, 323: 8–16. http://dx.doi.org/10.1016/j.desal.2013.02.013.

Curcio, E. & Drioli, E., 2005. Membrane distillation and related operations - review. *Seperation & Purification Reviews,* 34(1), pp. 35-36.

Damtie, M.M., Kim, B., Woo, Y.C. and Choi, J.S., 2018. Membrane distillation for industrial wastewater treatment: Studying the effects of membrane parameters on the wetting performance. *Chemosphere*, *206*, pp.793-801.

Dow, N. et al., 2008. *Membrane Distillation of Brine Wastes,* Adelaide: Water Quality Research Australia Limited.

Dow, N. et al., 2008. *Membrane Distillation of Brine Wastes,* Adelaide: Water Quality Research Australia Limited.

Drioli, E., Ali, A. & Macedonio., 2015. Membrane distillation:Recent developments and perspectives.. *Desalination,* Volume 356, pp. 56 - 84.

Du, Hongbo & Bandara, Subhani & Carson, Laura & Kommalapati, Raghava. (2019). Association of Polyethylene Glycol Solubility with Emerging Membrane Technologies, *Wastewater Treatment, and Desalination.*

EcologyDictionary.org, 2008. *EcologyDictionary.org.* [Online] Available at: http://www.ecologydictionary.org/MYPgV/EPA-Terms-of-Environment-Dictionary/BRINE [Accessed 23 07 2015].

El-Bourawi, M.S., Ding, Z., Ma, R. and Khayet, M., 2006. A framework for better understanding membrane distillation separation process. *Journal of membrane science*, *285*(1-2), pp.4-29.

EMIS, 2010. *Membrane distillation.* [Online] Available at: http://emis.vito.be/techniekfiche/membrane-distillation?language=en [Accessed 04 03 2015].

Essalhi, M. &. K., 2013. Self-sustained webs of polyvinylidene flouride electrospu nanofibres at different electrospinning times:1.Desalination by direct contact membrane distillation.

Journal of Membrane Science, Volume 433, pp. 167 - 179.

Eugster, H., 1980. Geochemistry of evaporitic lacustine desposits.. *Annual Review of Earth and Planetary Sciences.,* Volume 8, pp. 35-63.

Eykens, L., De Sitter, K., Dotremont, C., Pinoy, L. & Van Der Bruggen, B. 2016. How to Optimize the Membrane Properties for Membrane Distillation: A Review. *Industrial and Engineering Chemistry Research*, 55(35).

Fan, H. and Peng, Y., 2012. Application of PVDF membranes in desalination and comparison of the VMD and DCMD processes. *Chemical engineering science*, *79*, pp.94-102.

Field, R., Wu, H. & Wu, J., 2013. Multiscale Modelling of Membrane Distillation:Some Theoretical Considerations. *Industrial & Engineering Chemistry Research,* 52(26), pp. 8822 - 8828.

González, D., Amigo, J. & Suárez, F. 2017. Membrane distillation: Perspectives for sustainable and improved desalination. *Renewable and Sustainable Energy Reviews*.

Gostoli, C. & Sarti, G., 1987. Low Temperature Distillation through Hydrophobic Membranes. *Seperation Science and Technology,* 22(2&3), pp. 855 - 872.

Gryta, M., 2001. Direct Contact Membrane Distillation with Crystallization Applied to NaCl Solutions.

Gunko, S., Verbych, S., Bryk, M. & Hilal, N., 2006. Concentration of apple juice using direct contatc membrane distillation. *Desalination,* Volume 190, pp. 117 - 124.

Hausmann, A., 2013. *Membrane Distillation in Dairy Processing.* s.l.:s.n.

Hsu, S., Cheng, K. & Chiou, J., 2002. Seawater desalination by direct contact membrane distillation. *Desalination,* Volume 143, pp. 279 - 287.

Imdakm, A. & Matsuura, T., 2005. Simulation of heat and mass transfer in direct contatc membrane distillation (MD):The effect of membrane physical properties.. *Journal of Membrane Science,* 262(1 - 2), pp. 117 - 128.

Izquierdo-Gil, M.A., García-Payo, M.D.C. and Fernández-Pineda, C., 1999. Direct contact membrane distillation of sugar aqueous solutions. *Separation Science and Technology*, *34*(9), pp.1773-1801.

Jhariya, D.., Khan, R. & Thakur, G.. 2016. Impact of Mining Activity on environment: An Overview. *International Journal of Scientific and Research Publications (IJSRP)*, 10(05): 784–791.

Ji, X., Curcio, E., Al Obaidani, S., Di Profio, G., Fontananova, E. & Drioli, E. 2010. Membrane distillation-crystallization of seawater reverse osmosis brines. *Separation and Purification Technology*, 71(1): 76–82.

Jiang, X., Tuo, L., Lu, D., Hou, B., Chen, W. & He, G. 2017. Progress in membrane distillation crystallization: Process models, crystallization control and innovative applications. *Frontiers of Chemical Science and Engineering*, 11(4): 647–662.

July, P. 2017. Brazilian Journal of Chemical Engineering Evaluation of Sodium Chloride Crystallization in Membrane Distillation Crystallization Applied to Water Desalination. , 33(03): 1–26.

Kamranvand, F., Davey, C.J., Williams, L., Parker, A., Jiang, Y., Tyrrel, S. and McAdam, E.J., 2021. Membrane distillation of concentrated blackwater: Effect of temperature, solids concentration and membrane pore size.*Water Environment Research*, *93*(6), pp.875-886.

Kebria, M.R.S. & Rahimpour, A. 2020. Membrane Distillation: Basics, Advances, and Applications. *Intech*, (Advances in Membrane Technologies): 13. https://www.intechopen.com/books/advanced-biometric-technologies/liveness-detection-in-biometrics.

Kesieme, U.K. 2015. Mine waste water treatment and acid recovery using membrane distillation and solvent extraction.

Khalifa, A., Ahmad, H., Antar, M., Laoui, T. and Khayet, M., 2017. Experimental and theoretical investigations on water desalination using direct contact membrane distillation. *Desalination*, *404*, pp.22-34.

Khayet, M. & Matsuura, T., 2001. Preparation and characterisation of Polyvinylidene Flouride Membraness for Membrane Distillation.. *Industrial and Engineering Chemistry Research,* 40(24), pp. 5710 - 5718.

Khayet, M., 2011. *Desalination by Membrane Distillation.* [Online] Available at: http://www.desware.net/DESWARE-SampleAllChapter.aspx [Accessed 03 03 2015].

Kimura, S., Nakao, S.I. and Shimatani, S.I., 1987. Transport phenomena in membrane distillation. *Journal of membrane science*, *33*(3), pp.285-298.

Konig, A. & Weckesser, D., 2005. *Membrane Based Evaporation Crystallization.* s.l., s.n., pp. 1171-1176.

Kucera, J., 2010. *Reverse Osmosis: Industrial Applications and Processes.* Massachusetts(Salem): Scrivener Publishing LLC.

Kullab, A., 2011. *Desalination Using Membrane Distillation,* Stockholm

Lafuma, A. and Quéré, D., 2003. Superhydrophobic states. *Nature materials*, *2*(7), pp.457-460.

Lagana, F., Barbieri, G. & Drioli, E., 2000. Direct contact membrane distillation:modelling and concentration experiments. *Journal of Membrane Science,* 166(1), pp. 1 - 11.

Lawson, K.W. and Lloyd, D.R., 1997. Membrane distillation. *Journal of membrane Science*, *124*(1), pp.1-25.

Lee, K.P., Arnot, T.C. & Mattia, D. 2011. A review of reverse osmosis membrane materials for desalination-Development to date and future potential. *Journal of Membrane Science*, 370(1–2): 1–22. http://dx.doi.org/10.1016/j.memsci.2010.12.036.

Li, J., Guan, Y., Cheng, F. & Liu, Y. 2015. Treatment of high salinity brines by direct contact membrane distillation: Effect of membrane characteristics and salinity. *Chemosphere*, 140: 143–149. http://dx.doi.org/10.1016/j.chemosphere.2014.12.006.

Li, L. & Sirkar, K.K. 2016. Influence of microporous membrane properties on the desalination performance in direct contact membrane distillation. *Journal of Membrane Science*, 513: 280–293. http://dx.doi.org/10.1016/j.memsci.2016.04.015.

Liley, E. et al., 1999. Section 2: Physical and Chemical Data. In: D. W. Green, ed. *Perry's Chemical Engineers' Handbook.* 7th ed. s.l.:McGraw-Hill.

Mariah, L., 2006. *Membrane Distillation Of Concentrated Brines,* Durban: s.n.

Martinez, J. e. a., 2003. Estimation of vapour transfer coefficient of hydrophobic porous membranes for applications in membrane distillation.. *Seperation and Purification,* 33(1), pp. 45 - 55.

Martinez, L. and Rodriguez-Maroto, J.M., 2008. Membrane thickness reduction effects on direct contact membrane distillation performance. *Journal of Membrane Science*, *312*(1-2), pp.143-156.wood

Matheswaran, M., Kwon, T.O., Kim, J.W. and Moon, I.S., 2007. Factors affecting flux and water separation performance in air gap membrane distillation. *Journal of Industrial and Engineering Chemistry*, *13*(6), pp.965-970.

McCabe, W. L., Smith, J. & Harriott, P., 1993. Unit Operations of Chemical Engineering. Fifth Edition. In: B. J. Clark & E. Castelleno, eds. New York: McGraw-Hill Book Co, pp. 882-923.

Mericq, J.P., Laborie, S. and Cabassud, C., 2010. Vacuum membrane distillation of seawater reverse osmosis brines. *Water research*, *44*(18), pp.5260-5273.

Nathoo, J., Eggers, L., Randall, D. & Town, C. 2017. *Using Membrane Distillation Crystallisation For The Treatment Of Hypersaline Mining And Industrial Wastewater.*

Ochieng, G.M., Seanego, E.S. & Nkwonta, O.I. 2010. Impacts of mining on water resources in South Africa: A review. *Scientific Research and Essays*, 5(22): 3351–3357.

Onsekizoglu, P., 2012. Membrane Distillation: Principle, Advances, Limitations and Future Prospects in. In: S. Zereshki, ed. *Distillation - Advances from Modeling to Applications.* s.l.:Intech, pp. 233-266.

Osman, M.S., Schoeman, J.J. & Baratta, L.M. 2011. Desalination/concentration of reverse osmosis and electrodialysis brines with membrane distillation. *Desalination and Water Treatment*, 24(1–3): 293–301.

Otieno, F.A. and Ochieng, G.M., 2004. Water management tools as a means of averting a possible water scarcity in South Africa by the year 2025. *Water Sa*, *30*(5), pp.120-124.

Pantonja, C. e. a., 2016. Membrane Distillation Crystallisation Applied to Brine Desalination:Additional Design Criteria. *Industrial and Engineering Chemistry Research,* 55(4), pp. 1004-1012.

Payo, M. e. a., 1999. Air gap membrane distillation of aqueous alcohol solutions. *Journal of Membrane Science,* Volume 169, pp. 61 - 80.

Phattaranawik, J. & Jiraratananon, A., 2003. Effect of pore size distribution and air fluc pn mass transport in direct contact membrane distillation. *Journal of Membrane Science,* 215(1 - 2), pp. 75 - 85.

Qtaishat, M. & Banat, F., 2012. Desalination by solar powered membrane distillation systems. *Desalination,* Volume 308, pp. 186-197.

Qtaishat, M., Matsuura, T., Kruczek, B. & Khayet, M., 2007. Heat and mass transfer analysis in direct contact membrane distillation. *Desalination,* 219(1 - 3), pp. 272 - 292.

Ramirez, C., Patel, M. & Blok, K., 2006. From fluid milk to milk powder:Energy use and energy efficiency in the European dairy industry. *Energy,* Volume 31, pp. 1984 - 2004.

Rao, G., Hiibel, S. & Childress, A., 2014. Simplified flux prediction in direct-contact membrane distillation using a membrane structural parameter. *Desalination,* 351. 151 - 162.

Republic of South Africa. 1996. *Constitution of the Republic of South Africa, No. 108 of 1996*. South African Government.

Republic of South Africa. 1998. National Environmental Management Act, No. 107 of 1988. *Government Gazette*, 401(19519): 1–37.

Ruiz Salmón, I. & Luis, P. 2018. Membrane crystallization via membrane distillation. *Chemical Engineering and Processing: Process Intensification*, 123 (2017): 258–271. https://doi.org/10.1016/j.cep.2017.11.017.

Salehi, M. & Rostamani, R., 2013. Review of membrane distillation for the production of fresh water from saline water. *Journal of Novel Applied Sciences,* Volume 2, pp. 1072-1075.

Salzman, W., 2004. *The Melting Curve for Water; Vapor Pressure.* [Online] Available at: http://www.chem.arizona.edu/~salzmanr/480a/480ants/watvp/watvp.html [Accessed 06 04 2016].

Surapit, S., Jiraratananon, R. & Fane, A., 2006. Mass transfer mechanisms and transport resistances in direct contact membrane distillation process.. *Journal of Membrane Science,* Volume 277, pp. 186 - 194.

Susanto, H., 2011. Towards practical implementations of membrane distillation. *Chemical Engineering and Processing:Process Intensification,* 50(2). 139-150.

Taylor, P., Obaidani, S. Al, Curcio, E., Profio, G. Di & Drioli, E. 2009. Desalination and Water Treatment The role of membrane distillation / crystallization technologies in the integrated membrane system for seawater desalination. , (2013): 37–41.

Teoh, M.M. and Chung, T.S., 2009. Membrane distillation with hydrophobic macrovoid-free PVDF–PTFE hollow fiber membranes. *Separation and Purification Technology*, *66*(2), pp.229-236.

Tijing, L.D., Woo, Y.C., Choi, J.S., Lee, S., Kim, S.H. and Shon, H.K., 2015. Fouling and its control in membrane distillation—A review. *Journal of Membrane Science*, *475*, pp.215-244.

Tomaszewska, M., 2000. Membrane distillation-Examples of Applications in Technology and Environmental Protection.. *Polish Journal of Environmental Studies.,* 9(1), pp. 27 - 36.

Tun, C., Fane, A., Matheickal, J. & Sheikholeslami, R., 2005. Membrane distillation crystallization of concentrated salts—flux and crystal formation. *Journal of Membrane Science,* 07, 257(1-2), pp. 144-155.

University of Colorado at Boulder, 2015. *Organic Chemistry at CU Boulder.* [Online] Available at: http://orgchem.colorado.edu/Technique/Procedures/Crystallization/Crystallization.html [Accessed 21 04 2015].

Van Ness, H. C. & Abott, M. M., 1999. Section 4: Thermodynamics. In: D. W. Green, ed. *Perry's Chemical Engineerrs' Handbook.* 7th ed. s.l.:McGraw-Hill.

Walton, J. e. a., 2000. *Seperation and Waste Heat Desalination by Membrane Distillation,* Texas: s.n.

Wang, P. & Chung, T.S. 2015. Recent advances in membrane distillation processes: Membrane development, configuration design and application exploring. *Journal of Membrane Science*, 474: 39–56. http://dx.doi.org/10.1016/j.memsci.2014.09.016.

Water Research Commission. 2015. Background to Current Drought Situation in South Africa. *Water Reseach Commission Drought Factsheet 1*: 2015. http://www.wrc.org.za/SiteCollection Documents/ Background to current drought situation in South Africa (3).pdf 10 August 2017.

Winter, D., Koschikowski, J., Düver, D., Hertel, P. and Beuscher, U., 2013. Evaluation of MD process performance: effect of backing structures and membrane properties under different operating conditions. *Desalination*, *323*, pp.120-133.

World Bank Group, n.d. *Introduction to Wastewater Treatment Processes.* [Online] Available at: http://water.worldbank.org/shw-resource-guide/infrastructure/menu-technical-options/wastewater-treatment [Accessed 03 03 2015].

Woods, J., Pellegrino, J. and Burch, J., 2011. Generalized guidance for considering pore-size distribution in membrane distillation. *Journal of Membrane Science*, *368*(1-2), pp.124-133.

Wu, Y., Wang, R. & Field, R., 2014. Direct contact membrane distillation:An experimental and analytical investigatiuon of the effect of membrane thickness upon transmembrane flux.. *Journal of Membrane Science,* Volume 470, pp. 257 - 265.

WWF-SA. 2016. *Water: facts and futures*. www.wwf.org.za.

Xu, Y.F. and Huang, R.Y.M., 1988. Pervaporation separation of ethanol–water mixtures using ionically crosslinked blended polyacrylic acid (PAA)–nylon 6 membranes. *Journal of applied polymer science*, *36*(5), pp.1121-1128.

Yun, Y., Ma, R., Zhang, W., Fane, A.G. & Li, J. 2006. Direct contact membrane distillation mechanism for high concentration NaCl solutions. *Desalination*, 188(1–3): 251–262.

Zhang, J., Dow, N., Duke, M., Ostarcevic, E. and Gray, S., 2010. Identification of material and physical features of membrane distillation membranes for high performance desalination. *Journal of membrane science*, *349*(1-2), pp.295-303.

Zeng, L. & Gao, C., 2010. The prospective application of membrane distillation in the metallurgical industry. *Membrane Technology,* 05, 2010(5), pp. 6-10.

Appendices

Appendix A

Data from Experiment 1

Investigating the effect of pore size, Type 1 brine feed concentration and operating feed temperature on MD performance

APPENDIX A.1

Data from Experiment 1: Test number 1

MD experimental runs using 0.45 μm pore size membrane for the treatment of Type 1 brine with feed concentration of 65 g/L at a feed temperature of 80˚C.

Appendix A.1

Data from Experiment 1: Test number 1

Below in Table A- 1 the operating conditions are illustrated for the MD process and included are the membrane specifications:

Table A- 1: Membrane specification and initial operating conditions of experimental run

Membrane used	HVHP
Membrane pore size (µm)	0.45
Membrane Area (m^2)	0,00434
Feed Temperature (^oC)	80
Product Temperature (^oC)	10
Temperature Difference (^oC)	70
Feed Agitator (RPM)	600
Permeate Agitator (RPM)	600
Feed Flowrate (l/hr)	130
Permeate Flowrate (l/hr)	130
Feed Solution (g/L)	NaCl
	65
Feed volume (mL)	4000

Table A- 2: Test number 1 of experimental matrix for Experiment 1 (Run 1)

		Feed	Permeate			
	Time (min)	EC01 (mS/cm)	EC02 (µS/cm)	$Flux_P$ (L/m2.hr)	Salt Rejection (%)	ΔVP (ml)
RUN 1	0	92,20	4,44		100,00	
	10	93,30	5,83	62,54	99,99	45,24
	20	94,50	7,31	31,27	99,99	22,62
	30	95,60	8,84	31,27	99,99	22,62
	40	96,90	9,96	62,54	99,99	45,24
	50	98,00	10,92	87,56	99,99	63,34
	60	99,20	12,15	37,53	99,99	27,14
	70	100,50	13,22	46,91	99,99	33,93
	80	101,80	14,03	62,54	99,99	45,24
	90	103,30	14,82	78,18	99,99	56,55
	100	104,50	15,82	100,07	99,98	72,38
	110	105,90	15,96	46,91	99,98	33,93
	120	107,20	17,33	25,02	99,98	18,10
	130	108,70	18,13	46,91	99,98	33,93
	140	110,20	18,83	78,18	99,98	56,55
	150	111,50	19,64	46,91	99,98	33,93
	160	113,00	20,40	78,18	99,98	56,55
	170	114,50	21,10	68,80	99,98	49,76
	180	116,30	21,90	34,40	99,98	24,88

Table A- 3: Test number 1 of experimental matrix for Experiment 1 (duplicate)

		Feed	Permeate			
	Time (min)	EC01 (mS/cm)	EC02 (µS/cm)	$Flux_P$ (L/m2.hr)	Salt Rejection (%)	ΔVP (ml)
DUP	0	93,00	8,50			
	10	94,40	10,12	50,04	99,99	36,19
	20	95,50	11,25	28,14	99,99	20,36
	30	96,60	12,29	56,29	99,99	40,72
	40	97,90	13,31	37,53	99,99	27,14
	50	98,80	13,61	31,27	99,99	22,62
	60	100,10	14,83	31,27	99,99	22,62
	70	101,40	16,37	62,54	99,98	45,24
	80	102,60	17,01	71,93	99,98	52,03
	90	104,10	18,19	53,16	99,98	38,45
	100	105,20	19,15	62,54	99,98	45,24
	110	106,60	20,10	40,65	99,98	29,41
	120	108,00	21,30	21,89	99,98	15,83
	130	109,70	21,70	109,45	99,98	79,17
	140	111,00	22,50	40,65	99,98	29,41
	150	112,20	23,40	81,31	99,98	58,81
	160	113,80	24,30	18,76	99,98	13,57
	170	115,50	25,50	62,54	99,98	45,24
	180	116,70	26,40	71,93	99,98	52,03

Table A- 4: Test number 1 of experimental matrix for Experiment 1 (triplicate)

		Feed	Permeate			
	Time (min)	EC01 (mS/cm)	EC02 (µS/cm)	$Flux_P$ (L/m2.hr)	Salt Rejection (%)	ΔVP (ml)
TRIP	0	92,50	6,47			
	10	93,60	7,98	56,29	99,99	40,72
	20	94,80	9,28	29,71	99,99	21,49
	30	95,90	10,57	43,78	99,99	31,67
	40	97,20	11,64	50,04	99,99	36,19
	50	98,30	12,27	59,42	99,99	42,98
	60	99,50	13,49	34,40	99,99	24,88
	70	100,80	14,80	54,73	99,99	39,58
	80	102,10	15,52	67,23	99,98	48,63
	90	103,60	16,51	65,67	99,98	47,50
	100	104,80	17,49	81,31	99,98	58,81
	110	106,20	18,03	43,78	99,98	31,67
	120	107,50	19,32	23,45	99,98	16,96
	130	109,00	19,92	78,18	99,98	56,55
	140	110,50	20,67	59,42	99,98	42,98
	150	111,80	21,52	64,11	99,98	46,37
	160	113,30	22,35	48,47	99,98	35,06
	170	114,80	23,30	65,67	99,98	47,50
	180	116,60	24,15	37,53	99,98	27,14

Table A- 5: Average experimental flux rate for test number 1 of Experiment 1

Time (min)	Average $Flux_P$ ($L/m^2.hr$)
0	0,00
10	56,29
20	29,71
30	43,78
40	50,04
50	59,42
60	34,40
70	54,73
80	67,23
90	65,67
100	81,31
110	43,78
120	23,45
130	78,18
140	59,42
150	64,11
160	48,47
170	65,67
180	47,95

APPENDIX A.2

Data from Experiment 1: Test number 2

MD experimental runs using 0.22 μm pore size membrane for the treatment of Type 1 brine with feed concentration of 35 g/L at a feed temperature of 60˚C.

Appendix A.2

Data from Experiment 1: Test number 2

Below in Table A- 6 the operating conditions is illustrated for the MD process and included are the membrane specifications:

Table A- 6: Membrane specification and initial operating conditions of experimental run

Membrane used	HVHP
Membrane pore size (µm)	0.45
Membrane Area (m^2)	0,00434
Feed Temperature (^oC)	80
Product Temperature (^oC)	10
Temperature Difference (^oC)	70
Feed Agitator (RPM)	600
Permeate Agitator (RPM)	600
Feed Flowrate (l/hr)	130
Permeate Flowrate (l/hr)	130
Feed Solution (g/L)	NaCl
	65
Feed volume (mL)	4000

Table A- 7: Test number 2 of experimental matrix for Experiment 1 (Run 1)

		Feed	Permeate			
	Time (min)	EC01 (mS/cm)	EC02 (µS/cm)	FluxP (L/m2.hr)	Salt Rejection (%)	ΔVP (ml)
RUN 1	0	53,90	3,30		99,99	
	10	54,40	3,35	15,64	99,99	11,31
	20	55,10	3,40	-	99,99	
	30	55,50	3,42	15,64	99,99	11,31
	40	56,10	3,43	34,40	99,99	24,88
	50	56,70	3,43	40,65	99,99	29,41
	60	57,30	3,44	3,13	99,99	2,26
	70	57,90	3,50	37,53	99,99	27,14
	80	58,60	3,55	-	99,99	0,00
	90	59,30	3,58	43,78	99,99	31,67
	100	60,00	3,60	6,25	99,99	4,52
	110	60,60	3,62	28,14	99,99	20,36
	120	61,30	3,63	40,65	99,99	29,41
	130	62,00	3,68	12,51	99,99	9,05
	140	62,80	3,73	40,65	99,99	29,41
	150	63,50	3,75	9,38	99,99	6,79
	160	64,20	3,84	43,78	99,99	31,67
	170	65,20	3,91	9,38	99,99	6,79
	180	65,90	3,97	43,78	99,99	31,67

Table A- 8: Test number 2 of experimental matrix for Experiment 1 (duplicate)

		Feed	Permeate			
	Time (min)	EC01 (mS/cm)	EC02 (µS/cm)	FluxP (L/m2.hr)	Salt Rejection (%)	ΔVP (ml)
DUP	0	54,50	4,02			
	10	54,90	4,02	-	99,99	0,00
	20	55,30	4,09	31,27	99,99	22,62
	30	55,70	4,11	21,89	99,99	15,83
	40	56,20	4,13	25,02	99,99	18,10
	50	56,60	4,15	31,27	99,99	22,62
	60	57,10	4,19	15,64	99,99	11,31
	70	57,60	4,20	15,64	99,99	11,31
	80	58,10	4,22	18,76	99,99	13,57
	90	58,60	4,24	37,53	99,99	27,14
	100	59,10	4,27	37,53	99,99	27,14
	110	59,60	4,29	37,53	99,99	27,14
	120	60,10	4,30	-	99,99	0,00
	130	60,60	4,32	40,65	99,99	29,41
	140	61,20	4,35	21,89	99,99	15,83
	150	61,70	4,39	9,38	99,99	6,79
	160	62,20	4,41	31,27	99,99	22,62
	170	62,90	4,43	15,64	99,99	11,31
	180	63,40	4,50	25,02	99,99	18,10

Table A- 9: Test number 1 of experimental matrix for Experiment 1 (triplicate)

		Feed	Permeate			
	Time (min)	EC01 (mS/cm)	EC02 (µS/cm)	FluxP (L/m2.hr)	Salt Rejection (%)	ΔVP (ml)
TRIP	0	54,00	4,54			
	10	54,60	4,60	62,54	99,99	45,24
	20	55,10	4,64	46,91	99,99	33,93
	30	55,50	4,65	9,38	99,99	6,79
	40	56,00	4,66	46,91	99,99	33,93
	50	56,50	4,68	6,25	99,99	4,52
	60	57,00	4,70	15,64	99,99	11,31
	70	57,50	4,73	18,76	99,99	13,57
	80	58,00	4,76	12,51	99,99	9,05
	90	58,40	4,80	25,02	99,99	18,10
	100	59,00	4,82	-	99,99	0,00
	110	59,50	4,86	37,53	99,99	27,14
	120	60,00	4,95	31,27	99,99	22,62
	130	60,50	4,98	18,76	99,99	13,57
	140	61,20	5,03	25,02	99,99	18,10
	150	61,90	5,09	12,51	99,99	9,05
	160	62,50	5,13	-	99,99	0,00
	170	63,10	5,17	31,27	99,99	22,62
	180	63,80	5,22	21,89	99,99	15,83

Table A- 10: Average experimental flux rate for test number 2 of Experiment 1

Time (min)	Average FluxP (L/m2.hr)
0	0,00
10	39,09
20	39,09
30	15,64
40	35,44
50	26,06
60	11,47
70	23,98
80	15,64
90	35,44
100	21,89
110	34,40
120	35,96
130	23,98
140	29,19
150	10,42
160	37,53
170	18,76
180	30,23

APPENDIX A.3

Data from Experiment 1: Test number 3

MD experimental runs using 0.45 μm pore size membrane for the treatment of Type 1 brine with feed concentration of 65 g/L at a feed temperature of 40˚C.

Appendix A.3

Data from Response Surface Methodology experiments

Below in Table A- 11 the operating conditions is illustrated for the MD process and included are the membrane specifications:

Table A- 11: Membrane specification and initial operating conditions of experimental run

Membrane used	HVHP
Membrane pore size (µm)	0.45
Membrane Area (m^2)	0,00434
Feed Temperature (^oC)	80
Product Temperature (^oC)	10
Temperature Difference (^oC)	70
Feed Agitator (RPM)	600
Permeate Agitator (RPM)	600
Feed Flowrate (l/hr)	130
Permeate Flowrate (l/hr)	130
Feed Solution (g/L)	NaCl
	65
Feed volume (mL)	4000

Table A- 12: Test number 3 of experimental matrix for Experiment 1 (Run 1)

			Feed		Permeate	
	Time (min)	EC01 (mS/cm)	EC02 (µS/cm)	FluxP (L/m2.hr)	Salt Rejection (%)	ΔVP (ml)
RUN 1	0	87,70	3,54		100,00	
	10	88,10	3,90	-	100,00	0,00
	20	88,50	3,96	-	100,00	0,00
	30	88,90	4,00	-	100,00	0,00
	40	89,00	4,03	3,13	100,00	2,26
	50	89,40	4,15	3,13	100,00	2,26
	60	89,70	4,17	12,51	100,00	9,05
	70	90,00	4,19	3,13	100,00	2,26
	80	90,30	4,25	6,25	100,00	4,52
	90	90,40	4,28	9,38	100,00	6,79
	100	90,90	4,30	12,51	100,00	9,05
	110	91,10	4,36	6,25	100,00	4,52
	120	91,50	4,39	6,25	100,00	4,52
	130	91,70	4,41	9,38	100,00	6,79
	140	92,20	4,46	9,38	100,00	6,79
	150	92,30	4,48	9,38	100,00	6,79
	160	92,70	4,50	9,38	100,00	6,79
	170	93,00	4,53	12,51	100,00	9,05
	180	93,30	4,58	3,13	100,00	2,26

Table A- 13: Test number 3 of experimental matrix for Experiment 1 (duplicate)

			Feed		Permeate	
	Time (min)	EC01 (mS/cm)	EC02 (µS/cm)	FluxP (L/m2.hr)	Salt Rejection (%)	ΔVP (ml)
DUP	0	88,70	4,02			
	10	89,00	4,02	-	100,00	0,00
	20	89,30	4,09	-	100,00	0,00
	30	89,60	4,10	-	100,00	0,00
	40	89,90	4,13	6,25	100,00	4,52
	50	90,20	4,16	-	100,00	0,00
	60	90,40	4,17	6,25	100,00	4,52
	70	90,70	4,19	6,25	100,00	4,52
	80	91,00	4,22	6,25	100,00	4,52
	90	91,40	4,24	3,13	100,00	2,26
	100	91,50	4,27	3,13	100,00	2,26
	110	91,90	4,29	15,64	100,00	11,31
	120	92,30	4,30	9,38	100,00	6,79
	130	92,50	4,32	3,13	100,00	2,26
	140	92,80	4,35	6,25	100,00	4,52
	150	93,20	4,39	15,64	100,00	11,31
	160	93,40	4,41	3,13	100,00	2,26
	170	93,70	4,43	3,13	100,00	2,26
	180	93,90	4,50	6,25	100,00	4,52

Table A- 14: Test number 3 of experimental matrix for Experiment 1 (triplicate)

			Feed		Permeate	
	Time (min)	EC01 (mS/cm)	EC02 (µS/cm)	FluxP (L/m2.hr)	Salt Rejection (%)	ΔVP (ml)
TRIP	0	88,80	3,97			
	10	89,00	3,99	-	100,00	0,00
	20	89,20	4,01	-	100,00	0,00
	30	89,50	4,05	3,13	100,00	2,26
	40	89,90	4,09	-	100,00	0,00
	50	90,20	4,17	-	100,00	0,00
	60	90,40	4,24	3,13	100,00	2,26
	70	90,60	4,28	-	100,00	0,00
	80	91,00	4,30	3,13	100,00	2,26
	90	91,20	4,35	3,13	100,00	2,26
	100	91,50	4,37	-	100,00	0,00
	110	91,90	4,41	3,13	100,00	2,26
	120	92,30	4,47	3,13	100,00	2,26
	130	92,60	4,50	12,51	100,00	9,05
	140	92,80	4,53	9,38	100,00	6,79
	150	93,20	4,55	6,25	100,00	4,52
	160	93,50	4,59	3,13	100,00	2,26
	170	93,80	4,65	37,53	100,00	27,14
	180	94,10	4,70	15,64	100,00	11,31

Table A- 15: Average experimental flux rate for test number 3 of Experiment 1

Time (min)	Average FluxP (L/m2.hr)
0	-
10	-
20	-
30	3,13
40	4,69
50	3,13
60	7,30
70	4,69
80	5,21
90	5,21
100	7,82
110	8,34
120	6,25
130	8,34
140	8,34
150	10,42
160	5,21
170	17,72
180	8,34

APPENDIX A.4

Data from Experiment 1: Test number 4

MD experimental runs using 0.22 μm pore size membrane for the treatment of Type 1 brine with feed concentration of 50 g/L at a feed temperature of 40˚C.

Appendix A.4

Data from Response Surface Methodology experiments

Below in Table A- 16 the operating conditions is illustrated for the MD process and included are the membrane specifications:

Table A- 16: Membrane specification and initial operating conditions of experimental run

Membrane used	HVHP
Membrane pore size (µm)	0.45
Membrane Area (m^2)	0,00434
Feed Temperature (^oC)	80
Product Temperature (^oC)	10
Temperature Difference (^oC)	70
Feed Agitator (RPM)	600
Permeate Agitator (RPM)	600
Feed Flowrate (l/hr)	130
Permeate Flowrate (l/hr)	130
Feed Solution (g/L)	NaCl
	65
Feed volume (mL)	4000

Table A- 17: Test number 4 of experimental matrix for Experiment 1 (Run 1)

			Feed		Permeate	
	Time (min)	EC01 (mS/cm)	EC02 (µS/cm)	FluxP (L/m2.hr)	Salt Rejection (%)	ΔVP (ml)
RUN 1	0	70,50	6,70			
	10	70,90	7,10	-	99,99	0,00
	20	71,00	7,18	-	99,99	
	30	71,30	7,98	-	99,99	0,00
	40	71,40	8,07	-	99,99	0,00
	50	71,60	8,14	-	99,99	0,00
	60	71,60	8,35	-	99,99	0,00
	70	71,80	8,59	-	99,99	0,00
	80	72,10	8,62	-	99,99	0,00
	90	72,20	8,66	-	99,99	0,00
	100	72,30	8,74	31,27	99,99	22,62
	110	72,60	8,78	-	99,99	0,00
	120	72,70	8,83	15,64	99,99	11,31
	130	72,90	8,86	15,64	99,99	11,31
	140	73,10	8,90	-	99,99	0,00
	150	73,30	8,99	-	99,99	0,00
	160	73,50	9,09	-	99,99	0,00
	170	73,70	9,11	15,64	99,99	11,31
	180	73,70	9,23	15,64	99,99	11,31

Table A- 18: Test number 4 of experimental matrix for Experiment 1 (duplicate)

			Feed		Permeate	
	Time (min)	EC01 (mS/cm)	EC02 (µS/cm)	FluxP (L/m2.hr)	Salt Rejection (%)	ΔVP (ml)
DUP	0	69,80	5,02			
	10	70,10	5,09	-	99,99	0,00
	20	70,40	5,14	15,64	99,99	11,31
	30	70,60	5,16	31,27	99,99	22,62
	40	70,80	5,24	9,38	99,99	6,79
	50	71,00	5,36	6,25	99,99	4,52
	60	71,30	5,46	-	99,99	0,00
	70	71,50	5,64	6,25	99,99	4,52
	80	71,70	5,75	6,25	99,99	4,52
	90	71,80	5,80	12,51	99,99	9,05
	100	72,00	5,85	6,25	99,99	4,52
	110	72,30	5,86	21,89	99,99	15,83
	120	72,50	6,00	9,38	99,99	6,79
	130	72,70	6,01	6,25	99,99	4,52
	140	72,80	6,15	6,25	99,99	4,52
	150	73,20	6,27	6,25	99,99	4,52
	160	73,40	6,29	-	99,99	0,00
	170	73,60	6,51	18,76	99,99	13,57
	180	73,90	6,70	9,38	99,99	6,79

Table A- 19: Test number 4 of experimental matrix for Experiment 1 (triplicate)

			Feed		Permeate	
	Time (min)	EC01 (mS/cm)	EC02 (µS/cm)	FluxP (L/m2.hr)	Salt Rejection (%)	ΔVP (ml)
TRIP	0	71,70	5,35			
	10	72,00	5,55	-	99,99	0,00
	20	72,50	6,74	-	99,99	0,00
	30	72,80	6,30	-	99,99	0,00
	40	73,10	6,79	-	99,99	0,00
	50	73,30	6,90	-	99,99	0,00
	60	73,60	6,91	-	99,99	0,00
	70	73,80	6,96	-	99,99	0,00
	80	73,90	7,05	6,25	99,99	4,52
	90	74,30	7,23	9,38	99,99	6,79
	100	74,50	7,28	3,13	99,99	2,26
	110	74,80	7,31	9,38	99,99	6,79
	120	75,00	7,47	9,38	99,99	6,79
	130	75,30	7,65	15,64	99,99	11,31
	140	75,50	7,76	9,38	99,99	6,79
	150	75,70	7,86	6,25	99,99	4,52
	160	76,00	7,97	9,38	99,99	6,79
	170	76,30	8,01	15,64	99,99	11,31
	180	76,70	8,08	6,25	99,99	4,52

Table A- 20: Average experimental flux rate for test number 4 of Experiment 1

Time (min)	Average $Flux_P$ (L/m2.hr)
0	-
10	-
20	15,64
30	31,27
40	9,38
50	6,25
60	-
70	6,25
80	6,25
90	10,95
100	13,55
110	15,64
120	11,47
130	12,51
140	7,82
150	6,25
160	9,38
170	16,68
180	10,42

APPENDIX A.5

Data from Experiment 1: Test number 5

MD experimental runs using 0.45 μm pore size membrane for the treatment of Type 1 brine with feed concentration of 50 g/L at a feed temperature of 60˚C.

Appendix A.5

Data from Experiment 3: Test number 5

Below in Table A- 21 the operating conditions is illustrated for the MD process and included are the membrane specifications:

Table A- 21: Membrane specification and initial operating conditions of experimental run

Membrane used	HVHP
Membrane pore size (µm)	0.45
Membrane Area (m^2)	0,00434
Feed Temperature (^oC)	80
Product Temperature (^oC)	10
Temperature Difference (^oC)	70
Feed Agitator (RPM)	600
Permeate Agitator (RPM)	600
Feed Flowrate (l/hr)	130
Permeate Flowrate (l/hr)	130
Feed Solution (g/L)	NaCl
	65
Feed volume (mL)	4000

Table A- 22: Test number 5 of experimental matrix for Experiment 1 (Run 1)

			Feed		Permeate	
	Time (min)	EC01 (mS/cm)	EC02 (µS/cm)	FluxP (L/m2.hr)	Salt Rejection (%)	ΔVP (ml)
RUN 1	0	72,20	3,34			
	10	73,00	3,36	15,64	100,00	11,31
	20	73,60	3,68	-	100,00	6,79
	30	74,20	3,81	31,27	99,99	22,62
	40	74,70	3,91	21,89	99,99	15,83
	50	75,20	4,04	15,64	99,99	11,31
	60	75,80	4,12	21,89	99,99	15,83
	70	76,30	4,16	9,38	99,99	6,79
	80	76,90	4,21	56,29	99,99	40,72
	90	77,40	4,27	12,51	99,99	9,05
	100	78,00	4,31	50,04	99,99	36,19
	110	78,60	4,40	15,64	99,99	11,31
	120	79,20	4,43	21,89	99,99	15,83
	130	79,80	4,48	6,25	99,99	4,52
	140	80,50	4,56	25,02	99,99	18,10
	150	81,10	4,62	31,27	99,99	22,62
	160	81,70	4,66	31,27	99,99	22,62
	170	82,40	4,73	31,27	99,99	22,62
	180	83,00	4,82	25,02	99,99	18,10

Table A- 23: Test number 5 of experimental matrix for Experiment 1 (duplicate)

			Feed		Permeate	
	Time (min)	EC01 (mS/cm)	EC02 (µS/cm)	FluxP (L/m2.hr)	Salt Rejection (%)	ΔVP (ml)
DUP	0	72,60	3,84			
	10	73,30	3,79	6,25	99,99	4,52
	20	73,90	4,08	31,27	99,99	22,62
	30	74,50	4,18	12,51	99,99	9,05
	40	75,00	4,31	18,76	99,99	13,57
	50	75,60	4,36	28,14	99,99	20,36
	60	76,20	4,46	3,13	99,99	2,26
	70	76,80	4,61	37,53	99,99	27,14
	80	77,30	4,69	40,65	99,99	29,41
	90	78,00	4,83	9,38	99,99	6,79
	100	78,60	4,86	25,02	99,99	18,10
	110	79,20	5,06	15,64	99,99	11,31
	120	79,70	4,98	28,14	99,99	20,36
	130	80,50	5,15	15,64	99,99	11,31
	140	81,20	5,28	21,89	99,99	15,83
	150	81,80	5,47	37,53	99,99	27,14
	160	82,40	6,03	25,02	99,99	18,10
	170	83,10	6,77	31,27	99,99	22,62
	180	83,70	7,26	28,14	99,99	20,36

Table A- 24: Test number 5 of experimental matrix for Experiment 1 (triplicate)

			Feed		Permeate	
	Time (min)	EC01 (mS/cm)	EC02 (µS/cm)	FluxP (L/m2.hr)	Salt Rejection (%)	ΔVP (ml)
TRIP	0	71,20	3,42			
	10	71,90	3,56	15,64		11,31
	20	72,50	3,61	12,51	100,00	9,05
	30	73,00	3,72	28,14	99,99	20,36
	40	73,70	3,79	25,02	99,99	18,10
	50	74,40	3,91	12,51	99,99	9,05
	60	75,10	4,01	18,76	99,99	13,57
	70	75,80	4,09	15,64	99,99	11,31
	80	76,30	4,19	31,27	99,99	22,62
	90	77,00	4,31	37,53	99,99	27,14
	100	77,80	4,53	15,64	99,99	11,31
	110	78,50	4,60	6,25	99,99	4,52
	120	79,30	4,78	28,14	99,99	20,36
	130	80,00	4,84	25,02	99,99	18,10
	140	80,70	4,92	31,27	99,99	22,62
	150	81,30	5,03	28,14	99,99	20,36
	160	82,00	5,16	34,40	99,99	24,88
	170	82,70	5,29	34,40	99,99	24,88
	180	83,00	5,46	28,14	99,99	20,36

Table A- 25: Average experimental flux rate for test number 5 of Experiment 1

Time (min)	Average FluxP (L/m2.hr)
0	0,00
10	12,51
20	21,89
30	23,98
40	21,89
50	18,76
60	14,59
70	20,85
80	42,74
90	19,81
100	30,23
110	12,51
120	26,06
130	15,64
140	26,06
150	32,31
160	30,23
170	32,31
180	27,10

APPENDIX A.6

Data from Experiment 1: Test number 6

MD experimental runs using 0.22 µm pore size membrane for the treatment of Type 1 brine with feed concentration of 35 g/L at a feed temperature of 80˚C.

Appendix A.6

Data from Experiment 3: Test number 6

Below in Table A- 26 the operating conditions is illustrated for the MD process and included are the membrane specifications:

Table A- 26: Membrane specification and initial operating conditions of experimental run

Membrane used	HVHP
Membrane pore size (µm)	0.45
Membrane Area (m^2)	0,00434
Feed Temperature (^oC)	80
Product Temperature (^oC)	10
Temperature Difference (^oC)	70
Feed Agitator (RPM)	600
Permeate Agitator (RPM)	600
Feed Flowrate (l/hr)	130
Permeate Flowrate (l/hr)	130
Feed Solution (g/L)	NaCl
	65
Feed volume (mL)	4000

Table A- 27: Test number 6 of experimental matrix for Experiment 1 (Run 1)

			Feed		Permeate	
	Time (min)	EC01 (mS/cm)	EC02 (µS/cm)	FluxP (L/m2.hr)	Salt Rejection (%)	ΔVP (ml)
RUN 1	0	56,40	2,63			
	10	57,20	3,73	31,27	99,98	22,62
	20	58,00	4,06	93,82	99,98	67,86
	30	58,70	4,32	84,43	99,98	61,07
	40	59,40	4,56	65,67	99,98	47,50
	50	60,20	4,81	21,89	99,98	15,83
	60	60,90	4,98	15,64	99,98	11,31
	70	61,70	5,31	78,18	99,98	56,55
	80	62,60	5,55	62,54	99,98	45,24
	90	63,50	5,77	31,27	99,98	22,62
	100	64,40	6,00	62,54	99,98	45,24
	110	65,10	6,28	62,54	99,98	45,24
	120	66,20	6,66	71,93	99,98	52,03
	130	67,20	6,88	37,53	99,99	27,14
	140	68,20	7,29	46,91	99,99	33,93
	150	69,20	7,62	96,94	99,99	70,12
	160	70,10	8,01	28,14	99,99	20,36
	170	71,20	8,38	78,18	99,99	56,55
	180	72,30	8,88	25,02	99,99	18,10

Table A- 28: Test number 6 of experimental matrix for Experiment 1 (duplicate)

			Feed		Permeate	
	Time (min)	EC01 (mS/cm)	EC02 (µS/cm)	FluxP (L/m2.hr)	Salt Rejection (%)	ΔVP (ml)
DUP	0	55,80	4,98			
	10	56,50	5,94	31,27	99,98	22,62
	20	57,20	6,20	43,78	99,98	31,67
	30	58,10	6,80	34,40	99,98	24,88
	40	58,80	7,19	15,64	99,98	11,31
	50	59,50	7,58	50,04	99,98	36,19
	60	60,30	7,97	43,78	99,98	31,67
	70	61,10	8,24	46,91	99,98	33,93
	80	61,90	8,69	46,91	99,98	33,93
	90	62,70	9,19	46,91	99,98	33,93
	100	63,70	9,35	59,42	99,98	42,98
	110	64,60	9,95	56,29	99,98	40,72
	120	65,40	10,67	34,40	99,98	24,88
	130	66,40	11,11	37,53	99,98	27,14
	140	67,40	11,56	93,82	99,99	67,86
	150	68,30	12,05	50,04	99,99	36,19
	160	69,30	12,56	43,78	99,99	31,67
	170	70,30	12,93	31,27	99,99	22,62
	180	71,40	13,38	156,36	99,99	113,10

Table A- 29: Test number 6 of experimental matrix for Experiment 1 (triplicate)

			Feed		Permeate	
	Time (min)	EC01 (mS/cm)	EC02 (µS/cm)	FluxP (L/m2.hr)	Salt Rejection (%)	ΔVP (ml)
TRIP	0	56,00	4,63			
	10	56,70	5,73	31,27	99,98	22,62
	20	57,40	6,06	93,82	99,98	67,86
	30	58,20	6,32	84,43	99,98	61,07
	40	59,00	6,56	65,67	99,98	47,50
	50	59,90	6,81	21,89	99,98	15,83
	60	60,70	6,98	15,64	99,98	11,31
	70	61,40	7,31	78,18	99,98	56,55
	80	62,30	7,55	62,54	99,98	45,24
	90	63,20	7,77	31,27	99,98	22,62
	100	64,40	8,00	62,54	99,98	45,24
	110	65,20	8,28	62,54	99,98	45,24
	120	66,00	8,66	71,93	99,98	52,03
	130	67,10	8,88	37,53	99,99	27,14
	140	68,00	9,29	46,91	99,99	33,93
	150	68,90	9,62	96,94	99,98	70,12
	160	69,90	10,01	28,14	99,99	20,36
	170	70,80	10,38	78,18	99,99	56,55
	180	71,80	10,88	40,65	99,99	29,41

Table A- 30: Average experimental flux rate for test number 6 of Experiment 1

Time (min)	Average FluxP (L/m2.hr)
0	0,00
10	31,27
20	77,14
30	67,76
40	48,99
50	31,27
60	25,02
70	67,76
80	57,33
90	36,48
100	61,50
110	60,46
120	59,42
130	37,53
140	62,54
150	81,31
160	33,36
170	62,54
180	74,01

APPENDIX A.7

Data from Experiment 1: Test number 7

MD experimental runs using 0.45 μm pore size membrane for the treatment of Type 1 brine with feed concentration of 35 g/L at a feed temperature of 40˚C.

Appendix A.7

Data from Experiment 3: Test number 7

Below in Table A- 31 the operating conditions is illustrated for the MD process and included are the membrane specifications:

Table A- 31: Membrane specification and initial operating conditions of experimental run

Membrane used	HVHP
Membrane pore size (µm)	0.45
Membrane Area (m^2)	0,00434
Feed Temperature (^oC)	80
Product Temperature (^oC)	10
Temperature Difference (^oC)	70
Feed Agitator (RPM)	600
Permeate Agitator (RPM)	600
Feed Flowrate (l/hr)	130
Permeate Flowrate (l/hr)	130
Feed Solution (g/L)	NaCl
	65
Feed volume (mL)	4000

Table A- 32: Test number 7 of experimental matrix for Experiment 1 (Run 1)

			Feed		Permeate	
	Time (min)	EC01 (mS/cm)	EC02 (µS/cm)	FluxP (L/m2.hr)	Salt Rejection (%)	ΔVP (ml)
RUN 1	0	52,40	4,50			
	10	52,70	4,56	-	99,99	0,00
	20	52,90	4,60	-	99,99	0,00
	30	53,10	4,68	3,13	99,99	2,26
	40	53,30	4,80	15,64	99,99	11,31
	50	53,50	4,81	6,25	99,99	4,52
	60	53,70	4,82	6,25	99,99	4,52
	70	53,90	4,86	9,38	99,99	6,79
	80	54,00	4,92	3,13	99,99	2,26
	90	54,20	4,94	-	99,99	0,00
	100	54,50	4,94	6,25	99,99	4,52
	110	54,70	4,96	-	99,99	0,00
	120	54,90	4,98	-	99,99	0,00
	130	55,10	5,00	6,25	99,99	4,52
	140	55,30	5,06	6,25	99,99	4,52
	150	55,50	5,17	9,38	99,99	6,79
	160	55,60	5,20	6,25	99,99	4,52
	170	55,80	5,32	9,38	99,99	6,79
	180	56,10	5,46	3,13	99,99	2,26

Table A- 33: Test number 7 of experimental matrix for Experiment 1 (duplicate)

			Feed		Permeate	
	Time (min)	EC01 (mS/cm)	EC02 (µS/cm)	FluxP (L/m2.hr)	Salt Rejection (%)	ΔVP (ml)
DUP	0	52,10	5,20			
	10	52,30	5,30	-	99,99	0,00
	20	52,50	5,37	9,38	99,99	6,79
	30	52,70	5,50	9,38	99,99	6,79
	40	52,70	5,53	9,38	99,99	6,79
	50	52,90	5,60	6,25	99,99	4,52
	60	53,20	5,70	-	99,99	0,00
	70	53,40	5,75	9,38	99,99	6,79
	80	53,50	5,79	6,25	99,99	4,52
	90	53,70	5,85	-	99,99	0,00
	100	53,90	5,91	9,38	99,99	6,79
	110	54,10	5,95	9,38	99,99	6,79
	120	54,30	6,00	9,38	99,99	6,79
	130	54,50	6,07	15,64	99,99	11,31
	140	54,70	6,15	3,13	99,99	2,26
	150	54,90	6,24	9,38	99,99	6,79
	160	55,00	6,31	6,25	99,99	4,52
	170	55,20	6,36	15,64	99,99	11,31
	180	55,40	6,40	9,38	99,99	6,79

Table A- 34: Test number 7 of experimental matrix for Experiment 1 (triplicate)

			Feed		Permeate	
	Time (min)	EC01 (mS/cm)	EC02 (µS/cm)	FluxP (L/m2.hr)	Salt Rejection (%)	ΔVP (ml)
TRIP	0	48,80	3,73			
	10	48,80	3,74	-	99,99	0,00
	20	48,90	3,97	-	99,99	0,00
	30	49,00	4,02	-	99,99	0,00
	40	49,10	4,06	6,25	99,99	4,52
	50	49,30	4,10	-	99,99	0,00
	60	49,40	4,17	-	99,99	0,00
	70	49,50	4,22	9,38	99,99	6,79
	80	49,70	4,32	3,13	99,99	2,26
	90	49,80	4,40	6,25	99,99	4,52
	100	50,00	4,49	3,13	99,99	2,26
	110	50,20	4,53	3,13	99,99	2,26
	120	50,30	4,66	6,25	99,99	4,52
	130	50,50	4,73	-	99,99	0,00
	140	50,70	4,89	9,38	99,99	6,79
	150	50,80	4,96	12,51	99,99	9,05
	160	51,00	5,08	6,25	99,99	4,52
	170	51,10	5,15	15,64	99,99	11,31
	180	51,10	5,25	50,04	99,99	36,19

Table A- 35: Average experimental flux rate for test number 7 of Experiment 1

Time (min)	Average FluxP (L/m2.hr)
0	0,00
10	-
20	9,38
30	6,25
40	10,42
50	6,25
60	6,25
70	9,38
80	4,17
90	6,25
100	6,25
110	6,25
120	7,82
130	10,95
140	6,25
150	10,42
160	6,25
170	13,55
180	20,85

APPENDIX A.8

Data from Experiment 1: Test number 8

MD experimental runs using 0.22 μm pore size membrane for the treatment of Type 1 brine with feed concentration of 65 g/L at a feed temperature of 60˚C.

Appendix A.8

Data from Experiment 3: Test number 8

Below in Table A- 36 the operating conditions is illustrated for the MD process and included are the membrane specifications:

Table A- 36: Membrane specification and initial operating conditions of experimental run

Membrane used	HVHP
Membrane pore size (µm)	0.45
Membrane Area (m^2)	0,00434
Feed Temperature (^oC)	80
Product Temperature (^oC)	10
Temperature Difference (^oC)	70
Feed Agitator (RPM)	600
Permeate Agitator (RPM)	600
Feed Flowrate (l/hr)	130
Permeate Flowrate (l/hr)	130
Feed Solution (g/L)	NaCl
	65
Feed volume (mL)	4000

Table A- 37:Test number 8 of experimental matrix for Experiment 1 (Run 1)

			Feed		Permeate	
	Time (min)	EC01 (mS/cm)	EC02 (µS/cm)	FluxP (L/m2.hr)	Salt Rejection (%)	ΔVP (ml)
RUN 1	0	91,00	3,34			
	10	91,80	3,35	9,38	100,00	6,79
	20	92,40	4,24	-	100,00	0,00
	30	92,90	4,36	62,54	100,00	45,24
	40	93,40	4,93	15,64	99,99	11,31
	50	94,00	5,29	25,02	99,99	18,10
	60	94,60	5,36	28,14	99,99	20,36
	70	95,30	5,65	-	99,99	0,00
	80	95,90	5,81	9,38	99,99	6,79
	90	96,60	6,00	18,76	99,99	13,57
	100	97,10	6,34	53,16	99,99	38,45
	110	97,90	6,37	-	99,99	0,00
	120	98,40	6,45	43,78	99,99	31,67
	130	99,20	6,65	50,04	99,99	36,19
	140	99,90	6,86	-	99,99	0,00
	150	100,50	6,95	34,40	99,99	24,88
	160	101,10	7,15	-	99,99	0,00
	170	101,80	7,37	21,89	99,99	15,83
	180	102,60	7,64	59,42	99,99	42,98

Table A- 38: Test number 8 of experimental matrix for Experiment 1 (duplicate)

			Feed		Permeate	
	Time (min)	EC01 (mS/cm)	EC02 (µS/cm)	FluxP (L/m2.hr)	Salt Rejection (%)	ΔVP (ml)
DUP	0	91,20	4,40			
	10	92,00	4,75	6,25	99,99	4,52
	20	92,50	5,46	12,51	99,99	9,05
	30	93,00	5,84	6,25	99,99	4,52
	40	93,70	6,47	12,51	99,99	9,05
	50	94,30	6,99	40,65	99,99	29,41
	60	94,80	7,51	15,64	99,99	11,31
	70	95,40	7,67	15,64	99,99	11,31
	80	95,90	7,70	31,27	99,99	22,62
	90	96,60	7,97	-	99,99	0,00
	100	97,20	8,29	46,91	99,99	33,93
	110	97,80	8,55	15,64	99,99	11,31
	120	98,50	8,84	21,89	99,99	15,83
	130	99,20	9,11	18,76	99,99	13,57
	140	99,80	9,25	37,53	99,99	27,14
	150	100,40	9,51	25,02	99,99	18,10
	160	101,10	9,86	6,25	99,99	4,52
	170	101,60	10,15	12,51	99,99	9,05
	180	102,40	10,40	31,27	99,99	22,62

Table A- 39: Test number 8 of experimental matrix for Experiment 1 (triplicate)

			Feed		Permeate	
	Time (min)	EC01 (mS/cm)	EC02 (µS/cm)	FluxP (L/m2.hr)	Salt Rejection (%)	ΔVP (ml)
TRIP	0	91,30	4,01			
	10	91,94	4,02	15,64	100,00	11,31
	20	92,58	4,91	18,76	99,99	13,57
	30	93,22	5,03	3,13	99,99	2,26
	40	93,86	5,60	25,02	99,99	18,10
	50	94,50	5,96	37,53	99,99	27,14
	60	95,14	6,03	15,64	99,99	11,31
	70	95,78	6,32	12,51	99,99	9,05
	80	96,42	6,48	34,40	99,99	24,88
	90	97,06	6,67	25,02	99,99	18,10
	100	97,70	7,01	28,14	99,99	20,36
	110	98,34	7,04	34,40	99,99	24,88
	120	98,98	7,12	46,91	99,99	33,93
	130	99,62	7,32	31,27	99,99	22,62
	140	100,26	7,53	-	99,99	0,00
	150	100,90	7,62	37,53	99,99	27,14
	160	101,54	7,82	18,76	99,99	13,57
	170	102,18	8,04	12,51	99,99	9,05
	180	102,82	8,31	21,89	99,99	15,83

Table A- 40: Average experimental flux rate for test number 8 of Experiment 1

Time (min)	Average FluxP (L/m2.hr)
0	0,00
10	10,42
20	15,64
30	23,98
40	17,72
50	34,40
60	19,81
70	14,07
80	25,02
90	21,89
100	42,74
110	25,02
120	37,53
130	33,36
140	37,53
150	32,31
160	12,51
170	15,64
180	37,53

APPENDIX A.9

Data from Experiment 1: Test number 9

MD experimental runs using 0.45 μm pore size membrane for the treatment of Type 1 brine with feed concentration of 35 g/L at a feed temperature of 80˚C.

Appendix A.9

Data from Experiment 3: Test number 9

Below in Table A- 41 the operating conditions is illustrated for the MD process and included are the membrane specifications:

Table A- 41: Membrane specification and initial operating conditions of experimental run

Membrane used	HVHP
Membrane pore size (µm)	0.45
Membrane Area (m^2)	0,00434
Feed Temperature (^oC)	80
Product Temperature (^oC)	10
Temperature Difference (^oC)	70
Feed Agitator (RPM)	600
Permeate Agitator (RPM)	600
Feed Flowrate (l/hr)	130
Permeate Flowrate (l/hr)	130
Feed Solution (g/L)	NaCl
	65
Feed volume (mL)	4000

Table A- 42: Test number 9 of experimental matrix for Experiment 1 (Run 1)

			Feed		Permeate	
	Time (min)	EC01 (mS/cm)	EC02 (µS/cm)	FluxP (L/m2.hr)	Salt Rejection (%)	ΔVP (ml)
RUN 1	0	55,70	3,93			
	10	56,40	4,24	46,91	99,99	33,93
	20	57,20	4,69	-	99,99	
	30	58,00	5,11	25,02	99,99	18,10
	40	58,80	5,64	78,18	99,99	56,55
	50	59,70	6,14	62,54	99,99	45,24
	60	60,40	6,53	46,91	99,99	33,93
	70	61,50	7,14	62,54	99,99	45,24
	80	62,40	7,51	71,93	99,99	52,03
	90	63,40	8,51	37,53	99,99	27,14
	100	64,20	9,32	46,91	99,99	33,93
	110	65,30	9,99	78,18	99,98	56,55
	120	66,30	10,66	62,54	99,98	45,24
	130	67,40	11,08	31,27	99,98	22,62
	140	68,50	11,94	62,54	99,98	45,24
	150	69,40	12,52	62,54	99,98	45,24
	160	70,70	13,28	62,54	99,98	45,24
	170	71,80	13,93	46,91	99,98	33,93
	180	72,80	14,42	31,27	99,98	22,62

Table A- 43: Test number 9 of experimental matrix for Experiment 1 (duplicate)

			Feed		Permeate	
	Time (min)	EC01 (mS/cm)	EC02 (µS/cm)	FluxP (L/m2.hr)	Salt Rejection (%)	ΔVP (ml)
DUP	0	56,10	11,99			
	10	56,80	12,33	62,54	99,98	45,24
	20	57,70	12,74	56,29	99,98	40,72
	30	58,30	13,07	62,54	99,98	45,24
	40	59,00	13,45	62,54	99,98	45,24
	50	60,00	14,06	56,29	99,98	40,72
	60	60,80	14,49	43,78	99,98	31,67
	70	61,50	15,01	50,04	99,98	36,19
	80	62,40	15,45	37,53	99,98	27,14
	90	63,30	15,93	53,16	99,97	38,45
	100	64,10	16,40	43,78	99,97	31,67
	110	64,90	16,74	50,04	99,97	36,19
	120	66,10	17,12	71,93	99,97	52,03
	130	66,90	17,48	68,80	99,97	49,76
	140	67,90	17,89	31,27	99,97	22,62
	150	68,80	18,24	62,54	99,97	45,24
	160	69,90	18,46	62,54	99,97	45,24
	170	70,80	18,85	68,80	99,97	49,76
	180	72,00	19,18	71,93	99,97	52,03

Table A- 44: Test number 9 of experimental matrix for Experiment 1 (triplicate)

			Feed		Permeate	
	Time (min)	EC01 (mS/cm)	EC02 (µS/cm)	FluxP (L/m2.hr)	Salt Rejection (%)	ΔVP (ml)
TRIP	0	56,00	5,49			
	10	56,70	5,83	43,78	99,99	31,67
	20	57,50	6,24	40,65	99,99	29,41
	30	58,30	6,57	28,14	99,99	20,36
	40	59,10	6,95	75,05	99,99	54,29
	50	60,00	7,56	59,42	99,99	42,98
	60	60,70	7,99	50,04	99,99	36,19
	70	61,80	8,51	56,29	99,99	40,72
	80	62,70	8,95	78,18	99,99	56,55
	90	63,70	9,43	31,27	99,99	22,62
	100	64,50	9,90	53,16	99,98	38,45
	110	65,60	10,24	65,67	99,98	47,50
	120	66,60	10,62	75,05	99,98	54,29
	130	67,70	10,98	40,65	99,98	29,41
	140	68,80	11,39	62,54	99,98	45,24
	150	69,70	11,74	62,54	99,98	45,24
	160	71,00	11,96	62,54	99,98	45,24
	170	72,10	12,35	46,91	99,98	33,93
	180	73,10	12,68	40,65	99,98	29,41

Table A- 45: Average experimental flux rate for test number 9 of Experiment 1

Time (min)	Average FluxP (L/m2.hr)
0	0,00
10	51,08
20	48,47
30	38,57
40	71,93
50	59,42
60	46,91
70	56,29
80	62,54
90	40,65
100	47,95
110	64,63
120	69,84
130	46,91
140	52,12
150	62,54
160	62,54
170	54,20
180	47,95

APPENDIX A.10

Data from Experiment 1: Test number 10

MD experimental runs using 0.22 μm pore size membrane for the treatment of Type 1 brine with feed concentration of 50 g/L at a feed temperature of 80˚C.

Appendix A.10

Data from Experiment 3: Test number 10

Below in Table A- 46 the operating conditions is illustrated for the MD process and included are the membrane specifications:

Table A- 46: Membrane specification and initial operating conditions of experimental run

Membrane used	HVHP
Membrane pore size (µm)	0.45
Membrane Area (m^2)	0,00434
Feed Temperature (^oC)	80
Product Temperature (^oC)	10
Temperature Difference (^oC)	70
Feed Agitator (RPM)	600
Permeate Agitator (RPM)	600
Feed Flowrate (l/hr)	130
Permeate Flowrate (l/hr)	130
Feed Solution (g/L)	NaCl
	65
Feed volume (mL)	4000

Table A- 47: Test number 10 of experimental matrix for Experiment 1 (Run 1)

		Feed	Permeate			
	Time (min)	EC01 (mS/cm)	EC02 (µS/cm)	FluxP (L/m2.hr)	Salt Rejection (%)	ΔVP (ml)
RUN 1	0	74,90	4,19			
	10	76,10	4,54	56,29	99,99	40,72
	20	76,90	4,83	31,27	99,99	22,62
	30	77,80	5,30	56,29	99,99	40,72
	40	78,90	5,75	40,65	99,99	29,41
	50	79,80	6,06	43,78	99,99	31,67
	60	80,90	6,57	71,93	99,99	52,03
	70	81,90	6,61	34,40	99,99	24,88
	80	83,00	7,66	75,05	99,99	54,29
	90	84,00	8,01	78,18	99,99	56,55
	100	85,00	8,68	25,02	99,99	18,10
	110	86,10	9,16	78,18	99,99	56,55
	120	87,50	9,77	34,40	99,99	24,88
	130	88,40	10,15	62,54	99,99	45,24
	140	89,90	10,97	65,67	99,99	47,50
	150	91,20	11,45	-	99,99	0,00
	160	92,30	12,17	90,69	99,99	65,60
	170	93,70	12,74	21,89	99,99	15,83
	180	95,30	13,28	50,04	99,99	36,19

Table A- 48: Test number 10 of experimental matrix for Experiment 1 (duplicate)

		Feed	Permeate			
	Time (min)	EC01 (mS/cm)	EC02 (µS/cm)	FluxP (L/m2.hr)	Salt Rejection (%)	ΔVP (ml)
DUP	0	75,10	6,90			
	10	76,10	7,55	56,29	99,99	40,72
	20	76,90	8,18	31,27	99,99	22,62
	30	77,90	9,06	21,89	99,99	15,83
	40	79,00	9,86	62,54	99,99	45,24
	50	79,90	10,34	25,02	99,99	18,10
	60	81,00	11,18	62,54	99,99	45,24
	70	81,90	11,55	15,64	99,99	11,31
	80	83,00	12,44	46,91	99,99	33,93
	90	84,20	13,05	100,07	99,98	72,38
	100	85,40	13,61	25,02	99,98	18,10
	110	86,40	14,12	31,27	99,98	22,62
	120	87,40	14,77	62,54	99,98	45,24
	130	88,70	15,57	62,54	99,98	45,24
	140	89,80	16,13	78,18	99,98	56,55
	150	91,00	16,75	-	99,98	0,00
	160	92,30	17,44	31,27	99,98	22,62
	170	93,10	18,12	43,78	99,98	31,67
	180	94,70	18,67	81,31	99,98	58,81

Table A- 49: Test number 10 of experimental matrix for Experiment 1 (triplicate)

		Feed	Permeate			
	Time (min)	EC01 (mS/cm)	EC02 (µS/cm)	FluxP (L/m2.hr)	Salt Rejection (%)	ΔVP (ml)
TRIP	0	75,00	4,19			
	10	76,20	4,54	56,29	99,99	40,72
	20	77,00	4,83	31,27	99,99	22,62
	30	77,90	5,30	56,29	99,99	40,72
	40	79,00	5,75	40,65	99,99	29,41
	50	79,90	6,06	43,78	99,99	31,67
	60	81,00	6,57	71,93	99,99	52,03
	70	82,00	6,61	34,40	99,99	24,88
	80	83,10	7,66	75,05	99,99	54,29
	90	84,10	8,01	56,29	99,99	40,72
	100	85,10	8,68	31,27	99,99	22,62
	110	86,20	9,16	78,18	99,99	56,55
	120	87,60	9,77	34,40	99,99	24,88
	130	88,50	10,15	62,54	99,99	45,24
	140	90,00	10,97	43,78	99,99	31,67
	150	91,30	11,45	31,27	99,99	22,62
	160	92,40	12,17	90,69	99,99	65,60
	170	93,80	12,74	21,89	99,99	15,83
	180	95,40	13,28	50,04	99,99	36,19

Table A- 50: Average experimental flux rate for test number 10 of Experiment 1

Time (min)	Average FluxP (L/m2.hr)
0	0,00
10	56,29
20	31,27
30	44,82
40	47,95
50	37,53
60	68,80
70	28,14
80	65,67
90	78,18
100	27,10
110	62,54
120	43,78
130	62,54
140	62,54
150	31,27
160	70,88
170	29,19
180	60,46

Appendix B

Data from Experiment 2

Investigating the effect of scaling/fouling on the performance of MD using commercially available MD membranes for the treatment of Type 1 brine

Appendix B.1

Data from Experiment 2: Test number 1

Investigating the effect of scaling/fouling on the performance of MD using 0.22 μm pore size membrane for the treatment of Type 1 brine

Appendix B.1

Data from Experiment 2: Test number 1

Below in Table B- 1 the operating conditions is illustrated for the MD process and included are the membrane specifications:

Table B- 1: Membrane specification and initial operating conditions of experimental run

Membrane used	GVHP
Membrane pore size (µm)	0.22
Membrane Area (m^2)	0,00434
Feed Temperature (^oC)	60
Product Temperature (^oC)	10
Temperature Difference (^oC)	50
Feed Agitator (RPM)	600
Permeate Agitator (RPM)	600
Feed Flowrate (l/hr)	130
Permeate Flowrate (l/hr)	130
Feed Solution (g/L)	NaCl
	235
Feed volume (mL)	4000

Table B- 2: Test number 1 data for Experiment 2

	Feed	Permeate			
Time (min)	EC01 (mS/cm)	EC02 (µS/cm)	FluxP (L/m2.hr)	Salt Rejection (%)	ΔVP (ml)
0	203,00	3,99			
30	209,00	4,24	36,48	100,00	79,17
60	211,00	4,67	-	100,00	0,00
90	214,00	4,92	15,64	100,00	33,93
120	218,00	5,38	31,27	100,00	67,86
150	220,00	5,97	15,64	100,00	33,93
180	224,00	6,94	31,27	100,00	67,86
210	227,00	8,17	-	100,00	0,00
240	229,00	9,15	31,27	100,00	67,86
270	235,00	10,65	31,27	100,00	67,86
300	238,00	12,40	10,42	99,99	22,62
330	243,00	13,86	31,27	99,99	67,86
360	250,00	16,48	20,85	99,99	45,24

Appendix B.2

Data from Experiment 2: Test number 2

Investigating the effect of scaling/fouling on the performance of MD using 0.45 μm pore size membrane for the treatment of Type 1 brine

Appendix B.2

Data from Experiment 2: Test number 2

Below in Table B- 3 the operating conditions is illustrated for the MD process and included are the membrane specifications:

Table B- 3: Membrane specification and initial operating conditions of experimental run

Membrane used	HVHP
Membrane pore size (µm)	0.45
Membrane Area (m^2)	0,00434
Feed Temperature (^oC)	80
Product Temperature (^oC)	10
Temperature Difference (^oC)	70
Feed Agitator (RPM)	600
Permeate Agitator (RPM)	600
Feed Flowrate (l/hr)	130
Permeate Flowrate (l/hr)	130
Feed Solution (g/L)	NaCl
	65
Feed volume (mL)	4000

Table B- 4: Test number 2 data for Experiment 2

	Feed	Permeate			
Time (min)	EC01 (mS/cm)	EC02 (µS/cm)	FluxP (L/m2.hr)	Salt Rejection (%)	ΔVP (ml)
0	206,00	3,19			
30	209,00	3,20	5,21	100,00	11,31
60	213,00	3,31	5,21	100,00	11,31
90	217,00	3,67	26,06	100,00	56,55
120	220,00	4,33	20,85	100,00	45,24
150	223,00	5,34	10,42	100,00	22,62
180	227,00	6,30	46,91	100,00	101,79
210	230,00	7,64	26,06	100,00	56,55
240	236,00	10,51	10,42	100,00	22,62
270	237,00	11,46	5,21	100,00	11,31
300	243,00	14,27	52,12	99,99	113,10
330	248,00	16,00	20,85	99,99	45,24
360	253,00	18,25	20,85	99,99	45,24

Appendix C

Data from Experiment 3

Investigating the effect of pore size, Type 2 brine feed concentration and operating feed temperature on MD performance

Appendix C.1

Data from Experiment 3: Test number 1

Below in Table C- 1 the operating conditions is illustrated for the MD process and included are the membrane specifications:

Table C- 1: Membrane specification and initial operating conditions of experimental run

Membrane used	HVHP
Membrane pore size (µm)	0.45
Membrane Area (m^2)	0,00434
Feed Temperature (^oC)	80
Product Temperature (^oC)	10
Temperature Difference (^oC)	70
Feed Agitator (RPM)	600
Permeate Agitator (RPM)	600
Feed Flowrate (l/hr)	130
Permeate Flowrate (l/hr)	130
Feed Solution (g/L)	NaCl
	65
Feed volume (mL)	4000

Table C- 2: Test Number 1 data for Experiment 3 (Run1)

		Feed	Permeate			
	Time (min)	EC01 (mS/cm)	EC02 (µS/cm)	FluxP (L/m2.hr)	Salt Rejection (%)	ΔVP (ml)
RUN 1	0	13,70	5,53			
	10	13,72	5,65	-	99,96	0,00
	20	13,73	5,68	-	99,96	0,00
	30	13,74	5,63	-	99,96	0,00
	40	13,76	5,65	21,89	99,96	15,83
	50	13,78	5,64	3,13	99,96	2,26
	60	13,78	5,67	9,38	99,96	6,79
	70	13,78	5,67	-	99,96	0,00
	80	13,78	5,65	-	99,96	0,00
	90	13,81	5,67	-	99,96	0,00
	100	13,82	5,70	6,25	99,96	4,52
	110	13,83	5,82	-	99,96	0,00
	120	13,85	5,79	3,13	99,96	2,26
	130	13,85	5,83	-	99,96	0,00
	140	13,86	5,86	-	99,96	0,00
	150	13,90	5,91	-	99,96	0,00
	160	13,90	5,96	-	99,96	0,00
	170	13,91	5,97	-	99,96	0,00
	180	13,93	6,06	-	99,96	0,00

Table C- 3: Test Number 1 data for Experiment 3 (duplicate)

		Feed	Permeate			
	Time (min)	EC01 (mS/cm)	EC02 (µS/cm)	FluxP (L/m2.hr)	Salt Rejection (%)	ΔVP (ml)
DUP	0	12,66	3,67		99,97	
	10	12,71	3,83	-	99,97	0,00
	20	12,71	3,81	-	99,97	0,00
	30	12,74	3,76	18,76	99,97	13,57
	40	12,67	3,61	-	99,97	0,00
	50	12,69	3,50	6,25	99,97	4,52
	60	12,81	3,39	-	99,97	0,00
	70	12,83	3,29	-	99,97	0,00
	80	12,85	3,20	-	99,98	0,00
	90	12,88	3,15	-	99,98	0,00
	100	12,90	3,05	-	99,98	0,00
	110	12,92	3,08	-	99,98	0,00
	120	12,94	3,10	-	99,98	0,00
	130	12,96	3,10	-	99,98	0,00
	140	12,99	3,10	-	99,98	0,00
	150	13,01	3,10	-	99,98	0,00
	160	13,03	3,10	-	99,98	0,00
	170	13,05	3,10	15,64	99,98	11,31
	180	13,08	3,10	-	99,98	0,00

Appendix C.2

Data from Experiment 3: Test number 2

MD experimental runs using 0.45 μm pore size membrane for the treatment of Type 2 brine with feed concentration of 11870 mg/L at a feed temperature of 40˚C.

Appendix C.2

Data from Experiment 3: Test number 2

Below in Table C- 4 the operating conditions is illustrated for the MD process and included are the membrane specifications:

Table C- 4: Membrane specification and initial operating conditions of experimental run

Membrane used	HVHP
Membrane pore size (µm)	0.45
Membrane Area (m^2)	0,00434
Feed Temperature (^oC)	80
Product Temperature (^oC)	10
Temperature Difference (^oC)	70
Feed Agitator (RPM)	600
Permeate Agitator (RPM)	600
Feed Flowrate (l/hr)	130
Permeate Flowrate (l/hr)	130
Feed Solution (g/L)	NaCl
	65
Feed volume (mL)	4000

Table C- 5: Test Number 2 data for Experiment 3 (Run1)

			Feed		Permeate	
	Time (min)	EC01 (mS/cm)	EC02 (µS/cm)	FluxP (L/m2.hr)	Salt Rejection (%)	ΔVP (ml)
RUN 1	0	12,61	7,23			
	10	12,64	7,47	-	99,94	0,00
	20	12,67	7,50	-	99,94	4,52
	30	12,68	7,48	-	99,94	0,00
	40	12,70	7,46	15,64	99,94	11,31
	50	12,73	7,47	-	99,94	0,00
	60	12,75	7,40	6,25	99,94	4,52
	70	12,79	7,30	9,38	99,94	6,79
	80	12,81	7,20	-	99,94	0,00
	90	12,81	7,20	3,13	99,94	2,26
	100	12,85	7,20	12,51	99,94	9,05
	110	12,89	7,16	3,13	99,94	2,26
	120	12,90	7,07	12,51	99,94	9,05
	130	12,92	7,09	-	99,95	0,00
	140	12,92	7,03	15,64	99,95	11,31
	150	12,95	7,06	3,13	99,95	2,26
	160	12,98	7,10	6,25	99,95	4,52
	170	13,00	7,22	-	99,95	0,00
	180	13,02	7,26	6,25	99,94	4,52

Table C- 6: Test Number 2 data for Experiment 3 (duplicate)

			Feed		Permeate	
	Time (min)	EC01 (mS/cm)	EC02 (µS/cm)	FluxP (L/m2.hr)	Salt Rejection (%)	ΔVP (ml)
DUP	0	13,16	5,65		99,96	
	10	13,18	6,42	-	99,95	0,00
	20	13,21	6,96	-	99,95	0,00
	30	13,28	7,39	31,27	99,94	22,62
	40	13,31	7,97	15,64	99,94	11,31
	50	13,31	8,37	-	99,94	0,00
	60	13,33	8,87	15,64	99,93	11,31
	70	13,34	9,32	6,25	99,93	4,52
	80	13,35	9,72	-	99,93	0,00
	90	13,38	10,11	-	99,92	0,00
	100	13,41	10,51	9,38	99,92	6,79
	110	13,42	10,84	15,64	99,92	11,31
	120	13,48	11,21	6,25	99,92	4,52
	130	13,48	11,52	9,38	99,91	6,79
	140	13,49	11,81	9,38	99,91	6,79
	150	13,54	12,08	6,25	99,91	4,52
	160	13,54	12,42	15,64	99,91	11,31
	170	13,58	12,64	12,51	99,91	9,05
	180	13,60	12,95	-	99,90	0,00

Table C- 7: Average experimental flux rate for test number 2 of Experiment 3

Time (min)	Average $Flux_P$ ($L/m^2.hr$)
0	0,00
10	-
20	-
30	18,76
40	21,89
50	4,69
60	9,38
70	-
80	-
90	-
100	6,25
110	-
120	3,13
130	-
140	-
150	-
160	-
170	15,64
180	-

Appendix C.3

Data from Experiment 3: Test number 3

MD experimental runs using 0.22 μm pore size membrane for the treatment of Type 2 brine with feed concentration of 11870 mg/L at a feed temperature of 60˚C.

Appendix C.3

Data from Experiment 3: Test number 3

Below in Table C- 8 the operating conditions is illustrated for the MD process and included are the membrane specifications:

Table C- 8: Membrane specification and initial operating conditions of experimental run

Membrane used	HVHP
Membrane pore size (µm)	0.45
Membrane Area (m^2)	0,00434
Feed Temperature (^oC)	80
Product Temperature (^oC)	10
Temperature Difference (^oC)	70
Feed Agitator (RPM)	600
Permeate Agitator (RPM)	600
Feed Flowrate (l/hr)	130
Permeate Flowrate (l/hr)	130
Feed Solution (g/L)	NaCl
	65
Feed volume (mL)	4000

Table C- 9: Test Number 3 data for Experiment 3 (Run1)

			Feed		Permeate	
	Time (min)	EC01 (mS/cm)	EC02 (µS/cm)	FluxP (L/m2.hr)	Salt Rejection (%)	ΔVP (ml)
RUN 1	0	12,95	3,70			
	10	13,05	4,29	31,27	99,97	22,62
	20	13,15	4,65	-	99,97	15,83
	30	13,21	4,91	-	99,96	0,00
	40	13,27	5,14	34,40	99,96	24,88
	50	13,36	5,41	-	99,96	0,00
	60	13,42	5,69	12,51	99,96	9,05
	70	13,47	5,91	18,76	99,96	13,57
	80	13,56	6,15	21,89	99,96	15,83
	90	13,61	6,39	15,64	99,95	11,31
	100	13,69	6,62	15,64	99,95	11,31
	110	13,75	6,88	31,27	99,95	22,62
	120	13,84	7,14	31,27	99,95	22,62
	130	13,88	7,39	9,38	99,95	6,79
	140	13,95	7,59	6,25	99,95	4,52
	150	14,01	7,78	15,64	99,95	11,31
	160	14,08	7,99	25,02	99,94	18,10
	170	14,16	8,19	40,65	99,94	29,41
	180	14,24	8,43	6,25	99,94	0,00

Table C- 10: Test Number 1 data for Experiment 3 (duplicate)

			Feed		Permeate	
	Time (min)	EC01 (mS/cm)	EC02 (µS/cm)	FluxP (L/m2.hr)	Salt Rejection (%)	ΔVP (ml)
DUP	0	13,18	3,52		99,97	
	10	13,25	3,75	15,64	99,97	11,31
	20	13,32	3,91	9,38	99,97	6,79
	30	13,37	4,08	9,38	99,97	6,79
	40	13,49	4,26	53,16	99,97	38,45
	50	13,52	4,42	-	99,97	0,00
	60	13,55	4,63	6,25	99,97	4,52
	70	13,62	4,87	31,27	99,96	22,62
	80	13,68	5,08	15,64	99,96	11,31
	90	13,74	5,26	12,51	99,96	9,05
	100	13,83	5,48	6,25	99,96	4,52
	110	13,87	5,66	21,89	99,96	15,83
	120	13,93	5,84	12,51	99,96	9,05
	130	14,00	6,07	50,04	99,96	36,19
	140	14,06	6,22	6,25	99,96	4,52
	150	14,14	6,41	6,25	99,95	4,52
	160	14,21	6,59	25,02	99,95	18,10
	170	14,29	6,73	18,76	99,95	13,57
	180	14,35	6,89	12,51	99,95	9,05

Table C- 11: Average experimental flux rate for test number 3 of Experiment 3

Time (min)	Average $Flux_P$ (L/m2.hr)
0	0,00
10	23,45
20	9,38
30	9,38
40	43,78
50	-
60	9,38
70	25,02
80	18,76
90	14,07
100	10,95
110	26,58
120	21,89
130	29,71
140	6,25
150	10,95
160	25,02
170	29,71
180	9,38

Appendix C.4

Data from Experiment 3: Test number 4

MD experimental runs using 0.45 μm pore size membrane for the treatment of Type 2 brine with feed concentration of 11870 mg/L at a feed temperature of 60˚C.

Appendix C.4

Data from Experiment 3: Test number 4

Below in Table C- 12 the operating conditions is illustrated for the MD process and included are the membrane specifications:

Table C- 12: Membrane specification and initial operating conditions of experimental run

Membrane used	HVHP
Membrane pore size (µm)	0.45
Membrane Area (m^2)	0,00434
Feed Temperature (^oC)	80
Product Temperature (^oC)	10
Temperature Difference (^oC)	70
Feed Agitator (RPM)	600
Permeate Agitator (RPM)	600
Feed Flowrate (l/hr)	130
Permeate Flowrate (l/hr)	130
Feed Solution (g/L)	NaCl
	65
Feed volume (mL)	4000

Table C- 13: Test Number 4 data for Experiment 3 (Run1)

			Feed		Permeate	
	Time (min)	EC01 (mS/cm)	EC02 (µS/cm)	FluxP (L/m2.hr)	Salt Rejection (%)	ΔVP (ml)
RUN 1	0	12,95	3,65			
	10	13,08	4,00	-	99,97	0,00
	20	13,15	4,09	-	99,97	22,62
	30	13,22	4,14	9,38	99,97	6,79
	40	13,27	4,16	6,25	99,97	4,52
	50	13,37	4,19	-	99,97	0,00
	60	13,39	4,23	37,53	99,97	27,14
	70	13,47	4,27	18,76	99,97	13,57
	80	13,54	4,38	6,25	99,97	4,52
	90	13,61	4,43	31,27	99,97	22,62
	100	13,68	4,50	6,25	99,97	4,52
	110	13,75	4,55	25,02	99,97	18,10
	120	13,83	4,67	21,89	99,97	15,83
	130	13,91	4,79	6,25	99,97	4,52
	140	13,97	4,90	9,38	99,97	6,79
	150	14,02	4,96	50,04	99,97	36,19
	160	14,10	5,03	6,25	99,96	4,52
	170	14,19	5,14	25,02	99,96	18,10
	180	14,26	5,21	37,53	99,96	27,14

Table C- 14: Test Number 4 data for Experiment 3 (duplicate)

			Feed		Permeate	
	Time (min)	EC01 (mS/cm)	EC02 (µS/cm)	FluxP (L/m2.hr)	Salt Rejection (%)	ΔVP (ml)
DUP	0	13,21	3,07		99,98	
	10	13,29	3,61	15,64	99,97	11,31
	20	13,37	3,73	-	99,97	0,00
	30	13,43	3,77	46,91	99,97	33,93
	40	13,58	3,77	15,64	99,97	11,31
	50	13,58	3,77	31,27	99,97	22,62
	60	13,66	3,78	9,38	99,97	6,79
	70	13,73	3,80	28,14	99,97	20,36
	80	13,82	3,81	25,02	99,97	18,10
	90	13,88	3,89	31,27	99,97	22,62
	100	13,96	3,97	15,64	99,97	11,31
	110	14,04	4,00	12,51	99,97	9,05
	120	14,13	4,09	46,91	99,97	33,93
	130	14,21	4,18	18,76	99,97	13,57
	140	14,30	4,23	56,29	99,97	40,72
	150	14,39	4,36	-	99,97	0,00
	160	14,46	4,42	31,27	99,97	22,62
	170	14,54	4,55	37,53	99,97	27,14
	180	14,64	4,66	-	99,97	0,00

Table C- 15: Average experimental flux rate for test number 4 of Experiment 3

Time (min)	Average FluxP (L/m2.hr)
0	0,00
10	15,64
20	-
30	28,14
40	10,95
50	31,27
60	23,45
70	23,45
80	15,64
90	31,27
100	10,95
110	18,76
120	34,40
130	12,51
140	32,84
150	50,04
160	18,76
170	31,27
180	37,53

Appendix C.5

Data from Experiment 3: Test number 5

MD experimental runs using 0.22 μm pore size membrane for the treatment of Type 2 brine with feed concentration of 11870 mg/L at a feed temperature of 80˚C.

Appendix C.5

Data from Experiment 3: Test number 5

Below in Table C- 16 the operating conditions is illustrated for the MD process and included are the membrane specifications:

Table C- 16: Membrane specification and initial operating conditions of experimental run

Membrane used	HVHP
Membrane pore size (µm)	0.45
Membrane Area (m^2)	0,00434
Feed Temperature (^oC)	80
Product Temperature (^oC)	10
Temperature Difference (^oC)	70
Feed Agitator (RPM)	600
Permeate Agitator (RPM)	600
Feed Flowrate (l/hr)	130
Permeate Flowrate (l/hr)	130
Feed Solution (g/L)	NaCl
	65
Feed volume (mL)	4000

Table C- 17: Test Number 5 data for Experiment 3 (Run1)

			Feed		Permeate	
	Time (min)	EC01 (mS/cm)	EC02 (µS/cm)	FluxP (L/m2.hr)	Salt Rejection (%)	ΔVP (ml)
RUN 1	0	12,75	4,88			
	10	13,04	4,77	31,27	99,96	22,62
	20	13,24	4,74	-	99,96	45,24
	30	13,46	4,64	46,91	99,96	33,93
	40	13,62	4,59	62,54	99,97	45,24
	50	13,76	4,49	-	99,97	0,00
	60	13,93	4,44	46,91	99,97	33,93
	70	14,14	4,36	62,54	99,97	45,24
	80	14,34	4,25	62,54	99,97	45,24
	90	14,55	4,19	53,16	99,97	38,45
	100	14,75	4,13	65,67	99,97	47,50
	110	14,99	4,13	53,16	99,97	38,45
	120	15,22	4,30	62,54	99,97	45,24
	130	15,46	3,97	46,91	99,97	33,93
	140	15,69	3,95	56,29	99,97	40,72
	150	15,91	3,92	65,67	99,98	47,50
	160	16,16	3,84	34,40	99,98	24,88
	170	16,38	3,80	46,91	99,98	33,93
	180	16,65	3,80	71,93	99,98	52,03

Table C- 18: Test Number 5 data for Experiment 3 (duplicate)

			Feed		Permeate	
	Time (min)	EC01 (mS/cm)	EC02 (µS/cm)	FluxP (L/m2.hr)	Salt Rejection (%)	ΔVP (ml)
RUN 1	0	12,92	4,50		99,97	
	10	13,03	4,87	15,64	99,96	11,31
	20	13,22	4,75	46,91	99,96	33,93
	30	13,41	4,51	21,89	99,97	15,83
	40	13,68	4,28	78,18	99,97	56,55
	50	13,81	4,09	25,02	99,97	18,10
	60	14,00	3,97	40,65	99,97	29,41
	70	14,19	3,66	31,27	99,97	22,62
	80	14,36	3,87	31,27	99,97	22,62
	90	14,55	3,83	62,54	99,97	45,24
	100	14,76	3,81	37,53	99,97	27,14
	110	14,96	3,79	56,29	99,97	40,72
	120	15,18	3,82	37,53	99,97	27,14
	130	15,44	3,83	62,54	99,98	45,24
	140	15,69	3,88	71,93	99,98	52,03
	150	15,88	4,01	37,53	99,97	27,14
	160	16,11	4,09	40,65	99,97	29,41
	170	16,35	4,18	46,91	99,97	33,93
	180	16,58	4,31	43,78	99,97	31,67

Table C- 19: Average experimental flux rate for test number 5 of Experiment 3

Time (min)	Average FluxP (L/m2.hr)
0	0,00
10	23,45
20	46,91
30	34,40
40	70,36
50	25,02
60	43,78
70	46,91
80	46,91
90	57,85
100	51,60
110	54,73
120	50,04
130	54,73
140	64,11
150	51,60
160	37,53
170	46,91
180	57,85

Appendix C.6

Data from Experiment 3: Test number 6

MD experimental runs using 0.45 μm pore size membrane for the treatment of Type 2 brine with feed concentration of 11870 mg/L at a feed temperature of 80˚C.

Appendix C.6

Data from Experiment 3: Test number 6

Below in Table C- 20 the operating conditions is illustrated for the MD process and included are the membrane specifications:

Table C- 20: Membrane specification and initial operating conditions of experimental run

Membrane used	HVHP
Membrane pore size (µm)	0.45
Membrane Area (m^2)	0,00434
Feed Temperature (^oC)	80
Product Temperature (^oC)	10
Temperature Difference (^oC)	70
Feed Agitator (RPM)	600
Permeate Agitator (RPM)	600
Feed Flowrate (l/hr)	130
Permeate Flowrate (l/hr)	130
Feed Solution (g/L)	NaCl
	65
Feed volume (mL)	4000

Table C- 21: Test Number 6 data for Experiment 3 (Run1)

			Feed		Permeate	
	Time (min)	EC01 (mS/cm)	EC02 (µS/cm)	FluxP (L/m2.hr)	Salt Rejection (%)	ΔVP (ml)
RUN 1	0	12,71	3,39			
	10	12,91	4,00	9,38	99,97	6,79
	20	13,07	4,08	-	99,97	22,62
	30	13,27	3,94	31,27	99,97	22,62
	40	13,48	3,81	21,89	99,97	15,83
	50	13,69	3,72	37,53	99,97	27,14
	60	13,85	3,62	31,27	99,97	22,62
	70	14,04	3,64	71,93	99,97	52,03
	80	14,22	3,67	56,29	99,97	40,72
	90	14,39	3,74	21,89	99,97	15,83
	100	14,57	3,86	37,53	99,97	27,14
	110	14,79	4,04	65,67	99,97	47,50
	120	14,99	4,22	53,16	99,97	38,45
	130	15,25	4,49	21,89	99,97	15,83
	140	15,46	4,76	40,65	99,97	29,41
	150	15,69	5,08	71,93	99,97	52,03
	160	15,91	5,47	37,53	99,97	27,14
	170	16,15	5,89	93,82	99,97	67,86
	180	16,33	6,46	15,64	99,96	11,31

Table C- 22: Test Number 6 data for Experiment 3 (duplicate)

			Feed		Permeate	
	Time (min)	EC01 (mS/cm)	EC02 (µS/cm)	FluxP (L/m2.hr)	Salt Rejection (%)	ΔVP (ml)
RUN 1	0	12,68	3,52		99,97	
	10	12,75	3,87	6,25	99,97	4,52
	20	12,82	3,76	31,27	99,97	22,62
	30	12,97	3,55	40,65	99,97	29,41
	40	13,09	3,30	25,02	99,97	18,10
	50	13,12	3,11	37,53	99,98	27,14
	60	13,15	3,01	15,64	99,98	11,31
	70	13,22	2,92	46,91	99,98	33,93
	80	13,28	2,69	62,54	99,98	45,24
	90	13,34	2,72	68,80	99,98	49,76
	100	13,43	2,76	56,29	99,98	40,72
	110	13,47	2,82	31,27	99,98	22,62
	120	13,53	2,95	62,54	99,98	45,24
	130	13,60	2,99	43,78	99,98	31,67
	140	13,66	3,05	31,27	99,98	22,62
	150	13,74	3,18	40,65	99,98	29,41
	160	13,81	3,33	34,40	99,98	24,88
	170	13,89	3,62	21,89	99,97	15,83
	180	13,95	3,79	37,53	99,97	27,14

Table C- 23: Average experimental flux rate for test number 6 of Experiment 3

Time (min)	Average FluxP (L/m2.hr)
0	0,00
10	7,82
20	31,27
30	35,96
40	23,45
50	37,53
60	23,45
70	59,42
80	59,42
90	45,34
100	46,91
110	48,47
120	57,85
130	32,84
140	35,96
150	56,29
160	35,96
170	57,85
180	26,58

Appendix C.7

Data from Experiment 3: Test number 7

MD experimental runs using 0.22 μm pore size membrane for the treatment of Type 2 brine with feed concentration of 27025 mg/L at a feed temperature of 40˚C.

Appendix C.7

Data from Experiment 3: Test number 7

Below in Table C- 24 the operating conditions is illustrated for the MD process and included are the membrane specifications:

Table C- 24: Membrane specification and initial operating conditions of experimental run

Membrane used	HVHP
Membrane pore size (µm)	0.45
Membrane Area (m^2)	0,00434
Feed Temperature (^oC)	80
Product Temperature (^oC)	10
Temperature Difference (^oC)	70
Feed Agitator (RPM)	600
Permeate Agitator (RPM)	600
Feed Flowrate (l/hr)	130
Permeate Flowrate (l/hr)	130
Feed Solution (g/L)	NaCl
	65
Feed volume (mL)	4000

Table C- 25: Test Number 7 data for Experiment 3 (Run1)

			Feed		Permeate	
	Time (min)	EC01 (mS/cm)	EC02 (µS/cm)	FluxP (L/m2.hr)	Salt Rejection (%)	ΔVP (ml)
RUN 1	0	24,00	3,58			
	10	24,30	4,61	-	99,99	0,00
	20	24,30	4,86	-	99,98	0,00
	30	24,30	4,79	-	99,98	0,00
	40	24,30	4,61	-	99,98	0,00
	50	24,30	4,40	-	99,98	0,00
	60	24,40	4,27	-	99,98	0,00
	70	24,40	4,03	-	99,98	0,00
	80	24,40	3,93	-	99,98	0,00
	90	24,40	3,82	-	99,98	0,00
	100	24,50	3,69	-	99,98	0,00
	110	24,50	3,57	6,25	99,98	4,52
	120	24,50	3,45	-	99,99	0,00
	130	24,60	3,37	-	99,99	0,00
	140	24,60	3,29	-	99,99	0,00
	150	24,60	3,22	-	99,99	0,00
	160	24,60	3,11	-	99,99	0,00
	170	24,60	3,09	9,38	99,99	6,79
	180	24,60	3,01	6,25	99,99	4,52

Table C- 26: Test Number 7 data for Experiment 3 (duplicate)

			Feed		Permeate	
	Time (min)	EC01 (mS/cm)	EC02 (µS/cm)	FluxP (L/m2.hr)	Salt Rejection (%)	ΔVP (ml)
RUN 1	0	24,20	4,00		99,98	
	10	24,50	4,50	-	99,98	0,00
	20	24,50	4,92	-	99,98	0,00
	30	24,50	4,85	-	99,98	0,00
	40	24,50	4,76	-	99,98	0,00
	50	24,50	4,70	-	99,98	0,00
	60	24,50	4,58	-	99,98	0,00
	70	24,50	4,49	-	99,98	0,00
	80	24,50	4,42	9,38	99,98	6,79
	90	24,60	4,33	-	99,98	0,00
	100	24,60	4,30	-	99,98	0,00
	110	24,70	4,30	-	99,98	0,00
	120	24,70	4,26	-	99,98	0,00
	130	24,70	4,21	6,25	99,98	4,52
	140	24,80	4,15	-	99,98	0,00
	150	24,80	4,09	-	99,98	0,00
	160	24,80	4,02	9,38	99,98	6,79
	170	24,80	3,95	-	99,98	0,00
	180	24,90	3,88	3,13	99,98	2,26

Table C- 27: Average experimental flux rate for test number 7 of Experiment 3

Time (min)	Average FluxP (L/m2.hr)
0	0,00
10	-
20	-
30	-
40	-
50	-
60	-
70	-
80	9,38
90	-
100	-
110	6,25
120	-
130	6,25
140	-
150	-
160	9,38
170	9,38
180	4,69

Appendix C.7

Data from Experiment 3: Test number 8

MD experimental runs using 0.45 μm pore size membrane for the treatment of Type 2 brine with feed concentration of 27025 mg/L at a feed temperature of 40˚C.

Appendix C.8

Data from Experiment 3: Test number 8

Below in Table C- 28 the operating conditions is illustrated for the MD process and included are the membrane specifications:

Table C- 28: Membrane specification and initial operating conditions of experimental run

Membrane used	HVHP
Membrane pore size (µm)	0.45
Membrane Area (m^2)	0,00434
Feed Temperature (^oC)	80
Product Temperature (^oC)	10
Temperature Difference (^oC)	70
Feed Agitator (RPM)	600
Permeate Agitator (RPM)	600
Feed Flowrate (l/hr)	130
Permeate Flowrate (l/hr)	130
Feed Solution (g/L)	NaCl
	65
Feed volume (mL)	4000

Table C- 29: Test Number 8 data for Experiment 3 (Run1)

			Feed		Permeate	
	Time (min)	EC01 (mS/cm)	EC02 (µS/cm)	FluxP (L/m2.hr)	Salt Rejection (%)	ΔVP (ml)
RUN 1	0	24,10	4,04			
	10	24,10	4,59	-	99,98	0,00
	20	24,20	4,73	-	99,98	2,26
	30	24,20	4,52	-	99,98	0,00
	40	24,20	4,26	-	99,98	0,00
	50	24,30	4,00	-	99,98	0,00
	60	24,30	3,75	6,25	99,98	4,52
	70	24,30	3,57	-	99,98	0,00
	80	24,30	3,40	-	99,99	0,00
	90	24,30	3,19	-	99,99	0,00
	100	24,30	3,03	-	99,99	0,00
	110	24,40	2,89	-	99,99	0,00
	120	24,40	2,64	-	99,99	0,00
	130	24,40	2,64	3,13	99,99	2,26
	140	24,40	2,54	-	99,99	0,00
	150	24,40	2,42	6,25	99,99	4,52
	160	24,50	2,33	21,89	99,99	15,83
	170	24,50	2,27	15,64	99,99	11,31
	180	24,50	2,21	15,64	99,99	11,31

Table C- 30: Test Number 8 data for Experiment 3 (duplicate)

			Feed		Permeate	
	Time (min)	EC01 (mS/cm)	EC02 (µS/cm)	FluxP (L/m2.hr)	Salt Rejection (%)	ΔVP (ml)
DUP	0	23,80	3,40		99,99	
	10	23,80	3,78	-	99,98	0,00
	20	23,80	3,85	-	99,98	0,00
	30	23,90	3,75	-	99,98	0,00
	40	23,90	3,62	-	99,98	0,00
	50	23,90	3,58	-	99,99	0,00
	60	23,90	3,53	15,64	99,99	11,31
	70	23,90	3,24	-	99,99	0,00
	80	23,90	3,06	-	99,99	0,00
	90	23,90	2,99	-	99,99	0,00
	100	24,00	2,92	-	99,99	0,00
	110	24,00	2,92	-	99,99	0,00
	120	24,10	2,88	6,25	99,99	4,52
	130	24,10	2,80	-	99,99	0,00
	140	24,10	2,73	25,02	99,99	18,10
	150	24,20	2,51	-	99,99	0,00
	160	24,20	2,38	-	99,99	0,00
	170	24,20	2,15	15,64	99,99	11,31
	180	24,20	2,06	9,38	99,99	6,79

Table C- 31: Average experimental flux rate for test number 8 of Experiment 3

Time (min)	Average FluxP (L/m2.hr)
0	0,00
10	-
20	-
30	-
40	-
50	-
60	10,95
70	-
80	-
90	-
100	-
110	-
120	6,25
130	3,13
140	25,02
150	6,25
160	21,89
170	15,64
180	12,51

Appendix C.9

Data from Experiment 3: Test number 9

MD experimental runs using 0.22 μm pore size membrane for the treatment of Type 2 brine with feed concentration of 27025 mg/L at a feed temperature of 60˚C.

Appendix C.9

Data from Experiment 3: Test number 9

Below in Table C- 32 the operating conditions is illustrated for the MD process and included are the membrane specifications:

Table C- 32: Membrane specification and initial operating conditions of experimental run

Membrane used	HVHP
Membrane pore size (µm)	0.45
Membrane Area (m^2)	0,00434
Feed Temperature (^oC)	80
Product Temperature (^oC)	10
Temperature Difference (^oC)	70
Feed Agitator (RPM)	600
Permeate Agitator (RPM)	600
Feed Flowrate (l/hr)	130
Permeate Flowrate (l/hr)	130
Feed Solution (g/L)	NaCl
	65
Feed volume (mL)	4000

Table C- 33: Test Number 9 data for Experiment 3 (Run1)

			Feed		Permeate	
	Time (min)	EC01 (mS/cm)	EC02 (µS/cm)	FluxP (L/m2.hr)	Salt Rejection (%)	ΔVP (ml)
RUN 1	0	25,40	4,10			
	10	25,60	5,27	21,89	99,98	15,83
	20	25,70	5,33	-	99,98	0,00
	30	25,90	5,09	-	99,98	0,00
	40	25,90	4,77	15,64	99,98	11,31
	50	25,90	4,41	-	99,98	0,00
	60	26,00	4,15	15,64	99,98	11,31
	70	26,20	3,95	6,25	99,98	4,52
	80	26,30	3,72	-	99,98	0,00
	90	26,40	3,53	9,38	99,99	6,79
	100	26,50	3,37	-	99,99	0,00
	110	26,60	3,19	15,64	99,99	11,31
	120	26,70	3,05	15,64	99,99	11,31
	130	26,80	2,95	25,02	99,99	18,10
	140	27,20	3,02	15,64	99,99	11,31
	150	27,20	2,92	18,76	99,99	13,57
	160	27,30	2,89	18,76	99,99	13,57
	170	27,50	2,85	25,02	99,99	18,10
	180	27,50	2,85	18,76	99,99	13,57

Table C- 34: Test Number 9 data for Experiment 3 (duplicate)

			Feed		Permeate	
	Time (min)	EC01 (mS/cm)	EC02 (µS/cm)	FluxP (L/m2.hr)	Salt Rejection (%)	ΔVP (ml)
DUP	0	24,50	3,30		99,99	
	10	24,60	3,92	6,25	99,98	4,52
	20	24,80	4,18	9,38	99,98	6,79
	30	25,10	4,30	-	99,98	0,00
	40	25,30	4,19	12,51	99,98	9,05
	50	25,40	4,10	18,76	99,98	13,57
	60	25,60	3,92	31,27	99,98	22,62
	70	25,80	3,78	12,51	99,99	9,05
	80	25,90	3,65	18,76	99,99	13,57
	90	26,00	3,44	-	99,99	0,00
	100	26,00	3,42	15,64	99,99	11,31
	110	26,10	3,00	9,38	99,99	6,79
	120	26,30	2,88	15,64	99,99	11,31
	130	26,30	2,85	6,25	99,99	4,52
	140	26,40	2,81	18,76	99,99	13,57
	150	26,50	2,77	12,51	99,99	9,05
	160	26,70	2,71	6,25	99,99	4,52
	170	26,70	2,71	18,76	99,99	13,57
	180	26,80	2,70	9,38	99,99	6,79

Table C- 35: Average experimental flux rate for test number 9 of Experiment 3

Time (min)	Average FluxP (L/m2.hr)
0	0,00
10	14,07
20	9,38
30	-
40	14,07
50	18,76
60	23,45
70	9,38
80	18,76
90	9,38
100	15,64
110	12,51
120	15,64
130	15,64
140	17,20
150	15,64
160	12,51
170	21,89
180	14,07

Appendix C.10

Data from Experiment 3: Test number 10

MD experimental runs using 0.45 μm pore size membrane for the treatment of Type 2 brine with feed concentration of 27025 mg/L at a feed temperature of 60˚C.

Appendix C.10

Data from Experiment 3: Test number 9

Below in Table C- 36 the operating conditions is illustrated for the MD process and included are the membrane specifications:

Table C- 36: Membrane specification and initial operating conditions of experimental run

Membrane used	HVHP
Membrane pore size (µm)	0.45
Membrane Area (m^2)	0,00434
Feed Temperature (^oC)	80
Product Temperature (^oC)	10
Temperature Difference (^oC)	70
Feed Agitator (RPM)	600
Permeate Agitator (RPM)	600
Feed Flowrate (l/hr)	130
Permeate Flowrate (l/hr)	130
Feed Solution (g/L)	NaCl
	65
Feed volume (mL)	4000

Table C- 37: Test Number 10 data for Experiment 3 (Run1)

			Feed		Permeate	
	Time (min)	EC01 (mS/cm)	EC02 (µS/cm)	FluxP (L/m2.hr)	Salt Rejection (%)	ΔVP (ml)
RUN 1	0	24,80	5,08			
	10	24,90	5,16	-	99,98	0,00
	20	24,90	4,99	-	99,98	0,00
	30	25,20	4,81	15,64	99,98	11,31
	40	25,30	4,54	9,38	99,98	6,79
	50	25,40	4,19	6,25	99,98	4,52
	60	25,40	3,92	18,76	99,98	13,57
	70	25,50	3,73	21,89	99,98	15,83
	80	25,70	3,61	21,89	99,99	15,83
	90	25,90	3,47	21,89	99,99	15,83
	100	25,90	3,35	9,38	99,99	6,79
	110	26,00	3,24	25,02	99,99	18,10
	120	26,20	3,17	21,89	99,99	15,83
	130	26,20	3,09	6,25	99,99	4,52
	140	26,40	3,05	9,38	99,99	6,79
	150	26,50	3,00	15,64	99,99	11,31
	160	26,70	2,99	6,25	99,99	4,52
	170	26,80	2,98	9,38	99,99	6,79
	180	26,90	2,97	15,64	99,99	11,31

Table C- 38: Test Number 10 data for Experiment 3 (duplicate)

			Feed		Permeate	
	Time (min)	EC01 (mS/cm)	EC02 (µS/cm)	FluxP (L/m2.hr)	Salt Rejection (%)	ΔVP (ml)
DUP	0	24,60	4,26		99,98	
	10	24,70	4,39	6,25	99,98	4,52
	20	24,70	4,55	-	99,98	0,00
	30	24,80	4,61	9,38	99,98	6,79
	40	24,80	4,49	46,91	99,98	33,93
	50	25,00	4,32	46,91	99,98	33,93
	60	25,10	4,15	21,89	99,98	15,83
	70	25,20	4,08	18,76	99,98	13,57
	80	25,30	3,98	21,89	99,98	15,83
	90	25,50	3,71	9,38	99,99	6,79
	100	25,50	3,59	15,64	99,99	11,31
	110	25,60	3,48	12,51	99,99	9,05
	120	25,80	3,21	12,51	99,99	9,05
	130	25,90	3,10	12,51	99,99	9,05
	140	25,90	2,95	12,51	99,99	9,05
	150	26,10	2,92	9,38	99,99	6,79
	160	26,20	2,88	18,76	99,99	13,57
	170	26,30	2,86	9,38	99,99	6,79
	180	26,50	2,86	-	99,99	0,00

Table C- 39: Average experimental flux rate for test number 10 of Experiment 3

Time (min)	Average FluxP (L/m2.hr)
0	0,00
10	6,25
20	-
30	12,51
40	28,14
50	26,58
60	20,33
70	20,33
80	21,89
90	15,64
100	12,51
110	18,76
120	17,20
130	9,38
140	10,95
150	12,51
160	12,51
170	9,38
180	15,64

Appendix C.11

Data from Experiment 3: Test number 11

MD experimental runs using 0.22 μm pore size membrane for the treatment of Type 2 brine with feed concentration of 27025 mg/L at a feed temperature of 80˚C.

Appendix C.11

Data from Experiment 3: Test number 11

Below in Table C- 40 the operating conditions is illustrated for the MD process and included are the membrane specifications:

Table C- 40: Membrane specification and initial operating conditions of experimental run

Membrane used	HVHP
Membrane pore size (µm)	0.45
Membrane Area (m^2)	0,00434
Feed Temperature (^oC)	80
Product Temperature (^oC)	10
Temperature Difference (^oC)	70
Feed Agitator (RPM)	600
Permeate Agitator (RPM)	600
Feed Flowrate (l/hr)	130
Permeate Flowrate (l/hr)	130
Feed Solution (g/L)	NaCl
	65
Feed volume (mL)	4000

Table C- 41: Test Number 11 data for Experiment 3 (Run1)

			Feed		Permeate	
	Time (min)	EC01 (mS/cm)	EC02 (µS/cm)	FluxP (L/m2.hr)	Salt Rejection (%)	ΔVP (ml)
RUN 1	0	25,60	3,27			
	10	26,00	4,30	15,64	99,99	11,31
	20	26,10	4,50	15,64	99,98	11,31
	30	26,60	4,33	31,27	99,98	22,62
	40	27,00	4,02	31,27	99,98	22,62
	50	27,20	3,72	31,27	99,99	22,62
	60	27,50	3,48	56,29	99,99	40,72
	70	27,80	3,27	34,40	99,99	24,88
	80	28,10	3,12	28,14	99,99	20,36
	90	28,40	3,00	43,78	99,99	31,67
	100	28,60	2,93	40,65	99,99	29,41
	110	28,90	2,95	15,64	99,99	11,31
	120	29,20	3,01	-	99,99	0,00
	130	29,40	3,04	34,40	99,99	24,88
	140	29,60	3,08	28,14	99,99	20,36
	150	29,90	3,11	15,64	99,99	11,31
	160	30,10	3,22	37,53	99,99	27,14
	170	30,40	3,27	9,38	99,99	6,79
	180	30,40	3,35	28,14	99,99	20,36

Table C- 42: Test Number 11 data for Experiment 3 (duplicate)

			Feed		Permeate	
	Time (min)	EC01 (mS/cm)	EC02 (µS/cm)	FluxP (L/m2.hr)	Salt Rejection (%)	ΔVP (ml)
DUP	0	24,30	4,58		99,98	
	10	24,60	4,79	46,91	99,98	33,93
	20	25,00	5,05	31,27	99,98	22,62
	30	25,30	5,15	46,91	99,98	33,93
	40	25,70	5,08	31,27	99,98	22,62
	50	25,90	4,91	56,29	99,98	40,72
	60	26,20	4,75	21,89	99,98	15,83
	70	26,30	4,63	46,91	99,98	33,93
	80	26,50	4,43	21,89	99,98	15,83
	90	26,70	4,25	34,40	99,98	24,88
	100	27,00	4,28	21,89	99,98	15,83
	110	27,30	4,33	12,51	99,98	9,05
	120	27,50	4,37	3,13	99,98	2,26
	130	27,70	4,49	25,02	99,98	18,10
	140	27,80	4,56	34,40	99,98	24,88
	150	28,10	4,62	34,40	99,98	24,88
	160	28,40	4,71	18,76	99,98	13,57
	170	28,60	4,77	12,51	99,98	9,05
	180	28,90	4,81	31,27	99,98	22,62

Appendix C.12

Data from Experiment 3: Test number 12

MD experimental runs using 0.45 μm pore size membrane for the treatment of Type 2 brine with feed concentration of 27025 mg/L at a feed temperature of 80˚C.

Appendix C.12

Data from Experiment 3: Test number 12

Below in Table C- 43 the operating conditions is illustrated for the MD process and included are the membrane specifications:

Table C- 43: Membrane specification and initial operating conditions of experimental run

Membrane used	HVHP
Membrane pore size (µm)	0.45
Membrane Area (m^2)	0,00434
Feed Temperature (^oC)	80
Product Temperature (^oC)	10
Temperature Difference (^oC)	70
Feed Agitator (RPM)	600
Permeate Agitator (RPM)	600
Feed Flowrate (l/hr)	130
Permeate Flowrate (l/hr)	130
Feed Solution (g/L)	NaCl
	65
Feed volume (mL)	4000

Table C- 44: Test Number 12 data for Experiment 3 (Run1)

			Feed		Permeate	
	Time (min)	EC01 (mS/cm)	EC02 (µS/cm)	FluxP (L/m2.hr)	Salt Rejection (%)	ΔVP (ml)
RUN 1	0	26,40	4,63			
	10	26,70	5,33	62,54	99,98	45,24
	20	27,00	5,46	-	99,98	27,14
	30	27,30	5,32	9,38	99,98	6,79
	40	27,70	5,15	53,16	99,98	38,45
	50	28,10	4,95	46,91	99,98	33,93
	60	28,40	4,85	31,27	99,98	22,62
	70	28,50	4,85	6,25	99,98	4,52
	80	28,80	4,90	-	99,98	0,00
	90	29,00	5,94	9,38	99,98	6,79
	100	29,20	6,12	25,02	99,98	18,10
	110	29,40	6,30	31,27	99,98	22,62
	120	29,70	6,67	25,02	99,98	18,10
	130	30,00	7,54	31,27	99,98	22,62
	140	30,20	8,16	-	99,98	0,00
	150	30,40	9,06	25,02	99,97	18,10
	160	30,70	9,93	9,38	99,97	6,79
	170	30,90	10,80	6,25	99,97	4,52
	180	31,10	11,85	25,02	99,97	18,10

Table C- 45: Test Number 12 data for Experiment 3 (duplicate)

		Feed	Permeate			
	Time (min)	EC01 (mS/cm)	EC02 (µS/cm)	FluxP (L/m2.hr)	Salt Rejection (%)	ΔVP (ml)
DUP	0	23,20	4,36		99,98	
	10	23,50	4,34	46,91	99,98	33,93
	20	23,80	4,18	31,27	99,98	22,62
	30	23,90	4,12	46,91	99,98	33,93
	40	24,10	4,09	31,27	99,98	22,62
	50	24,30	4,06	56,29	99,98	40,72
	60	24,60	4,22	21,89	99,98	15,83
	70	24,70	4,53	46,91	99,98	33,93
	80	24,90	5,00	21,89	99,98	15,83
	90	25,10	5,86	34,40	99,98	24,88
	100	25,20	6,84	21,89	99,97	15,83
	110	25,40	8,02	12,51	99,97	9,05
	120	25,60	9,56	3,13	99,96	2,26
	130	25,80	10,05	15,64	99,96	11,31
	140	26,00	10,38	21,89	99,96	15,83
	150	26,30	10,86	12,51	99,96	9,05
	160	26,50	11,39	15,64	99,96	11,31
	170	26,70	11,88	18,76	99,96	13,57
	180	27,00	12,18	9,38	99,95	6,79

Table C- 46: Average experimental flux rate for test number 12 of Experiment 3

Time (min)	Average FluxP (L/m2.hr)
0	0,00
10	54,73
20	31,27
30	28,14
40	42,22
50	51,60
60	26,58
70	26,58
80	21,89
90	21,89
100	23,45
110	21,89
120	14,07
130	23,45
140	21,89
150	18,76
160	12,51
170	12,51
180	17,20

Appendix D

Appendix D.1

Data from Experiment 4: Test number 2

Investigating the effect of scaling/fouling on the performance of MD using 0.45 μm pore size membrane for the treatment of type Type 2 brine

Appendix D.1

Data from Experiment 4: Test number 1

Below in Table D- 1 the operating conditions is illustrated for the MD process and included are the membrane specifications:

Table D- 1: Membrane specification and initial operating conditions of experimental run

Membrane used	GVHP
Membrane pore size (µm)	0.22
Membrane Area (m^2)	0,00434
Feed Temperature (^oC)	60
Product Temperature (^oC)	10
Temperature Difference (^oC)	50
Feed Agitator (RPM)	600
Permeate Agitator (RPM)	600
Feed Flowrate (l/hr)	130
Permeate Flowrate (l/hr)	130
Feed Solution (g/L)	NaCl
	235
Feed volume (mL)	4000

Table D- 2: Test Number 1 data for Experiment 4

		Feed		Permeate			
	Time (min)	TSS (mg/L)	EC01 (mS/cm)	EC02 (µS/cm)	FluxP (L/m2.hr)	Salt Rejection (%)	ΔVP (ml)
RUN 1	0		25,00	5,12			
	60	3935,08	25,70	4,52	15,64	99,98	67,86
	120	3891,80	26,20	3,52	15,64	99,99	67,86
	180	3880,98	27,00	3,47	18,24	99,99	79,17
	240	3880,98	27,50	3,22	23,45	99,99	101,79
	300	3870,16	28,10	3,22	7,82	99,99	33,93
	360	3880,98	28,90	3,32	18,24	99,99	79,17
	420	3891,80	29,60	3,65	18,24	99,99	79,17
	480	3880,98	30,30	4,08	23,45	99,99	101,79
	540	3859,34	31,30	4,57	20,85	99,99	90,48
	600	3880,98	32,20	5,14	20,85	99,98	90,48
	660	3913,44	33,00	5,71	10,42	99,98	45,24
	720	3913,44	33,50	6,09	15,64	99,98	67,86
	780	3902,62	33,80	6,43	5,21	99,98	22,62
	840	3924,26	33,80	6,82	15,64	99,98	67,86
	900	3924,26	33,30	7,09	10,42	99,98	45,24

	960	3924,26	32,70	7,54	5,21	99,98	22,62
	1020	3913,44	31,60	7,88	10,42	99,98	45,24
	1080	3945,90	30,10	8,18	5,21	99,97	22,62
	1140	3924,26	31,90	8,52	15,64	99,97	67,86
	1200	3924,26	33,90	9,09	5,21	99,97	22,62
	1260	3924,26	33,50	9,51	5,21	99,97	22,62
	1320	3935,08	35,60	9,89	5,21	99,97	22,62
	1380	3935,08	33,50	10,40	5,21	99,97	22,62
	1440	3935,08	31,80	10,82	5,21	99,97	22,62
	1500	3935,08	31,20	11,16	5,21	99,96	22,62
	1560	3924,26	29,80	11,51	5,21	99,96	22,62
	1620	3924,26	28,90	11,95	2,61	99,96	11,31
	1680	3935,08	27,40	12,45	7,82	99,95	33,93
	1740	3945,90	26,70	12,88	2,61	99,95	11,31
	1800	3924,26	26,00	13,33	5,21	99,95	22,62
	1860	3935,08	25,60	13,82	7,82	99,95	33,93
	1920	3935,08	25,40	14,33	-	99,94	0,00
	1980	3956,72	25,10	15,08	2,61	99,94	11,31
	2040	3924,26	24,60	15,65	7,82	99,94	33,93

Appendix D.2

Data from Experiment 4: Test number 2

Investigating the effect of scaling/fouling on the performance of MD using 0.45 μm pore size membrane for the treatment of type Type 2 brine

Appendix D.2

Data from Response Surface Methodology experiments

Below in Table D- 3 the operating conditions is illustrated for the MD process and included are the membrane specifications:

Table D- 3: Membrane specification and initial operating conditions of experimental run

Membrane used	GVHP
Membrane pore size (µm)	0.22
Membrane Area (m^2)	0,00434
Feed Temperature (^oC)	60
Product Temperature (^oC)	10
Temperature Difference (^oC)	50
Feed Agitator (RPM)	600
Permeate Agitator (RPM)	600
Feed Flowrate (l/hr)	130
Permeate Flowrate (l/hr)	130
Feed Solution (g/L)	NaCl
	235
Feed volume (mL)	4000

Table D- 4: Test Number 1 data for Experiment 4

		Feed		Permeate			
	Time (min)	TSS (mg/L)	EC01 (mS/cm)	EC02 (µS/cm)	FluxP (L/m2.hr)	Salt Rejection (%)	ΔVP (ml)
RUN 1	0	2552,87	25,70	4,49			
	60	2629,43	26,50	4,39	33,88	99,98	147,03
	120	2670,81	27,30	3,68	18,24	99,99	79,17
	180	2734,91	28,20	3,00	28,67	99,99	124,41
	240	2799,01	29,10	2,57	28,67	99,99	124,41
	300	2869,29	29,90	2,45	31,27	99,99	135,72
	360	2902,37	30,90	2,45	15,64	99,99	67,86
	420	2995,40	31,80	2,52	41,70	99,99	180,96
	480	3065,71	33,20	2,61	31,27	99,99	135,72
	540	3065,71	34,40	2,78	-	99,99	0,00
	600	3100,87	35,80	2,91	15,64	99,99	67,86
	660	3194,01	37,10	3,06	41,70	99,99	180,96
	720	3276,90	38,60	3,25	36,48	99,99	158,34
	780	3299,71	40,00	3,50	10,42	99,99	45,24
	840	3328,76	41,50	4,01	13,03	99,99	56,55
	900	3393,16	42,40	4,62	28,67	99,99	124,41
	960	3434,76	42,00	5,18	18,24	99,99	79,17
	1020	3486,83	40,70	5,70	23,45	99,99	101,79
	1080	3509,78	39,40	6,24	10,42	99,98	45,24
	1140	3545,27	38,90	6,85	15,64	99,98	67,86
	1200	3580,82	38,30	7,46	15,64	99,98	67,86
	1260	3580,82	38,40	8,18	-	99,98	0,00
	1320	3635,31	39,00	8,88	23,45	99,98	101,79
	1380	3639,50	39,00	9,71	2,61	99,98	11,31
	1440	3694,16	40,20	10,52	23,45	99,97	101,79

Appendix E

Data from Experiment 5

Investigating the effect of pore size on the performance of MD using actual brine emanating from mining and industrial wastewater

Appendix E.1

Data from Experiment 5: Test number 1

Investigating the effect of pore size on the performance of MD using 0.22 μm pore size membrane for the treatment of actual brine emanating from mining and industrial wastewater

Appendix E.1

Data from Experiment 5: Test number 1

Below in Table E- 1 the operating conditions is illustrated for the MD process and included are the membrane specifications:

Table E- 1: Membrane specification and initial operating conditions of experimental run

Membrane used	GVHP
Membrane pore size (µm)	0.22
Membrane Area (m^2)	0,00434
Feed Temperature (^oC)	60
Product Temperature (^oC)	10
Temperature Difference (^oC)	50
Feed Agitator (RPM)	600
Permeate Agitator (RPM)	600
Feed Flowrate (l/hr)	130
Permeate Flowrate (l/hr)	130
Feed Solution (g/L)	NaCl
	235
Feed volume (mL)	4000

			Feed		Permeate	
	Time (min)	EC01 (mS/cm)	EC02 (µS/cm)	FluxP (L/m2.hr)	Salt Rejection (%)	ΔVP (ml)
RUN 1	0	6,44	1,53			
	60	6,58	1,96	13,03	99,97	56,55
	120	6,99	2,12	28,67	99,97	124,41
	180	7,08	2,22	15,64	99,97	67,86
	240	7,25	2,16	33,88	99,97	147,03
	300	7,42	2,17	15,64	99,97	67,86
	360	7,60	2,21	28,67	99,97	124,41
	420	7,68	2,34	2,61	99,97	11,31
	480	7,76	2,56	13,03	99,97	56,55

Appendix E.2

Data from Experiment 5: Test number 2

Investigating the effect of pore size on the performance of MD using 0.22 μm pore size membrane for the treatment of actual brine emanating from mining and industrial wastewater

Appendix E.2

Data from Experiment 5: Test number 2

Below in Table E- 2 the operating conditions is illustrated for the MD process and included are the membrane specifications:

Table E- 2: Membrane specification and initial operating conditions of experimental run

Membrane used	GVHP
Membrane pore size (µm)	0.22
Membrane Area (m^2)	0,00434
Feed Temperature (^oC)	60
Product Temperature (^oC)	10
Temperature Difference (^oC)	50
Feed Agitator (RPM)	600
Permeate Agitator (RPM)	600
Feed Flowrate (l/hr)	130
Permeate Flowrate (l/hr)	130
Feed Solution (g/L)	NaCl
	235
Feed volume (mL)	4000

Table E- 3: Test Number 2 data for Experiment 5

			Feed		Permeate	
	Time (min)	EC01 (mS/cm)	EC02 (µS/cm)	FluxP (L/m2.hr)	Salt Rejection (%)	ΔVP (ml)
RUN 1	0	6.21	1,39			
	60	6.25	1,53	18,24	99,97	79,17
	120	6,45	1,89	10,42	99,97	45,24
	180	6,68	2,11	15,64	99,97	67,86
	240	6,77	2,29	13,03	99,97	56,55
	300	6,84	2,48	18,24	99,96	79,17
	360	6,97	2,83	10,42	99,96	45,24
	420	7,10	3,35	15,64	99,95	67,86
	480	7,25	3,86	13,03	99,95	56,55

Appendix F

Tank level calibration

Table F. 1: Feed tank level calibration

Level (cm)	ΔL (cm)	volume added (ml)	ml/cm
404	0	0	0
406,3	2,3	480	208,7
408,6	2,3	495	215,2
410,8	2,2	474	215,5
412,9	2,1	475	226,2
		Average	**216,4**

Table F. 2: Product tank level calibration

Level (cm)	ΔL (cm)	volume added (ml)	ml/cm
435,5	0	0	0
433,3	2,2	482	219,1
431,2	2,1	486	231,4
428,9	2,3	491	213,5
426,9	2	482	241
		Average	**226,2**

Appendix G

Sample Calculations

Sample calculations are based on short run data in Appendix D.1:

Flux

The permeate flux was calculated using the following formula:

$$Flux = \frac{Volume\ of\ water\ extracted\ (l)}{Membrane\ area\ (m^2) \times Timeperiod(h)} = \frac{(56.55\ ml \div 1000)}{0.00434\ m^2 \times (1hr)} = \frac{0.05655\ l}{0.00434\ m^2.hr}$$

$$= 13.03\ \frac{l}{m^2.hr}$$

Salt Rejection

The observed salt rejection was calculated using the conductivities of the feed and the permeate:

$$\%\ Rejection = \left(1 - \frac{EC_{permeate}}{EC_{feed}}\right) \times\ 100\ = \left(1 - \frac{\left(\frac{1.96\mu S}{cm} \div 1000\right)}{6.58\frac{mS}{cm}}\right) = 99.97\%$$

Water Recovery

The water recovery was calculated using the following formula:

$$\%\ Recovery = \left(\frac{Cumulative\ volume\ (ml)}{Total\ feed\ volume\ (ml)}\right) \times 100 = \left(\frac{56.55ml}{4000}\right) \times 100 = 1.41\%$$